MAGYAR ÁLLAMI
EÖTVÖS LORÁND
GEOFIZIKAI INTÉZET

GEOFIZIKAI
KÖZLEMÉNYEK

ВЕНГЕРСКИЙ
ГЕОФИЗИЧЕСКИЙ
ИНСТИТУТ
ИМ Л. ЭТВЕША

ГЕОФИЗИЧЕСКИЙ
БЮЛЛЕТЕНЬ

BUDAPEST

EOTVOS LORÁND
GEOPHYSICAL INSTITUTE
OF HUNGARY

GEOPHYSICAL TRANSACTIONS

SPECIAL ISSUE
ON
ANISOTROPY, SHEAR WAVES AND
POLARIZATION MEASUEREMENTS

CONTENTS

VOL. 34. NO. 1. JULY 1988. (ISSN 0016-7177)

KÜLÖNKIADÁS
ANIZOTRÓPIA, NYIRÓHULLÁMOK ÉS POLARIZÁCIÓS MÉRÉSEK

TARTALOMJEGYZÉK

СПЕЦИАЛНЫЙ ВЫПУСК
АНИЗОТРОПИЯ, ПОПЕРЕЧНЫЕ ВОЛНЫ И ПОЛЯРИЗАЦИОННЫЕ ИЗМЕРЕНИЯ

СОДЕРЖАНИЕ

GEOPHYSICAL TRANSACTIONS 1988
Vol. 34. No. 1. p. 3

EDITOR'S NOTE

By publishing the material of an EAEG Workshop, Geophysical Transactions set on a new venture. The novelty is twofold: in the first place a journal independent of EAEG is publishing this material and, secondly, a primary journal is publishing a tutorial-type material. Let us start by considering the second aspect: even at the workshop itself it was felt that the material was not homogeneous, there were papers of real tutorial character—for one such paper special thanks are due to Prof. Grau—but others contained material that could easily be qualified as new. For those who have to start working with shear waves (and their number will surely grow because of the increasing interest in the topic) it is advantageous if, just after reading a good tutorial review, they can get an insight into the research aspects of the subject matter.

Back to the first point, i.e. the connection between EAEG and ELGI. It has been proven in many ways that a divided world means a great disadvantage to science. In its efforts towards uniting European geophysicists, EAEG has organized annual meetings in socialist countries (Zagreb 1977, Budapest 1985, Belgrade 1987) thereby enabling a much higher participation rate for those who —for currency reasons—would otherwise have been unable to take part in such meetings. We regard this special issue as a similar gesture.

The idea of publishing the material of the workshop came as a sudden thought while listening to the lectures at Belgrade. As the different accents poured knowledge on our poor heads that were becoming increasingly tired, I wondered how much of all the lectures I should be able to transmit to my colleagues at home. Not too much, I admitted to myself. My notes were inadequate, and the material received was short of being comprehensive. Thus, in the form of this special issue, we would like to pass over the information originally received by a few participants only.

Originally we had hoped to be ready with this special issue by the beginning of 1988. But time passed and manuscripts trickled in slowly. Of the eight lectures we are only able to publish six, and one of these six is in the form of an expanded abstract. But to compensate for the delay, some of the papers have been worked up to a much higher level than the original presentations.

Taking everything into consideration, practice will decide whether our venture is a success or a failure. This special issue is available to non subscribers through both the EAEG Business Office and the Association of Hungarian Geophysicists using the attached card.

Budapest, May 1988

Éva Kilényi
Editor

GEOPHYSICAL TRANSACTIONS 1988
Vol. 34. No. 1. pp. 5—6

FOREWORD FOR THE SPECIAL ISSUE 'ANISOTROPY, SHEAR WAVES AND POLARIZATION MEASUREMENTS'

Hans A. K. EDELMANN*

The immediate reaction of my colleagues and I after looking at shear-wave recordings some fifteen years ago was emphatic. As predicted, a new artificially generated wave type could be used to produce a subsurface image. The reaction of the Establishment, however, was less encouraging and we all soon became aware that a long way lay ahead of us during which the method had to be improved and the sceptics convinced. There were many proposals at that time suggesting how the new tool should be used — one of the most conservative theories being to determine Poissons's ratio from *P*- and *S*-wave velocities. Many misunderstandings, too, had to be cleared out of the way, for example shear-wave records were not suitable for replacing *P*-wave records. Neither velocities nor reflection coefficients could be assumed to be equal for both types of waves so that the differences in appearance of *P*- and *S*-wave records, that embarrassed most of the seismologists, proved to be the real potential of the method. We had to learn to interpret these differences with respect to subsurface lithology because we knew too little about the relationship between lithology and *P*- and *S*-wave appearance.

Obtaining good shear-wave sections was not simple at that time because of the predominant ground roll and the strong but obscure local influence of near-surface layers. It was therefore a relief to discover that the quality of data proved to be strongly dependent upon anisotropy, which explained many of the phenomena previously not readily understood. But as always it had to be decided which physical effects were to be used and which were to be eliminated. Theoretically, the influence of polarization, meaning the dependence of propagation velocity on propagation direction, can have a high diagnostic value. The German engineer Otto von Guericke said in 1672: "...therefore scientists who merely rely upon ideas and deductions and do not accept practical experience will never make conclusive statements about the constitution of this Universe. Because if human thinking is not based upon experiments, it will deviate from truth farther than the sun is separated from the earth". It was obvious from the beginning that experience could only be gained from practical application. Among the first geophysicists who successfully applied shear waves in reflection seismic work was Kenneth Waters from CONOCO. He showed

* PRAKLA-SEISMOS AG, POB 510530, D 3000 Hannover 51
Manuscript received: 18 January, 1988

convincingly that the cross-sectional view of the earth need no longer be based on the sole method of compressional wave reflection seismics. He proposed a means of generating shear-wave cross-sections which had all the features necessary for becoming a routine method using the VIBROSEIS® technique. No other method tested since that time has ever achieved the same quality of data acquisition and degree of professionalism.

It can be said today that the theory of shear waves exists and the tools necessary for proving this theory are also available. Even so, the exploration geophysicist must realize he will be asked questions if he highlights an important subject. It is not sufficient to discover things in nature, then isolate and describe them. That is equivalent to discovering a new geophysical effect in test-tube experiments. A new geophysical method must first of all prove its usefulness under the critical eyes of those who are responsible for the success of exploration and production drilling. Little by little it is becoming evident that there is a great deal known about shear waves. But this information has been given very reluctantly by the bright people in the oil industry who have held back good ideas for refinement and finishing, instead of aggressively selling their methods to the decision makers who urgently need more reliable information. This is what I call the tolerated information gap in a company.

Ludger Mintrop, the inventor of the refraction seismic technique did one thing. He offered purely and simply to delineate salt domes, which at that time were known to be the centres of oil accumulation. Neither he nor anyone else could exhaustively explain the physical process of refraction seismics, but notwithstanding that, many people succeeded in finding oil by his technique. When we offer the shear-wave technique today as an aid to finding and developing specific oil and gas fields we must ensure it gets into the hands of those who are ready and able to use it to achieve higher success rates, i.e. production and petroleum engineers.

The purpose of the E. A. E. G. workshop held at the Belgrade Convention in 1987 was to present an opportunity to learn more about the theoretical background and to improve our practical knowledge. In addition, it was intended to give an impetus to think about a more efficient application of shear waves.

Acknowledgement is due to the Eötvös Loránd Geophysical Institute, who kindly undertook to publish the work. I would like to thank all participants for their contributions and my co-chairman Robert Garotta for his help in making the workshop a success.

Hannover, January 1988

GEOPHYSICAL TRANSACTIONS 1988
Vol. 34. No. 1. pp. 7—43

S-WAVES AND SEISMIC ANISOTROPY

Gérard GRAU*

In some instances where *P*-wave records are of poor quality, *S*-waves have been used in order to produce exploitable seismic sections. In most cases, *S*-waves recording serves as a useful complement to *P*-wave surveys for lithology studies or for the verification of gas bright spots. *S*-wave seismology is able to yield more information about geological formations than *P*-waves alone because of the variety of *S*-wave polarization effects that can be observed. Indications about rock fractures, a characteristic of great interest to oil production engineers, may be obtained by careful analysis of such effects. This paper is meant to be an introduction to the study of *S*-, or transverse waves and of seismic anisotropy in *in-situ* sedimentary rocks, to their meaning and to their use for hydrocarbon prospecting. It aims at presenting a résumé of the main physical principles involved, of current seismic practice, and of research directions to be pursued.

Keywords: seismic method, shear waves, wave polarization, seismic anisotropy

1. Introduction

The existence of body waves of two different types was predicted in early studies by Poisson, Green, Lamé and others. Later on, seismologists identified two of the main events visible on records from teleseisms as arrivals of these body waves. The particle displacement of the slower ones is shown to be perpendicular to the ray, hence their name of *transverse waves*, whereas the faster waves are described as *longitudinal*, the direction of their particle motion being oriented along the ray.

As will be seen later on, exploration geophysicists usually generate both types of waves even when they mean to produce and record only longitudinal vibrations. The seismic reflection method for investigating sedimentary basins is almost always described, and its data are interpreted in terms of longitudinal wave propagation only. The positive results oil explorationists have met with so far have been obtained in this manner. It is interesting however to examine what the properties of the transverse waves are and to describe what additional information can be derived from their observation. This paper is meant to be an introduction to such a study.

The subject matter is divided according to hypotheses of growing complexity regarding the elastic properties of the geological media in which the disturbance is to propagate. In this respect, I am following the usual course taken by books dealing with wave propagation: the more realistic the description of propagation in actual rocks, the more sophisticated and intricate the theory.

* Institut Français du Pétrole, 4 Avenue de Bois-Préau, 92500 Rueil-Malmaison, France
Manuscript received: 6 January, 1988

A glossary will be found annexed to this paper. It is designed for the use of readers who might not be familiar with the technical terms of wave propagation theory. A classified list of books and papers is also included for further reading. Against common practice and in order to simplify this paper, I have taken the liberty of not giving any references in the course of the text; a few references have, however been cited in relation to the figures. The reader is kindly invited to consult the bibliography depending on the subject matter involved.

2. Homogeneous, isotropic, elastic solids

Let us first examine the case of a solid material that would be homogeneous, with isotropic properties, and that would be perfectly elastic. Even though geological formations exhibiting these properties would be very difficult to find, such hypotheses are convenient for study. Moreover, the theory yields a good approximation of a number of properties of real media as studied by exploration geophysicists. It is the basis for conventional descriptions of the seismic method.

As first shown by Poisson, theory indicates that body waves of two distinct kinds can propagate in an isotropic homogeneous elastic medium. One of these waves is such that the curl of the particle displacement vector is zero everywhere and at all times. This is the *P*-, *irrotational* or *compressional* wave. Elements of volume in the body do not undergo any rotation when waves of this type travel through them. The other one corresponds to a displacement vector that has a zero divergence. This is the *S*-, *equivoluminal* or *shear* wave. Such disturbances do not involve any volume change, but only distortion of the elementary domains agitated by the passage of the wave *(Fig. 1)*. Resistance to shearing stresses is the reason why the medium supports *S*-wave propagation.

Theory further states that in an infinite isotropic homogeneous medium the two different waves travel without interference, because the general wave equation splits nicely into two independent wave equations, one for *P*- waves, one for *S*-waves. In the presence of a boundary, however, waves of one type usually undergo conversion into waves of the other type: some *P*-vibration energy can be transformed into *S*-vibration energy or conversely. As a result, a wave incident on an interface separating two media usually generates two reflected and two transmitted waves, one of each type. The most notable exceptions correspond to cases where the dynamic equilibrium of the interface requires one reflected and one transmitted wave only. This occurs when the incident disturbance is either a plane *P*-wave at normal incidence, or a plane *S*-wave with its particle motion parallel to the interface. In the latter case, the phenomenon is simply described by a wave equation similar to that for propagation in a fluid.

P- and *S*-waves are polarized. The particle motion for homogeneous *P*-waves is perpendicular to wave surfaces (or wavefronts); that of *S*-waves is contained in a plane tangent to such surfaces. As the direction of propagation of the energy – the ray direction in the high-frequency approximation – is

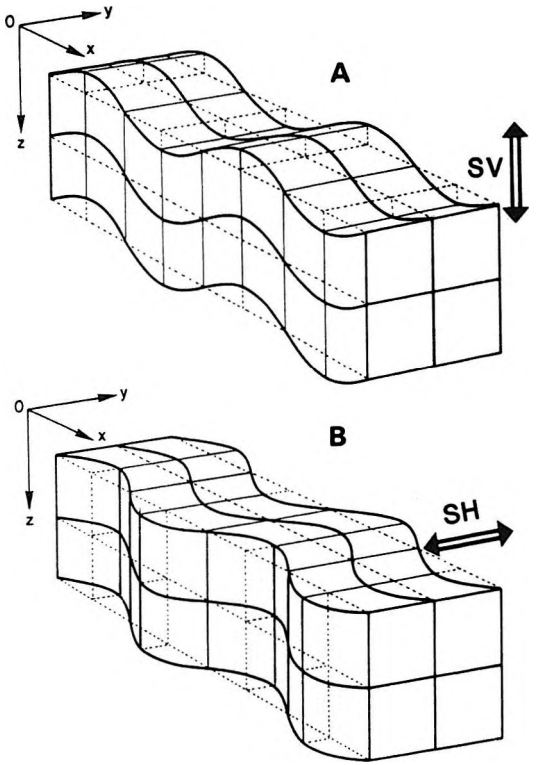

Fig. 1. Displacement for plane shear wave propagating in the *x* direction
A) Displacement in the *z* direction
B) Displacement in the *y* direction
Note that planes parallel to *xOy* move parallel to each other without ever altering their distance · [after AULD 1973]

1. ábra. Részecske elmozdulás *x*-irányban terjedő sík *S*-hullámok esetén
A) *z*-irányú elmozdulás
B) *y*-irányú elmozdulás
Megjegyezzük, hogy az *xOy* síkkal párhuzamos síkok egymással párhuzamosan mozognak anélkül, hogy a távolságukat megváltoztatnák [AULD 1973 nyomán]

Рис. 1. Смещение частиц при плоских поперечных волнах, распространяющихся в направлении *x*
A) Смещение в направлении *z*
B) Смещение в направлении *y*
Примечание: плоскости, параллельные плоскости *xOy* смещаются параллельно друг другу без изменения расстояний между ними [по AULD 1973].

perpendicular to the surfaces with equal phase, *P*-wave movement is oriented along the ray and *S*-wave movement perpendicular to it. In *Fig. 2* suppose a wavefront *(F)* originating at *(O)* on a horizontal surface plane *(H)* is observed at subsurface point *M*. *P*- waves are polarized along ray *OM*. The particle displacement of *S*- waves takes place in a plane tangent to *(F)* at point *M*. The

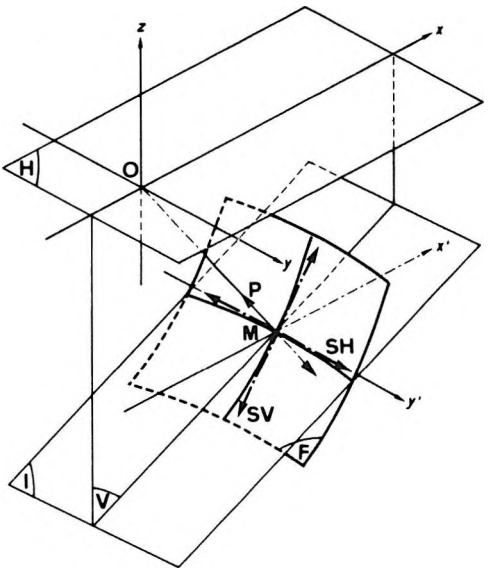

Fig. 2. Particle motions for *P*- and *S*-waves in an isotropic medium [after POLŠKOV et al. 1980]

2. ábra. Részecske elmozdulás *P*- és *S*-hullámokra izotróp közegben [POLŠKOV et al. 1980 nyomán]

Рис. 2. Движение частиц для продольных и поперечных волн в изотропной среде [по POLŠKOV et al. 1980].

S-wave that has its particle motion contained in the vertical plane *(V)* of *OP* is called *SV*. The arrivals will be observed on vertical geophones and on horizontal geophones with their axis along *Ox*. The *S*- wave with horizontal polarization *(SH)* has its motion oriented along *My'* normal to plane *(V)*. It would be reflected without conversion on a plane such as *(I)* and the events would be best recorded on horizontal phones with their axis parallel to *Oy*. The best line orientation for *SH*-wave surveying is *Ox* with source and geophone polarization parallel to *Oy*. There is thus a great difference between *P*- and *S*-wave polarization. Particle motion of *P*-waves is rectilinear. On the contrary, the only constraint on *S*-wave displacement is that the particle has to remain in a plane.

For practical purposes, a distinction is commonly made between *S*-waves with different polarizations, by using their relationship with respect to the horizontal. An *S*-wave with horizontal particle motion is called *SH* (see *Figs. 2 and 3)*. If the movement occurs in the vertical plane of the ray, the wave is called *SV*. The medium being isotropic, all *S*-waves, whether *SH* or *SV*, or any transverse wave with intermediate polarization, travel with the same velocity. Such an ideal situation, as in *Fig. 3*, corresponds to tabular series of geological formations and to a low-velocity layer with very simple properties. In real cases, things may not be as clear-cut as on this figure [ENSLEY 1985].

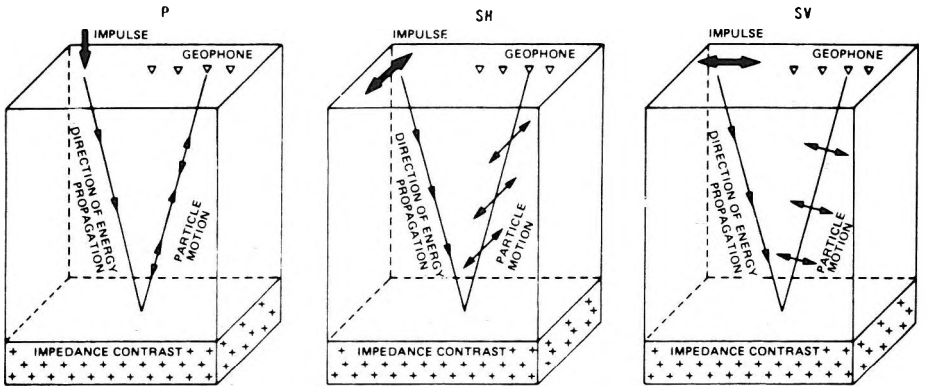

Fig. 3. A schematic drawing showing paths and polarization of *P*-, *SH*- and *SV*-waves. *P*- and *SV*-waves appear on vertical geophones and on geophones oriented along the line, *SH*-waves are detected only on geophones oriented normal to the line

3. ábra. Vázlat a *P*-, *SH*- és *SV*-hullámok útjáról és polarizációjáról. A *P*- és *SV*-hullámok a vertikális geofonokon és a vonal mentén irányított geofonokon jelennek meg, az *SH*-hullámok csak a vonalra merőleges irányítottságú geofonokon észlelhetők

Рис. 3. Схема пути и поляризации продольных и поляризованных поперечных волн. Продольные волны и поперечные, поляризованные в вертикальной плоскости, регистрируются вертикальными сейсмоприемниками и сейсмоприемниками, ориентированными вдоль профилей. Поперечные волны, поляризованные в горизонтальной плоскости, регистрируются лишь сейсмоприемниками, ориентированными вкрест профилям.

It is important to remember that the polarization of *P*- or *S*-waves is defined at any one point with respect to the direction of the ray going through that point. An *S*-wave arriving at a geophone at the surface is polarized horizontally if of the *SH* type. If it is not *SH*, it has a non-zero vertical component. An *SV*-wave arriving at a well geophone may very easily have a vertical component larger than the horizontal one. Similarly, a *P*-wave, as recorded by a sonde in a well, may appear to have greater amplitudes on the horizontal phones than on the vertical ones *(Fig. 4)*. Hence the importance of referring 3-component measurements to a coordinate system tied to the direction of arrival of the wave rather than to the horizontal plane.

There are several cases in which *S*-wave generation can be obtained while performing seismic surveys:

— transverse waves with horizontal polarization are intentionally created by a surface source;
— or a conventional source, such as an underground explosion, emits mostly compressional-wave energy, but geophone-to-source offset is such that conversion from *P* to *S* occurs at subsurface interfaces;
— or, finally, a vertical surface source generates shear waves in non-vertical directions, the echoes of which, however weak they may be, are picked up by vertical geophones.

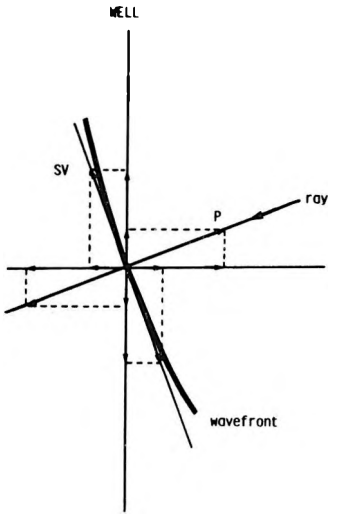

Fig. 4. Horizontal and vertical components of *P*- and *SV*-waves arriving at a seismic sonde in a well
4. ábra. Fúrólyukban levő szeizmikus szondába érkező *P*- és *SV*-hullámok horizontális és vertikális komponense

Рис. 4. Горизонтальные и вертикальные компоненты волн, продольных и поперечных, поляризованных в вертикальной плоскости, поступающих в сейсмический зонд, помещенный в буровую скважину.

Generally speaking, it is difficult to create *S*-waves with enough energy when surface materials are loose. When they are compact, the efficiency of surface sources is much higher. The intentional generation of *SH*-waves makes it possible to have these waves polarized in such a way that particle motion is parallel to the interfaces at the reflection points. If one is in the presence of two-dimensional structures, it is then possible to obtain simple *S*-wave propagation without any conversion throughout: *S*-waves are transmitted and reflected as *S*-waves, irrespective of the angle of incidence. In order to prevent wave conversion, *S*-waves must be generated and recorded at the surface with polarization parallel to the strike of the interfaces. Should the line be located in the vertical plane of the dip vector of the interfaces waves that have a horizontal polarization perpendicular to the line, are best recorded by geophones with a horizontal-directivity maximum oriented perpendicularly to the line. This is the basis for the *SH*-method which can be utilized in regions where all interfaces have the same strike. Unfortunately, two-dimensional structures are rare and *SH* seismic results, although theoretically free from interference, may be polluted by *P*-waves and by *S*-waves with non-horizontal polarization.

In the second case, if one has in mind the production of a *P*-section, *S*-waves reaching the vertical geophones may be considered as a nuisance, and corresponding events as noise. But, with a view to using these waves, one may lay down horizontal geophones with their axes parallel to the line direction. One may thus register *SV*-waves resulting from a conversion at depth, and obtain at the same time both a *P*- and an *S*-section. Horizontal geophones are sensitive to the horizontal component of *SV*-waves and to the weak horizontal component of *P*-wave arrivals. The records obtained with vertical geophones will contain *P*-reflections and the vertical component of *SV* arrivals. An appropriate CDP processing must be applied and the stacking must take into account the geometry of *P-S* (or *S-P*) rays. A difficulty lies in the fact that the suitable

intertrace distances and the correct offsets are usually not the same for both types of waves. As *S*-noise waves have shorter wavelengths, the horizontal geophone groups must be shorter and closer to each other. However, there are distinct advantages in the converted-wave method. Cost is of course lower. Static corrections are easier to obtain and more accurate, and resolution is often better. In *Fig. 5* the paths from surface point *A* to surface point *B* are notably different for *S-S* waves and for *P-S* waves. Layer 2 is assumed to be birefringent (see below). On the *S-S* path, wave splitting occurs twice, the arrivals are complicated and the source of the phenomenon is not easily localized. When using converted waves, any observed wave splitting has to have taken place on the *S*-branch only and the corresponding arrival is more simply analysed [after GAROTTA and MARÉCHAL 1987].

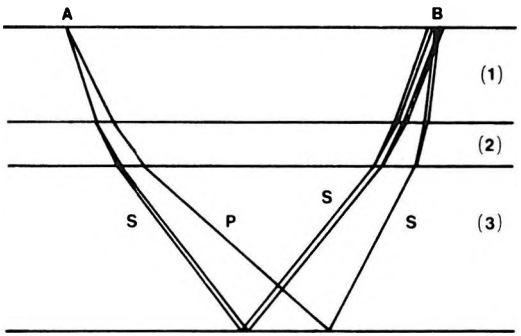

Fig. 5. Geometry for *S–S* and *P–S* travel paths
For simplicity, the figure has been drawn with horizontal interfaces and only the paths that give rise to reflections on the lowest interface have been represented

5. ábra. A sugárút geometriája *S–S* és *P–S* hullámra.
Egyszerűség kedvéért az ábrát vízszintes határfelületekkel rajzoltuk, és csak a legalsó határfelületen reflexiókat keltő sugarakat tüntettük fel

Рис. 5. Геометрия пути лучей для поперечно-поперечных и продольно-поперечных волн.
Для простоты изображены горизонтальные поверхности раздела и лишь лучи, вызывающие отражения на самой нижней из поверхностей.

The third case is of rather minor importance since it corresponds to transverse wave energy that is sent into the ground at slanting angles. The echoes produced are therefore to be observed only at high offsets.

Whether the relatively cheap method using converted waves or the more expensive one of generating and recording *SH*-waves is used, *S*-wave energy has to propagate through the low velocity layer. In this medium, *S*-waves travel very slowly. Their velocity may sometimes be as low as only a few hundred metres per second. The static corrections are therefore very large and known only with relatively poor accuracy. Furthermore the LVL, as seen by *S*-waves, is often thicker than for *P*-waves, since *S*-waves are not influenced very much by the water table. It follows that *S*-statics generally cannot be deduced from *P*-statics. As a result, the resolution of CDP stacks from *S*-wave surveys is often deficient.

Another reason for the lack of resolution is that energy absorption, and the loss of high frequencies that follows from it, are usually larger for *S*- than for *P*-waves. This goes against one of the theoretical benefits one could hope to find by working with *S*-waves, namely the possibility of taking advantage of their shorter wavelengths. Only when shooting in a well and recording in another well, can one hope to increase resolution significantly by using *S*-waves. Generally, the noise is stronger on *S*-wave surveys because of the presence of Love waves. It is also more difficult to discriminate against by means of wavenumber and velocity filters. All these particular features make *S*-wave field operations and processing rather delicate and expensive.

Some time ago, *SH*-waves were generated by successively shooting two rows of buried charges separated by a narrow patch of softened soil. With such an arrangement, both emissions generate *P*- and *S*-waves, but the polarization of the *SH*-component depends on the location of the row that is being detonated with respect to the soft patch. Subtraction of the seismograms obtained does away with *P*-waves and reinforces *SH*-waves. Most often now, industrial surveys are conducted with horizontal vibrators, although arrangements of properly phased vertical vibrators have been proposed. Horizontal hammers were also developed for the generation of *SH*-waves (see a comparison of results in *Fig. 6*). Some of the well sources now being prepared will deliver a large proportion of their acoustic energy as *S*-waves.

One may ask: why take pains to do *S*-wave surveys when one so easily obtains *P*-wave sections? In some rare instances, it is possible to obtain good-quality *S*-wave records in areas where *P*-wave data are rather poor. This may occur where outcrops of high-velocity rocks are present and this may be of great importance because of the useful subsurface information thus provided, which could not have been obtained from *P*-wave surveys.

But then, why spend money conducting additional surveys with special sources and geophones and performing extra processing in areas where *P*-wave records are already of a satisfactory quality? One answer is that the observation of *S*-wave reflections and of their lateral variations, together with the knowledge of *S*-wave velocities, can provide enhanced resolution and bring forth additional information about rocks and their fluids. In favourable instances, the elastic coefficients of the formation can be estimated. Moreover, it will be seen further on that *S*-waves are a particularly well suited tool for the study of rock anisotropy.

The velocity V_S of *S*-wave propagation in an isotropic solid is always smaller than V_P, that of *P*-waves. The factor $\gamma = V_S/V_P$ is a decreasing function of Poisson's ratio. There is therefore some degree of correspondence between γ values and the lithological nature of the rock: when lower than 0.5, they correspond to poorly consolidated water-saturated rocks or to clays. Values between 0.50 and 0.55 indicate the presence of carbonates. Sandstones have γ's ranging from 0.57 to 0.65. When saturated with gas, rocks may have γ values 10 to 20 per cent higher than these. In an unconsolidated formation such as the low-velocity surface layer, γ can reach values as low as 0.15. On the other hand,

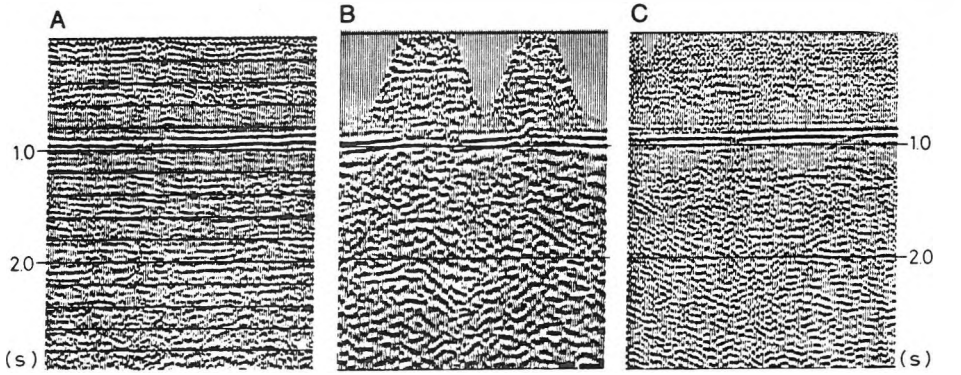

Fig. 6. A comparison of results obtained with three different ways of generating *SH*-waves [EDELMANN and SCHMOLL 1983]
A) Horizontal hammer, 8-fold vertical stack, 1200% horizontal stack
B) Buried charges, 2-fold vertical stack 200 to 1400% horizontal stack
C) Phased vertical vibrators, 16-fold vertical stack, 3000% horizontal stack

6. ábra. Három különböző *SH*-hullámgerjesztéssel nyert eredmény összehasonlítása [EDELMANN és SCHMOLL 1983]
A) Vízszintes kalapács, 8-szoros vertikális, 1200% horizontális összegzés
B) Betemetett töltet, 2-szeres vertikális, 200%-tól 1400%-ig terjedő horizontális összegzés
C) Fázisban eltolt vertikális vibrátorok, 16-szoros vertikális, 3000% horizontális összegzés

Рис. 6. Сопоставление результатов по трем различным способам возбуждения поперечных волн, поляризованных в горизонтальной плоскости [по EDELMANN–SCHMOLL 1983].
A) Горизонтальный молот, вертикальное суммирование — восьмикратное, горизонтальное — 1200%
B) Засыпанный заряд, вертикальное суммирование — двухкратное, горизонтальное — от 200 до 1400%
C) Вертикальные вибраторы, сдвинутые по фазе, вертикальное суммирование — шестнадцатикратное, горизонтальное — 3000%.

in compact rocks such as are considered in earthquake seismology, γ is close to 0.58, or $1/\sqrt{3}$, the value that corresponds to solids with equal Lamé constants, or a Poisson's ratio of 1/4. In *Fig. 7* both V_P/V_S and V_S/V_P ratios are plotted versus porosity in consolidated rocks. For a given porosity, the range of variations of V_P/V_S is large enough for this ratio to be a good indicator of the nature of the fluid.

As said above, a theoretical advantage of *S*-wave surveys is that the wavelengths ought to be shorter than those of *P*-waves. *S*-wavelengths can be smaller than those of *P*-waves only if γ multiplied by the ratio of the corresponding frequencies, f_P/f_S, is smaller than 1. In such a case, resolution is higher on the *S*-wave section. This may happen mostly when $\gamma < 0.5$. However, as mentioned above, the higher attenuation of transverse waves usually makes it difficult to obtain the same spectrum as commonly observed with *P*-waves and, consequently, no increase in subsurface resolution can be procured.

Lithological studies make use of pseudo-logs of the γ coefficient. The correspondence between γ values and formation characteristics is useful for the

detection of lateral changes of facies, or of fluid content, in a layer. If no well survey is available, common practice is to determine a γ_t coefficient, the ratio of the time differences between top and bottom horizons of the layer on *P*- and *S*-wave records. This γ_t is equal to $\gamma_V = V_S/V_P$ if the medium is isotropic.

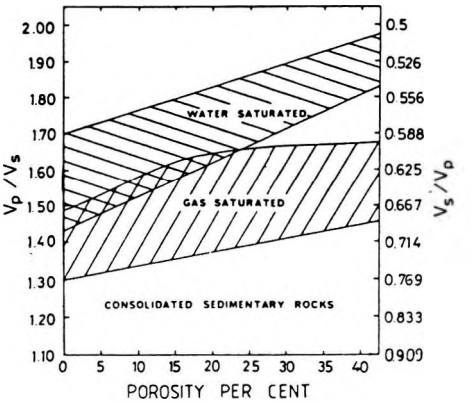

Fig. 7. V_P/V_S (or V_S/V_P) ratio as a function of porosity in consolidated rocks [GREGORY 1976].

7. ábra. V_P/V_S (vagy V_S/V_P) hányadosok a porozitás függvényében, konszolidált kőzetekben [GREGORY 1976]

Рис. 7. Отношения скоростей продольных и поперечных волн как функция пористости в консолидированных породах [по GREGORY 1976].

Some difficulty is usually experienced when attempting to estimate γ, since one has to determine V_P and V_S in the same layer. Indeed, the reflections visible on *P*- and *S*-wave records may not be due to the same geological interfaces and the layers may not be defined in the same manner on both sections. If the interpreter has a VSP at his disposal, then he knows where the seismic *P*- and *S*-events have originated from and the identification of corresponding *P*- and *S*-reflections is greatly facilitated. Otherwise, he would have to rely on visual correlations. These are easy in structured regions but may be impossible where the formations are tabular. In areas where velocity anisotropy is high, different γ factors have to be considered depending on which *S*-wave velocity is being taken into account.

As the propagation of transverse waves depends on the material being able to store shear elastic energy, *S*-wave propagation velocity is only slightly affected by the fluid content of the rock, which does not contribute to the shear strength. Hence the use of *S*-wave surveys as a complement for the interpretation of *P*-wave sections. Should a reflection-coefficient anomaly, a bright or flat spot, be observed on conventional *P*-wave data, a question that immediately arises is whether this anomaly is due to a variation of rock-matrix properties or to a variation of the fluid that is contained in its pores. If the anomaly is present on both *P*- and *S*-wave sections, then it is highly probable that the rock itself (its facies or its porosity) can be incriminated *(Fig. 8)*. If it is present on the *P*-wave records and does not show on the *S*-wave section, the nature of the fluid, or its variations, may be held responsible for the effect and the presence of gas can legitimately be inferred *(Fig. 9)*.

Another application of *S*-wave measurements in connection with *P*-wave observations consists in estimating the elastic properties of rock massifs. In

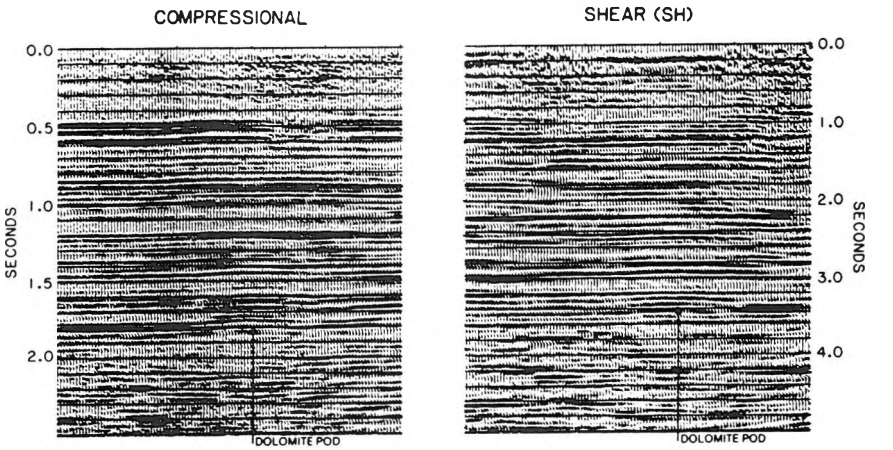

Fig. 8. 2400% stacks of *P*- and *SH*-wave reflections generated by the buried charges method. Average velocity ratio is of the order of 0.5. A dolomite pod gives similar seismic expressions on the *P*-wave section at 1.75 s and on the *S*-wave section at 3.2 s [GAROTTA 1978]

8. ábra. Betemetett töltet eljárással mért *P*- és *SH*-hullám reflexiós szelvény 2400% összegzéssel. Az átlagos gerjesztett sebességhányados 0,5 körüli. Egy dolomit lencse a *P*-hullám szelvényen 1,75 s-nál, az *S*-hullám szelvényen 3,2 s-nál hasonló szeizmikus képet ad [GAROTTA 1978]

Рис. 8. Разрез по методу отраженных волн с засыпанным зарядом по продольным и поперечным, поляризованным в горизонтальной плоскости, волнам, суммирование — 2400%. Среднее отношение возбужденных скоростей — около 0,5. Линза доломитов при 1,75 с на разрезе продольных волн и при 3,2 с на разрезе поперечных волн дает сходную сейсмическую картину [GAROTTA 1978].

cases where tomographic studies make it possible to determine *P*- and *S*-wave velocities in some volume of material, a good estimate can be made of the elastic coefficients, and particularly of the Poisson's ratio of the material. Clearly, when modern inversion techniques are ready to be used industrially, these methods will be able to provide a detailed description of the distribution of elastic coefficients and of density.

VSP's are often run with 3-component sondes and *P*- and *S*-wave surface sources at a marginal additional cost. Present industrial practice, however, is not much in favour of conducting *S*-wave surface surveys, for exploration managers often do not expect benefits worth the trouble and the expense. Nevertheless, it will be seen that *S*-waves can be used to detect some characteristics of rock anisotropy which, in turn, may be diagnostic of properties of great utility to reservoir engineers. The recognition of this possibility may stimulate the interest of oil explorationists.

The simplicity of analysing propagation characteristics in a homogeneous, isotropic, elastic solid must be considered as the result of a simplification that is usually made for the sake of easier theorizing, for natural solids are neither completely homogeneous nor really isotropic, and they have some degree of anelasticity. In the following chapter we are going to consider more realistic hypotheses and are going to dwell for some time on the problem of anisotropy.

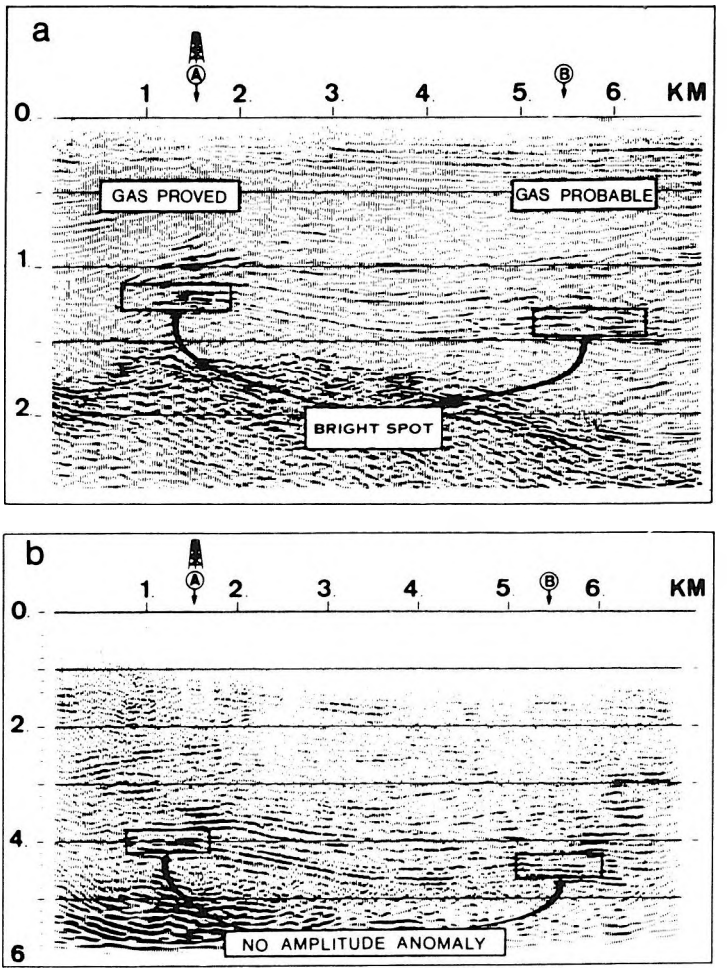

Fig. 9. Gas bright spots. The amplitude anomalies visible in locations *A* and *B* on the *P*-wave section do not show on the *S*-wave section. The *A* bright spot was proven to be due to the presence of gas [AUDET et al. 1981]
a) *P*-wave section; b) *SH*-wave section

9. ábra. Gáztelepek által okozott fényes foltok. A *P*-hullám szelvényen az *A* és *B* pontban látható amplitúdó anomáliák nem jelentkeznek az *S*-hullám szelvényen. Utólag beigazolódott, hogy az *A* pontbeli fényes folt gázt jelez [AUDET et al. 1981]
a) *P*-hullám szelvény; b) *SH*-hullám szelvény

Рис. 9. Светлые пятны, вызываемые наличием газовых залежей. На разрезе продольных волн в точках *A* и *B* видны аномалии амплитуд, не проявляющиеся на разрезе поперечных волн. Впоследствии было подтверждено, что светлое пятно в пункте *A* связано с газовой залежью [AUDET et al. 1981].
а) Разрез по продольным волнам; b) Разрез по поперечным волнам, поляризованным в горизонтальной плоскости.

3. Anelastic, homogeneous, isotropic media

Anelastic media absorb some of the energy from the waves and transform it into heat. Suppose an anelastic wedge (2) is comprised between two elastic media (1) and (3) *(Fig. 10)*. A plane wave with constant amplitude along its wave surfaces is assumed to travel in medium (1) and to reach interface (I_{12}) with normal incidence. In (1), surfaces with constant amplitude are planes parallel to φ_1, a constant-phase surface. In (2), they are also parallel to φ_1. When arriving in medium (3), the wave amplitude is smaller on ray AA' than on ray BB'. Constant-amplitude surfaces in medium (3) are perpendicular to φ_3 a constant-phase surface in that medium. In other words, constant-phase surfaces are not parallel to constant-amplitude surfaces. In the general case, when the wave crosses an interface, constant-amplitude surfaces are refracted according to a generalization of Snell's law.

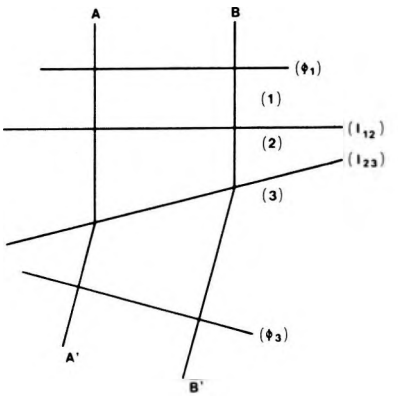

Fig. 10. Attenuating-wedge effect. For legend see text

10. ábra. Csillapító ékhatás. Jelmagyarázatokat lásd a szövegben

Рис. 10. Затухание под влиянием клина. Условные обозначения – см. в тексте.

It has been shown that the particle motion for such waves is usually elliptical. Since *P*- and *S*-waves are elliptically polarized, they are no longer either purely longitudinal or purely transverse. In most instances however, the ellipticity of particle trajectories that theory can forecast from such a cause is rather small and it would seem that anelasticity alone cannot explain the rather round shape of many of the particle trajectories actually observed.

Attenuation of *S*-waves may exhibit some degree of correlation with lithology or with rock fracturing. As the estimation of attenuation in thin layers is extremely difficult, applications are rare.

4. Heterogeneous, isotropic, elastic solids

When the properties of the medium cannot be considered to be constant within a wavelength, the equation of motion can no longer be separated into two simpler wave equations. The material does not support independent *P*- and *S*-waves. Both kinds of disturbance cannot travel to and fro without interacting.

For a given degree of heterogeneity, the effect is of course more pronounced for the high-frequency components of the spectrum. In view of the complexity of the theoretical analysis, the heterogeneity of density and of elastic properties is generally ignored when interpreting seismic results and geological media are commonly considered to be made up of a juxtaposition of homogeneous ones. Clearly, neglecting heterogeneity has not been too detrimental to prospecting in the past. Nevertheless, when detailed and accurate simulation of wave propagation is needed in order to invert seismic data, the effect may have to be taken into account.

5. Anisotropic, homogeneous, elastic solids

Most geological formations are anisotropic with regard to their elastic properties. The study of seismic wave propagation in such media is therefore of great significance, be it only for the sake of obtaining exact depths to the reflectors — a major requirement for seismic prospecting. Other possible applications deal with lithological or rock fracture studies. Causes for anisotropy of sedimentary rocks may be the following:

— deposition of clastic sediments with a preferred orientation in the Earth's gravity field (probably not a prominent cause),
— stress (not a very important cause either),
— deposition in estuaries and in sedimentary fans with channels and bars,
— compaction of formations with the frequent occurrence of stylolites,
— fine layering of sediments of different natures,
— and, finally, the presence of oriented joints or cracks of various sizes which the stresses may maintain gaping open and filled with water.

Orders of magnitude for the velocity anisotropy (the ratio of horizontal to vertical velocity) may vary substantially from point to point. However, values generally observed are in the range of 1.05 to 1.15 for *P*-waves and 1.10 to 1.50 for *S*-waves. An example of experimental results is shown in *Figure 11*.

At any point in an elastic medium and at any time, Hooke's law states that the stress-strain relationship is linear. The proportionality coefficients constitute a fourth-order tensor, the elasticity tensor. Out of its 81 components, at most 21 are independent because of the symmetry of the strain and stress tensors on one hand, and of thermodynamic considerations on the other hand. Moreover, anisotropic rock formations may possess some symmetries. This means that, at a given point, directions that are symmetrical with respect to a symmetry plane or to a symmetry axis are equivalent as far as elastic behaviour and wave propagation are concerned. In such a case, the number of independent elastic coefficients required to describe the medium is reduced and is therefore smaller than 21.

The most drastic simplification is that which results from isotropy. The properties of the material being the same in all directions, all planes are symmetry planes and the elastic coefficients do not depend on the system of coordinates chosen. Therefore, the wave-propagation equation must have a vectorial

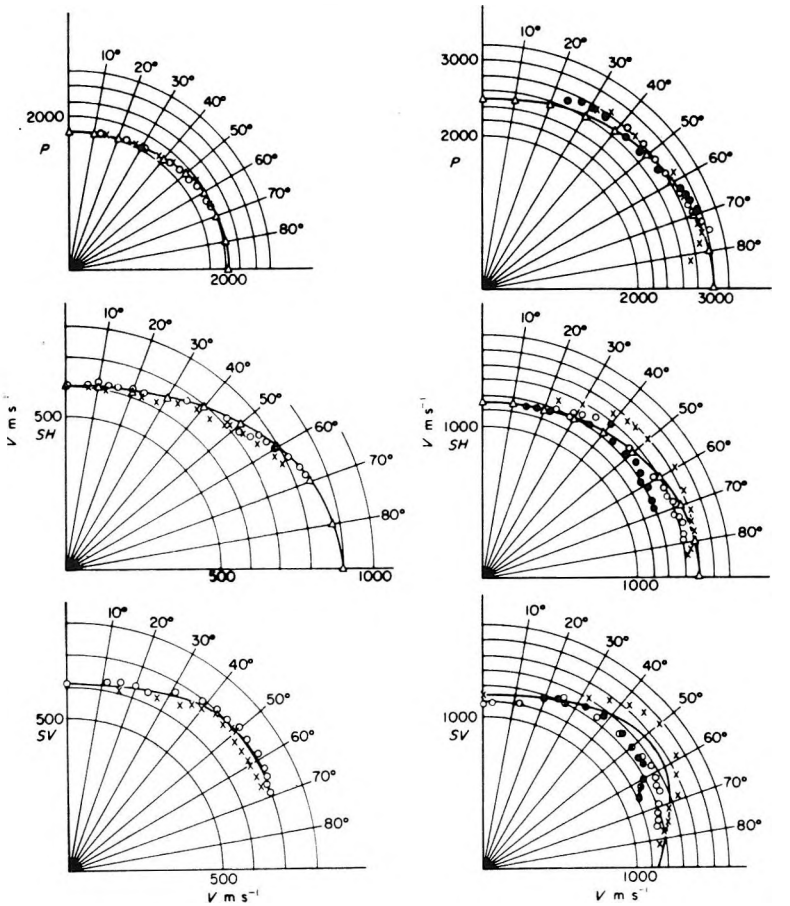

Fig. 11. ***P***-, ***SH***- and ***SV***-velocities obtained from borehole measurements in terrigenous and carbonate sequences. Left column from terrigenous, mostly clayey series; right column from carbonate series. Observations were made along the strike of the formation. *SH*-waves exhibit an elliptic velocity characteristic [Brodov et al. 1984]

11. ábra. Fúrólyuk mérésekből nyert *P*-, *SH*- és *SV*-sebességek szárazföldi és karbonátos összletben. A bal oldali oszlop szárazföldi, többnyire agyagos sorozatból, a jobb oldali karbonátos sorozatból való. A megfigyeléseket a formáció csapásiránya mentén végezték. Az *SH*-hullámok elliptikus sebesség karakterisztikájúak [Brodov et al. 1984]

Рис. 11. Скорости волн продольных и поперечных, поляризованных в горизонтальной и вертикальной плоскостях, полученные в терригенной и карбонатной толщах по скважинным измерениям. В левом столбце приведены результаты по терригенной, существенно глинистой толще, а в правом — по карбонатной. Измерения проводились по простиранию толщи. Поперечные волны, поляризованные в горизонтальной плоскости, обладают эллиптической характеристикой скоростей [по Brodov et al. 1984].

nature. As stresses depend on the spatial second derivatives of the displacement vector, the equation has to involve only those second derivative operators that are vectors. Mathematics teaches us that only two of them are independent. If we use the gradient of the divergence and the Laplacian, we obtain the conventional equation for elastodynamics. Expressing the displacement vector in terms of Helmholtz potentials, the particle motion field can be shown to split into divergence-free and irrotational components. Each of these corresponds to a wave which can travel in a boundless medium independently of the other, and with a different velocity. This is another way of saying that isotropic materials have only two independent elastic coefficients.

Fine layering with horizontal bedding is such that any vertical line is a symmetry axis, any vertical plane is a symmetry plane. The elastic properties are the same in all azimuths and wave-propagation velocity at any point depends only on the angle of the ray through that point with the axis of symmetry. If the beds are thin with respect to wavelength, the stratified formation can be considered as made up of a single homogeneous and anisotropic material, even if the individual beds are isotropic by themselves. This equivalent medium is described as *transversely isotropic* because it behaves as if it were isotropic in directions perpendicular to a symmetry axis. This type of anisotropy has been called a polar one. It involves only five independent elastic coefficients which can be computed, given the elastic coefficients of the materials constituting the individual beds and some statistics concerning their thicknesses. It must be noticed here that extremely few experimenters have succeeded in measuring all five coefficients of natural formations *in situ*, because of the difficulty of gathering enough independent measurements.

The criterion about the possibility of replacing a succession of isotropic layers by an equivalent homogeneous anisotropic medium depends on seismic wavelengths being substantially larger than the thickness of the individual layers. Therefore, it will often happen that this equivalence will be justified for seismic surveys but will break down for acoustic well-logging. In some cases, a layered medium may even look like a transversely isotropic medium for the long-wavelength part of the spectrum of a disturbance and, for its shorter wavelengths, like a succession of isotropic layers.

If a medium contains a large number of fluid-filled parallel cracks with small dimensions, we again have a transversely isotropic medium. Any straight line perpendicular to the cracks is an axis of symmetry and any plane containing such an axis is a symmetry plane. The elastic properties are the same in all directions contained in a plane parallel to the cracks. If the microcracks are vertical, rock properties vary with the azimuth and the corresponding anisotropy is said to be azimuthal. An example of mis-ties of *SH*-wave reflections obtained in different azimuths is shown in *Fig. 12*. Shear velocity is lower in east–west direction than north–south. This anisotropy appears to be related to an east–west fracture set which was recognized in outcrops [LYNN and THOMSEN 1986]*.

* Note, however, that azimuthal anisotropy can result also from other causes than the presence of microcracks.

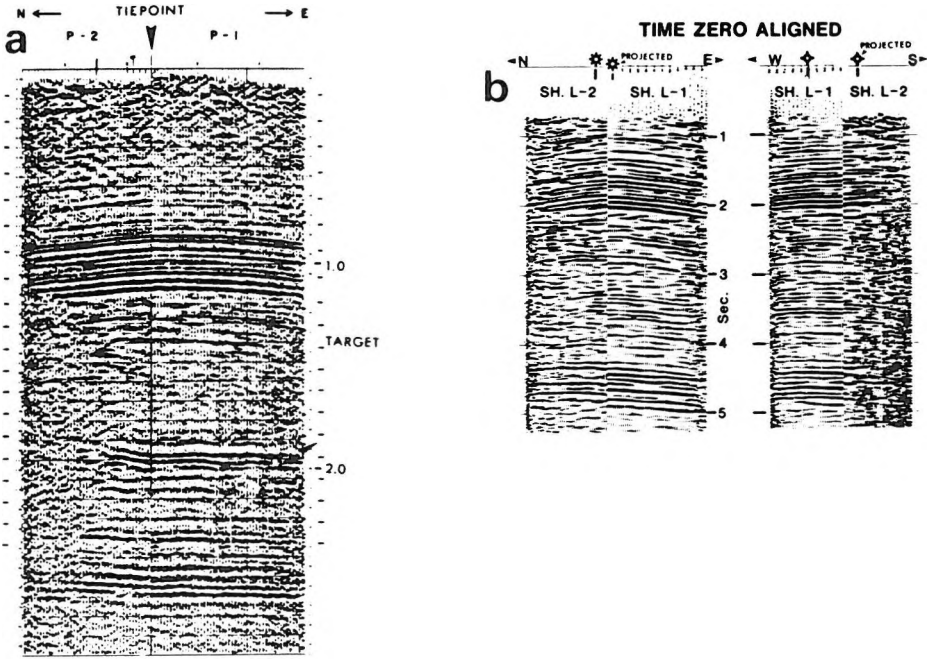

Fig. 12. Azimuthal anisotropy
a) Two *P*-wave time sections showing that the sections tie at the intersection point
b) Intersection of *S*-wave time sections with mis-ties growing with reflection time

12. ábra. Azimut anizotrópia
a) Két *P*-hullám időszelvény, a metszéspontban jól korreláló reflexiókkal
b) *S*-hullám időszelvények kereszteződése, a reflexiós idővel növekszik a korrelációs hiba

Рис. 12. Анизотропия азимутов
a) Два разреза продольных волн с отражениями, легко скоррелируемыми в точке пересечения профилей
b) Пересечение временных разрезов поперечных волн; с увеличением времени отражения возрастает ошибка корреляции.

The behaviour of such media is again fully described when five independent elastic coefficients are given.

Suppose now that a finely-layered medium is affected by the presence of parallel liquid-filled microcracks, then the symmetry is drastically reduced. If the cracks are perpendicular to the bedding, the anisotropy of the formation is of orthorhombic symmetry with nine independent coefficients. Should the cracks still be parallel but not be perpendicular to the layers, then we would observe the symmetry of monoclinic crystals. Such models may not be extremely exact but they can be expected to describe reality locally to a reasonable degree of approximation.

Theory shows the main features of wave propagation in anisotropic media to be the following:

1. For each direction of space, there can exist three plane body waves propagating with different velocities and different linear polarizations. This results from the fact that wave velocities and polarizations for a given propagation direction can be shown to be the eigenvalues and eigenvectors, respectively, of a 3 × 3 matrix, the Christoffel matrix. In each phase-propagation direction, the medium allows particles to oscillate only along three directions. These three polarizations are orthogonal to each other *(Fig. 13)* and depend exclusively on the direction in which the wave is travelling, or more exactly, on the orientation of this direction with respect to the symmetry planes of the medium. One polarization is generally close to the direction of phase-propagation: it corresponds to a *quasi-longitudinal* vibration. The other two are usually *quasi-transverse*. Only in special directions can the waves be purely longitudinal or purely transverse. As a rule, the three waves with orthogonal polarizations that can travel in a given direction do so with different velocities. In an infinite medium, if excited simultaneously, they will propagate independently of each other, a coupling between them being possible only at boundaries. At an interface separating two anisotropic media, an incident wave usually generates three reflected waves (one quasi-longitudinal and two quasi-transverse) and three transmitted waves (again one quasi-longitudinal and two quasi-transverse).

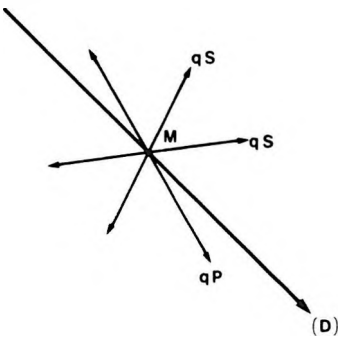

Fig. 13. Three plane waves with orthogonal particle-displacement polarizations correspond to a given phase-propagation direction (*D*); *qP* is a quasi longitudinal wave, the two *qS* waves are quasi transverse

13. ábra. Három síkhullám, ortogonális részecske-elmozdulás polarizációval, az adott (*D*) fázis terjedési iránynak megfelelően. A *qP* hullám kvázi longitudinális, a két *qS* hullám kvázi transzverzális

Рис. 13. Три плоские волны с ортогональной поляризацией смещения частиц в соответствии с направлением распространения данной фазы (*D*). Волна *qP* является квази-продольной, а две волны *qS* — квази-поперечными.

2. The direction of energy propagation for a given wave does not usually coincide with the normal to surfaces with constant phase. One must therefore make a distinction between the direction of propagation of the energy and that of the phase *(Fig. 14)*. The plane-wave surface (*W*) is tangential to (*S*)

the locus of all points reached at the same time from point O. Ray OM is a segment of a straight line since the medium is homogeneous. Energy-propagation velocity is directed along the ray. Phase-propagation velocity is parallel to the normal (N) to the wave surface at M. Phase-propagation vector $\vec{V}$ is the projection of energy-propagation vector $\vec{V}_e$ on a direction parallel to N. The energy velocity (which is often called group velocity) and the phase velocity are in general different and, as a result, the rays usually are not normal to the surfaces with constant phase. Reflection and transmission are governed by Snell's law *(Fig. 15)*. Equilibrium conditions for interface (I) between two media (1) and (2) require the wavenumber vectors of all seven waves to be coplanar with the normal at the point of incidence M and to have equal projections on (I).

Given the velocity of the incident wave (here, a P-wave) and the distributions of S- and P-velocities as a function of orientation around point M, the phase-propagation directions of the three reflected waves and of the three refracted waves are found. Then the anisotropy properties of media (1) and (2) determine the polarizations.

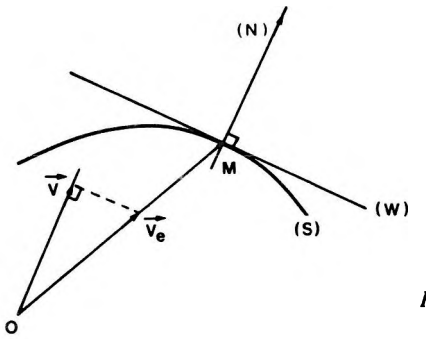

Fig. 14. Phase and energy velocities for a plane wave in a homogeneous, anisotropic solid

14. ábra. Fázis- és energia sebességek sikhullámra homogén, anizotrop közegben

Рис. 14. Скорости фаз и энергий плоской волны в анизотропной среде.

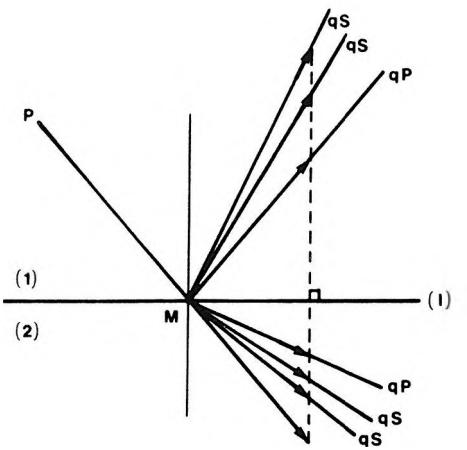

Fig. 15. Snell's law for anisotropic media

15. ábra. A Snellius–Descartes törvény anizotróp közegben

Рис. 15. Закон Снеллия–Декарта в анизотропной среде.

3. The phase velocity of longitudinal or quasi-longitudinal waves is usually larger than that of transverse or quasi-transverse waves. There is no theoretical reason why it should always be so and, as a matter of fact, crystals are known where there is a direction in which one of the quasi-transverse waves may travel faster than the other two possible waves. In a transversely isotropic medium, the *S*-wave velocity in a plane perpendicular to the symmetry axis is commonly larger than in other directions, but evidence to the contrary has been reported.
4. Energy-velocity surfaces may have cusps. This may be the source of anomalies in the amplitude distribution of seismic events arriving at neighbouring points, especially when the wavefronts are curved.

Point 1 shows how different wave propagation in anisotropic media is from that in isotropic ones. We have seen that transverse body waves could propagate in isotropic materials with an infinite number of polarization directions, all of them lying in a plane tangent to the wave surface. In general, this is no longer the case in anisotropic media since only two orientations of the particle displacement vector are admissible for quasi-transverse waves. As these polarizations are determined by the medium, given the phase-propagation direction, a careful study of the quasi-transverse waves can provide precious indications concerning the anisotropy properties of the material. On the contrary, quasi *P*-waves' polarization is usually quite close to the ray direction and cannot convey much information.

An important exception to the foregoing must be noted, however, when propagation occurs along a symmetry axis or in a symmetry plane of a transversely isotropic medium. Assuming that the direction of phase propagation is oriented along a vertical symmetry axis, then a pure *P*-wave can exist, i.e. a wave with purely longitudinal particle movement. *S*-waves, if excited, will therefore have horizontal polarizations: they are purely transverse. Because of the symmetry around the axis, their displacement vectors are oriented in any arbitrary horizontal direction and their propagation velocities do not depend on azimuth. If the transverse isotropy in question is caused by layering, then the velocity of these *SH*-waves is a simple function of the *S*-wave velocities of the individual beds.

Suppose now that a plane wave propagates in a direction contained in a symmetry plane. Any polarization direction must either be contained in the plane or perpendicular to it. It follows that the displacement of the quasi-longitudinal perturbation takes place in the symmetry plane. One quasi-transverse wave may propagate in the same direction with its polarization in the plane. One purely transverse wave is also possible with its displacement vector perpendicular to the symmetry plane. In *Fig. 16* the medium is symbolically represented by its lower part, but it is assumed to be of infinite extent and homogeneous. The parallel planes depict either interfaces between thin beds or planes parallel to fluid-filled microcracks. At point *M*, axis (*A*) is a symmetry axis. Assume (*I*) is the direction of phase propagation for a plane wave. One of the *S*-waves that is allowed to propagate will be polarized in the plane of incidence (Π_1) which contains (*I*) and (*A*): it is a quasi *S*-wave. The other one

will have its particle motion normal to the plane of incidence: it is a pure *S*-wave polarized in plane (Π_2) perpendicular to (Π_1). There is therefore always a pure *S*-wave polarization parallel to the bedding or to the microcracks.

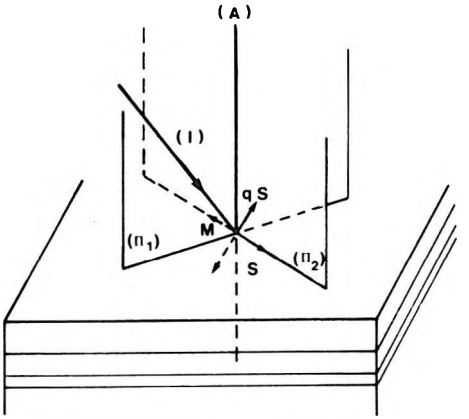

Fig. 16. The two legitimate *S*-waves in a transversely isotropic medium

16. ábra. A két szabályos *S*-hullám transzverzálisan izotróp közegben

Рис. 16. Две правильные попречные волны в попречноизотропной среде

Should we be in the presence of a stack of finely stratified horizontal beds, the symmetry axis would be vertical. Any vertical plane would be a symmetry plane. Therefore, the plane which contains the phase-propagation direction of a plane wave and the axis is such a symmetry plane. A plane wave can either be a quasi *P*-wave or a quasi *SV*-wave with particle motion in the plane or a pure *SH*-wave with displacement normal to the plane. Upon reflection on and transmission through horizontal interfaces, the first two will be coupled, whereas the *SH*-wave will behave independently. If the phase-propagation direction lies along axis (*A*), then both *S*-waves are pure and they travel with identical velocities.

Assume now that we have a rock massif with vertical, liquid-filled, parallel microcracks. The symmetry axis is horizontal. Any plane containing it is a symmetry plane. In particular, the incidence plane defined by the phase-propagation direction of the wave and the axis is a symmetry plane. A pure *S*-wave can propagate in the given direction with polarization perpendicular to the plane. The particle motion is therefore normal to the axis and it takes place in a plane parallel to the microcracks. If the incidence plane is vertical, and only in this case, the pure *S*-wave is an *SH*-wave with its particle motion vector parallel to the strike of the cracks. The other *S*-wave will then be a quasi *SV*-wave vibrating in the vertical plane.

These considerations show that a careful study of *S*-wave polarization may be able to yield interesting information, especially when the phase-propagation direction is not too distant from a symmetry axis. Three-component geophones should be used systematically for such investigations and it would be advantageous to generate the disturbances by means of a source with controlled emission orientation. One should not minimize, however, the great difficulty of such polarization studies. Let us mention only some of the effects that will

constitute obstacles and will have to be compensated for: possible inhomogeneity of the rock massif, presence of other anisotropic formations, variable or inefficient coupling of well seismic sondes, influence of both surface layer and free surface. Many research problems will have to be attacked in this domain. One of the most difficult ones will be that of finding ways of transforming surface records for easy comparison with well records.

Detailed resolution of a practical reservoir engineering survey would call for a very elaborate analysis of propagation characteristics in and near the layers of interest. Amplitude-versus-offset studies, which are commonly performed in order to determine the nature of the fluid in rock pores, would certainly benefit from interpreters taking into consideration the directions of wave-propagation and of polarization. As always, lateral variations of seismic propagation properties may be much easier to detect and to quantify than the actual properties.

When arriving in a transversely-isotropic medium, a transverse vibration with an arbitrary polarization direction generates the two orthogonally-polarized quasi *S*-waves that fit the propagation direction: *wave-splitting* occurs. This is the seismic equivalent of optical birefringence. It can be observed only with *S*- or quasi *S*-waves. A condition for the phenomenon to take place is for the phase-propagation direction in the anisotropic medium not to lie along a symmetry axis, that is to say not to be normal to bedding in a finely stratified formation, or to microcrack faces in a cracked medium. The two waves thus created usually travel with different velocities. For instance, a shear wave with polarization parallel to fluid-filled cracks will travel faster than a wave with its polarization oblique to them. The maximum magnitude of the effect is of the order of a few per cent. Since the pulses have the same shape, accurate determination of their arrival-time difference can be attempted by the use of some correlation algorithm.

A detailed study of shear-wave splitting can provide interesting information on the preferential directions which characterize the structure of a layer in particular on the distribution of natural fluid-filled microcracks, should they all be oriented in the same way in a large volume of rock, and possibly also about the density of such cracks. Such an investigation can lead to the detection of fractured reservoirs and to the estimation of the most probable direction for the creation of a fracture by a hydrofracturing operation. The differential-time method is particularly elegant. It does not make it necessary to actually invert the data and to estimate all the elastic coefficients as would be required in order to get a complete understanding of the anisotropy of the formation. However, it can be expected to give good results only in the most favourable cases, i.e. when the anisotropy is simple enough and is restricted to the reservoir itself. Analysing more complicated situations would most probably require extensive mathematical simulations of wave propagation. It would then be difficult to find numerical values with which to feed the computer.

Shear-wave splitting is a very plausible cause for the ellipticity or pseudo-ellipticity observed on particle trajectories, at least when the time lag between the two *S*-waves is short enough, with respect to period, to allow them to interfere

(Fig. 17). Correcting this effect by an appropriate deconvolution would enhance deep reflections. It has also been shown that a rotation of the data obtained with multicomponent geophones and multiorientation sources can improve overall quality because this is equivalent to recording in the preferred directions of the medium. Results of such a processing are shown in *Fig. 18*. Splitting effects disappear, interferences have been minimized, correlations are easy, and the characteristic mis-ties of events appear clearly [ALFORD 1986].

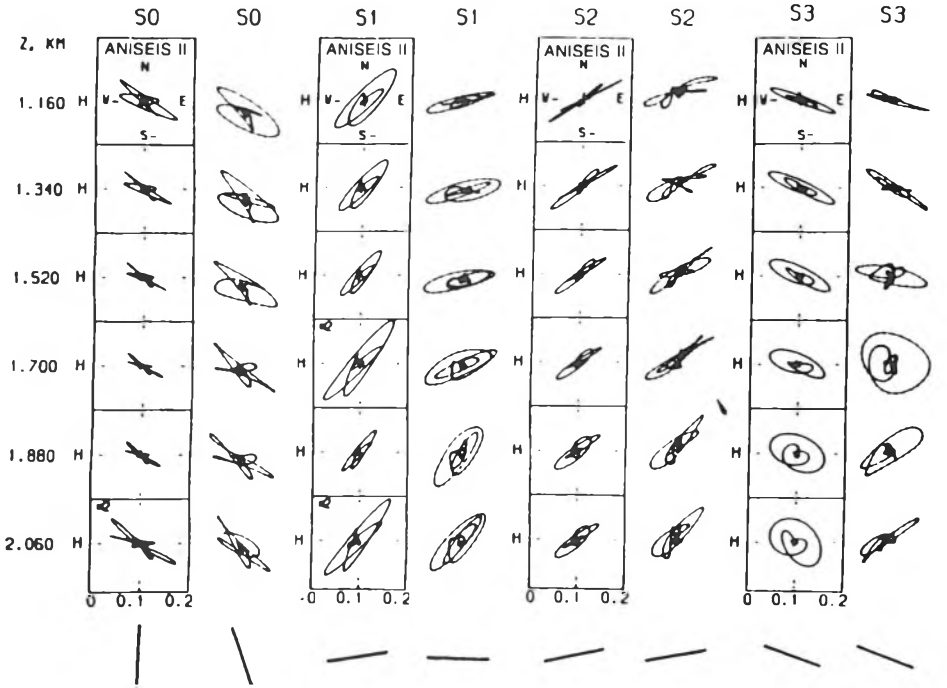

Fig. 17. Synthetic and observed horizontal hodographs of particle displacements. The particle-motion patterns correspond to measurements in well (depth scale at left) of waves generated at various surface points, S_0, S_1, S_2 and S_3, the latter being located the farthest away from the wellhead. The hodographs in boxes are the result of numerical simulation. Bars beneath patterns indicate vibration orientation [CRAMPIN et al. 1986]

17. ábra. Részecske elmozdulások szintetikus és észlelt vízszintes trajektóriái. A részecske elmozdulás ábrák fúrólyukban végzett mérésekből származnak (mélységskála bal oldalt) különböző S_0, S_1, S_2 és S_3 felszíni pontban generált hullámok esetén (a legutolsó van legtávolabb a fúrólyuktól). A bekeretezett trajektóriák numerikus szimuláció eredményei. A minták alatti vonalak a vibrátor irányítottságát jelzik [CRAMPIN et al. 1986]

Рис. 17. Синтетические в наблюденные горизонтальные траектории перемещений частиц. Примеры перемещения частиц взяты по скважинным измерениям (шкала глубин — слева) волн, возбужденных в различных точках S_0, S_1, S_2 и S_3 дневной поверхности (из них дальше всего от скважины находится последняя). Траектории, обведенные рамками, получены в результате цифровой симуляции. Линии под примерами обозначают ориентировку вибратора [по CRAMPIN et al. 1986].

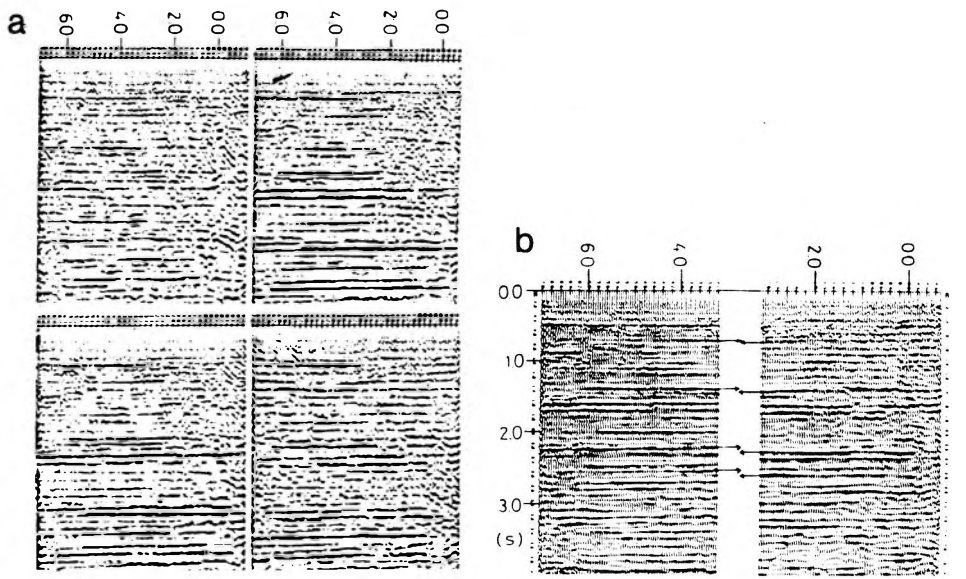

Fig. 18. Compensation of *S*-wave splitting effect
a) Time sections with different vibrator and geophone orientations. Left column shows in-line source, right column crossline vibrator orientation. Upper row displays in-line geophones, bottom row corresponds to geophones with crossline orientation. Signal-to-noise ratios are higher when orientations of source and receivers are perpendicular
b) Time sections obtained after mathematical rotation of data so as to be parallel or perpendicular to the symmetry axis direction of the azimuthally anisotropic medium
[ALFORD 1986]

18. ábra. Az *S*-hullám hasadás hatásának ellensúlyozása
a) Időszelvények különböző vibrátor és geofon irányítottság mellett. A bal oldali oszlopban vonalba eső, a jobb oldaliban keresztirányú a vibrátor irányítottsága. A felső sorban vonalba eső, az alsó sorban keresztirányú a geofonok tájolása. A jel/zaj viszony nagyobb, ha a forrás és vevő irányítottsága egymásra merőleges
b) Az adatok matematikai rotációjával nyert időszelvények. Egyik párhuzamos, a másik merőleges az iránytól függően anizotróp közeg szimmetria tengelyére
[ALFORD 1986]

Рис. 18. Компенсация эффекта от расщепления поперечных волн.
a) Временные разрезы при различных ориентировках вибраторов и сейсмоприемников. В левой колонке — ориентировка вибраторов по профилю, в правой — вкрест профилю. В верхней полосе — ориентировка сейсмоприемников по профилю, в нижней — вкрест профилю. Отношение сигнал/шум больше при взаимноперпендикулярной ориентировке источника и приемника.
b) Временные разрезы, полученные путем математической ротации данных. Один из них параллелен оси симметрии азимутально анизотропной среды, другой перпендикулярен ей
[по ALFORD 1986].

The discrepancy between phase- and energy-velocity vectors mentioned above in chapter 2 introduces a complication with respect to the behaviour at an interface, as compared with the classical situation prevailing at the boundary between isotropic media. The equilibrium of the interface has to do

with phase velocities and Snell's law applies, as was mentioned above. The incident, reflected and transmitted rays, however, are not generally coplanar. An exception occurs when the ray lies in a symmetry plane. Phase- and group-velocity vectors are then located in this same plane. In view of the complexity of wave propagation in anisotropic media, practical problems ought to be tackled with the help of computer simulations of geometrical relationships, traveltimes and wave forms. Among other things, this would enable interpreters to know which path the waves have followed and therefore which subsurface zones have been investigated.

In contrast with the richness of information *S*-wave surveys will be able to offer if they can hold their promise, *P*-wave behaviour in anisotropic formations appears to have much less potential. A well-known effect of anisotropy, that was noticed by early observers, is that *P*-wave velocities — as determined by usual reflection-curvature analyses — do not coincide with vertical velocities, with the result that computed depths may be inaccurate. Detecting a velocity anisotropy from surface records only is not an easy proposition, and often is impossible. As a matter of fact, it has been shown that in a special case where all beds of a given horizontal formation would have equal values of Poisson's ratio, the curvature of *P*-wave surfaces near the vertical would be consistent with a model with a velocity equal to the vertical *P*-wave velocity. Anyhow, when recorded on short spreads, *P*-waves usually appear to have propagated in an isotropic medium. However, if observed on long spreads, *P*-wave $t^2 - x^2$ curves for transverse isotropic media deviate slightly from a straight line, but this effect does not provide a valid diagnosis even if the observations are unambiguous, for it could just as well result from vertical inhomogeneity. Partial understanding of this anisotropy may be obtained by means of special experiments allowing a comparison of the propagation times from various points at the surface to a sonde in a well, varying the angles of incidence to the geophone.

This relative insensitivity of vertically-travelling *P*-waves has been the reason why anisotropy has not aroused more interest among oil exploration geophysicists. *S*-waves are intimately connected with anisotropy investigations because they are much more affected by anisotropic effects than are *P*-waves and because of their higher number of degrees of freedom. *S*-wave anisotropy can be observed by means of determination of transit-time ratios in a given layer for *P*-, *SH*- and *P*-converted-to-*SV*-waves. Lateral variations of the *SH*–*SV* velocity ratio are an indication of lithological modifications. Variations of the *P*–*SH* velocity ratio can result from modifications in the sand–shale ratio of the layer and/or from changes in the nature of the fluid in the pores. As mentioned above, how reliable such an analysis can be will depend on the quality of the correlation between corresponding events in the different seismic sections. Numerical simulations may help interpreters overcome this difficulty.

SH-waves in a transversely isotropic medium with horizontal layering have elliptical wave surfaces with arrival times and curvatures similar to those of the spherical wave surfaces that one would observe in an isotropic medium. The moveout velocity is the velocity for waves travelling in a horizontal direction

and is of course independent of direction. As the wave surfaces are elliptical, the $t^2 - x^2$ curve is a straight line, exactly like that of a wave propagating in an isotropic medium. By themselves, such *SH*-observations do not yield any clue as to the anisotropy of the medium. The t^2–x^2 curve for *SV*-waves is convex downwards and, if the quality of the data permits this observation, this could be a diagnosis of transverse isotropy since such a curvature cannot be caused by vertical inhomogeneity.

6. Anisotropic, anelastic solids

As the three body waves travel with different velocities, they are also certainly affected by attenuation coefficients that depend on wave type and on wave travel direction. The dependence of this attenuation on azimuth angle is easily derived in theory, but it would be extremely difficult to find actual values for the parameters that appear in the equations. Very little is known on this subject and it is hard to imagine how field experiments could yield suitable data with a high degree of accuracy. It would also be difficult in most practical cases to derive useful information about attenuation from amplitude-versus-offset observations. Conversely, how can one correct such observations in order to isolate reflectivity effects from anelastic effects in the upper strata? These problems, which are not without practical interest, stand in front of us as a formidable challenge.

7. Anisotropic, inhomogeneous, elastic solids

Textbook discussions of wave propagation in anisotropic media, or of the properties of grossly anisotropic formations, consider only homogeneous anisotropic media. As was mentioned above, a stack of thin isotropic layers is equivalent to a block of homogeneous anisotropic material. In natural conditions, however, statistics on thin bed elastic properties and thicknesses vary with depth. It follows that the anisotropy properties of the equivalent medium seen by long-wavelength perturbations also depend on depth. The elasticity tensor varies with location: the medium cannot be considered homogeneous for the shorter wavelengths. Most probably, fluid-filled microcracks in structured rock formations ought to display similar characteristics because of variations in elastic properties, porosity, stress distribution and so on.

Detailed and accurate investigations in areas with complicated tectonics will have to be conducted taking such effects into account. Numerical simulations of wave propagation in inhomogeneous, anisotropic media will become an essential tool for interpreters.

8. Conclusions

Exploration geophysicists have so far made *S*-wave surface surveys with two principal objectives in mind. One of these was obtaining interpretable data in areas of poor *P*-wave quality. In favourable but rare circumstances, *S*-wave reflections indeed have a higher resolving power than their *P*-wave counterparts. The second goal was the discrimination of gas bright spots from bright spots caused by lithological variations. This application has often met with success and has enabled geophysicists to provide reservoir engineers with reliable results. An extension of such studies has made it possible to correlate V_S/V_P ratios with lithology. The main difficulty lies in obtaining proper correlations of *P*- and *S*-wave events. Besides, this ratio cannot be estimated very accurately unless large time intervals are taken for analysing velocities, a choice that would remove all interest in this operation because of the corresponding loss in resolution.

Additional uses for *S*-wave surveys are being investigated. They take advantage of the higher number of degrees of freedom of *S*-waves. Unlike *P*-waves which are always polarized in a direction close to the ray, *S*-waves are polarized in directions which depend on the anisotropy properties of the formation. Because of their sensitivity, *S*-waves are a tool that is very well suited for such investigations. Exploration geophysicists will aim at going beyond classical resolution limits by obtaining information concerning the very structure of the material. A fundamental problem that will arise is that of the detectability limits of anisotropy properties. How thick, how wide, how anisotropic must a volume of rock be in order to be easily detected and investigated with a sufficient degree of accuracy?

One application of great potential importance for the exploitation of hydrocarbon pools is the detection and study of rocks with microfractures. In simple enough circumstances, *S*-waves travelling through a cracked formation suffer birefringence effects. A rapid diagnosis about microcrack orientation may be obtained by a determination of the time delay between the two split waves and of their polarization directions. In a number of cases, however, things may not be so simple because of the complexity of the anisotropy and the lack of homogeneity of natural media. Possibly, an analysis of the symmetry properties of the medium may already provide useful information. But it may well be that a proper interpretation of the data cannot be made without some kind of elaborate inversion.

However, because of the large number of independent elastic coefficients theoretically necessary to correctly represent the behaviour of a natural medium, it is difficult to imagine how an efficient inversion algorithm could be applied to real data. Research is necessary in order to determine whether incomplete inversions would be of any practical use. Some of the questions to be answered should be the following: are some of the coefficients more strongly affected by characteristics of interest or, in other words, are they all of equal significance? What are the limits within which differential-time studies are

feasible, especially in dipping formations? In which conditions can one separate the effects of two or more media with different anisotropy characteristics? What is the result of attenuation anisotropy added to velocity anisotropy? How can one compensate for the influence of the low-velocity layer on surface records?

Without any doubt, theoretical and practical research work, together with laboratory and field measurements, will be needed. Efficient software for computer simulations will be necessary and more experimental work will have to be performed before all the benefits of anisotropy determination can be obtained and its limits established. In particular, as it is important to be able to observe accurately polarizations and amplitudes of surface arrivals, the distortions caused by the LVL and the free surface should be actively and carefully studied. As a by-product, a better knowledge of the low-velocity layer may be expected.

Field measurements will more and more necessitate the use of three-component recordings and of multidirectional sources. Powerful tools for numerical simulation of wave propagation are a requisite for correct interpretation. Specialized processing software is also necessary.

Taking into account the high cost of *S*-wave surface surveys with complete 3-D, three-component recordings and multidirectional sources, the industrial use of the converted-waves method should also be thoroughly investigated. Of course, it cannot provide complete information, but it may constitute a cheap and easily implemented means of obtaining useful results — especially for amplitude-versus-offset and wave-splitting studies. The main advantage of the *P*–*S* method, besides its low cost, probably lies in its better lateral resolution for localizing wave-splitting layers. More elaborate methods may be used in a second step.

Until now, *S*-wave surveys have often been less reliable and of poorer quality than *P*-wave ones. The signal-to-noise ratio, in particular, and the determination of static corrections have been rather deficient. There are positive indications, however, that the quality of *S*-wave surveys may significantly be improved by taking anisotropy effects into account, for instance shear-wave splitting and azimuthal discrepancies of times and amplitudes, and by somehow compensating for them through proper processing. Better quality *S*-wave data may, in turn, yield more and clearer information about deep reflectors and about the anisotropy characteristics of layers at intermediate depth.

Most certainly, amplitude-versus-offset analyses will benefit from *P*- and *S*-waves being examined together, with anisotropy effects taken into account. And it can be expected that there is ample room for a detailed study of *S*-wave polarization and amplitude when monitoring production from a field or fluid injection into a reservoir.

As a final conclusion, it can be hoped that the renewal of interest in *S*-wave propagation will keep its promises, especially in the domain of fractured reservoir delineation and of lithological studies. This will not be achieved, however, without ample theoretical investigations and the corresponding field tests.

Appropriate processing procedures will have to be designed with the extensive use of interactive procedures in order to cope with the large number of different parameters that will have to be adjusted.

Acknowledgments

I would like to thank M. Dubesset, L. Nicoletis and P. Rasolofosaon for helpful discussions.

SELECTED BIBLIOGRAPHY

This classified list of references was compiled with a view to helping beginners in the study of *S*-waves and seismic anisotropy find their way through a particularly extensive literature.

No attempt was made at giving credit to all authors who have written important contributions in the field. For further study, a much more complete bibliography by R. A. Ensley (*in* Danbom and Domenico, 255–270) may be consulted.

S-WAVES

General

Dohr G. P. (ed.) 1985: Seismic shear waves. Geophysical Press, London–Amsterdam, A: Theory, 356 p., B: Applications, 273 p.

Edelmann H. A. K. and others 1986: Scherwellenseismik. Prakla–Seismos A. G., Hannover, 47 p.

Garotta R. 1978: Land seismic shear waves. C. G. G. Technical Series, N° 507.78.05, Massy, 16 p.

Danbom S. H. and Domenico S. N. (ed.) 1987: Shear wave exploration. Soc. of Exploration Geophysicists, Tulsa, 275 p.

Polarization

Cliet C. and Dubesset M. 1987: Three-component recordings: Interest for land seismic source study. Geophysics, **52**, 8, pp. 1048–1059

Douma J. and Helbig K. 1987: What can the polarization of shear waves tell us? First Break, **5**, 3, pp. 95–104

Gal'perin E. I. 1984: The polarization method of seismic exploration. Reidel, Dordrecht, 267 p.

Garotta R. J. and Maréchal P. 1987: Shear wave polarization survey using converted waves. Expanded Abstracts of 59th SEG Mtg., New Orleans, pp. 657–658

Velocity and attenuation

Bourbié T., Coussy O. and Zinszner B. 1986: Acoustique des milieux poreux. Ed. Technip, Paris, 339 p. (see Ch. 2, 5, 7)

Domenico S. N. 1984: Rock lithology and porosity determination from shear and compressional wave velocity. Geophysics, **49**, 8, pp. 1188–1195

Garotta R. 1983: Le rôle des ondes transverses en exploration sismique. Proc. Eleventh World Petroleum Congress, London, vol. 2, pp. 207–214

Gregory A. R. 1976: Fluid saturation effects on dynamic elastic properties of sedimentary rocks. Geophysics, **41**, 5, pp. 895–921

Mcdonal F. J., Angona F. A., Mills R. L., Sengbush R. L., van Nostrand R. G. and White J. E. 1981: Attenuation of shear waves in Pierre shale, *in* Seismic Wave Attenuation, Soc. of Exploration Geophysicists, Tulsa, pp. 252–270

Tatham R. H. 1982: V_P/V_S and lithology, Geophysics, **47**, 3, pp. 336–344

Tatham R. H. and Stoffa P. L. 1976: V_P/V_S – A potential hydrocarbon indicator. Geophysics, **41**, 5, pp. 837–849

Static corrections

MARI J. L. 1984: Estimation of static corrections for shear wave profiling using the dispersion properties of Love waves. Geophysics, **49,** 8, pp. 1169–1179

WIEST B. and EDELMANN H. A. K. 1984: Static corrections for shear wave sections. Geophysical Prospecting, **32,** 6, pp. 1091–1102

S-wave sources

CHERRY J. T. and WATERS K. H. 1968: Shear wave recording using continuous signal methods. I Early development. Geophysics, **33,** 2, pp. 229–239

EDELMANN H. A. K. and SCHMOLL J. 1983: Seismische Messungen mit horizontal polarisierten Scherwellen. Erdöl Erdgas Zeitschrift, **99,** 1, pp. 23–32

ERICKSON E. L., MILLER D. E. and WATERS K. H. 1968: Shear waves recording using continuous signal methods, II Later experimentation. Geophysics, **33,** 2, pp. 240–254

FERTIG J. 1984: Shear waves by an explosive point-source: the earth surface as a generator of converted *P–S* waves. Geophysical Prospecting, **32,** 1, pp. 1–17

KÄHLER S. and MEISSNER R. 1983: Radiation and receiver pattern of shear and compressional waves as a function of Poisson's ratio. Geophysical Prospecting, **31,** 3, pp. 421–435

MEISSNER R. 1965. *P-* and *SV*-waves from uphole shooting. Geophysical Prospecting, **13,** 3, pp. 433–459

WHITE J. E. and SENGBUSH R. L. 1963: Shear waves from explosive sources. Geophysics **28,** 6, pp 1001–1019

Case histories

AUDET J., DELVAUX J. and GAROTTA R. 1981: Exemples d'utilisation d'études combinées ondes *P*-ondes *S* en exploration pétrolière. Pétrole et Techniques, **283,** pp. 128–143

DOHR G. and JANLE H. 1980: Improvements in the observation of shear waves. Geophysical Prospecting, **28,** 2, pp. 208–220

ENSLEY R. A. 1985: Evaluation of direct hydrocarbon indicators through comparison of compressional- and shear-wave seismic data: a case study of the Myrnam gas field. Alberta. Geophysics, **50,** 1, pp. 37–48

MCCORMACK M. D., DUNBAR J. A., and SHARP W. W. 1984: A case study of stratigraphic interpretation using shear and compressional seismic data. Geophysics, **49,** 5, pp. 509–520

POLŠKOV M. K., BRODOV L. JU., MIRONOVA L. V., MICHON D., GAROTTA R., LAYOTTE P. C. and COPPENS F. 1980: Utilisation combinée des ondes longitudinales et transversales en sismique réflexion, Geophysical Prospecting, **28,** 2, pp. 185–207

ROBERTSON J. D. 1987: Carbonate porosity from S/P traveltime ratios. Geophysics, **52,** 10, pp. 1346–1354

STÜMPEL H., KÄHLER S., MEISSNER R. and MILKEREIT B., 1984: The use of seismic shear waves and compressional waves for lithological problems of shallow sediments. Geophysical Prospecting, **32,** 4, pp. 662–675

ANISOTROPY

Elastic waves in anisotropic media. Tensors

AULD B. A. 1973: Acoustic fields and waves in solids. Vol. 2., J. Wiley, New York, London, 423 and 414 p. (See Ch. 1, 2, 3, 7, 9)

DIEULESAINT E. and ROYER D. 1974: Ondes élastiques dans les solides. Masson, Paris, 407 p. (see Ch. 1, 3, 5)

JEFFREYS H. 1961: Cartesian tensors. Cambridge University Press, 93 p. (see Ch. 1, 8)

Stratified media

BACKUS, G. E. 1962: Long-wave elastic anisotropy produced by horizontal layering. J. Geophys. Research, **67**, 11, pp. 4427–4440

BRODOV L. Y., EVSTIFEYEV V. I., KARUS E. V. and KULICHIKHINA T. N. 1984: Some results of the experimental study of seismic anisotropy of sedimentary rocks using different types of waves. Geophys. J. R. astr. Soc., **76**, 1, pp. 191–200

CRAMPIN S. 1977: A review of the effects of anisotropic layering on the propagation of seismic waves. Geophys. J. R. astr. Soc., **49**, 1, pp. 9–27

CRAMPIN S. 1986: Anisotropy and transverse isotropy. Geophysical Prospecting, **34**, 1, pp. 94–99

HAKE H., HELBIG K. and MESDAG C. S. 1984: Three-term Taylor series for t^2–x^2 curves of *P*- and *S*-waves over layered transversely isotropic ground. Geophysical Prospecting, **32**, 5, pp. 828–850

HELBIG K. 1981: Systematic classification of layer-induced transverse isotropy. Geophysical Prospecting, **29**, 4, pp. 550–577

HELBIG K. 1983: Elliptical anisotropy — Its significance and meaning. Geophysics, **48**, 7, pp. 825–832

LEVIN F. K. 1979: Seismic velocities in transversely isotropic media. Geophysics, **44**, 5, pp. 918–936

LEVIN F. K. 1980: Seismic velocities in transversely isotropic media II. Geophysics, **45**, 1, pp. 3–17

POSTMA G. W. 1955: Wave propagation in a stratified medium. Geophysics, **20**, 4, pp. 780–806

WHITE J. E., MARTINEAU-NICOLETIS L. and MONASH C. 1983: Measured anisotropy in Pierre shale. Geophysical Prospecting, **31**, 5, pp. 709–725

WINTERSTEIN D. F. 1986: Anisotropy effects in *P*-wave and *SH*-wave stacking velocities contain information on lithology. Geophysics, **51**, 3, pp. 661–672

Cracked solids. Azimuthal anisotropy

ALFORD R. M. 1986: Shear data in the presence of azimuthal anisotropy: Dilley, Texas. Expanded Abstracts, 56th SEG Mtg., Houston, pp. 476–479

CRAMPIN S. 1981: A review of wave motion in anisotropic and cracked elastic media. Wave Motion, **3**, pp. 343–391

CRAMPIN S., BUSH I., NAVILLE C. and TAYLOR D. 1986: Estimating the internal structure of reservoirs with shear wave VSPs. The Leading Edge, **5**, 11, pp. 35–39

CRAMPIN S., MCGONIGLE R. and BAMFORD D. 1980: Estimating crack parameters from observations of *P*-wave velocity anisotropy. Geophysics, **45**, 3, pp. 345–360

LYNN H. B. and THOMSEN L. A. 1986: Reflection shear wave data along the principal axes of azimuthal anisotropy. Expanded Abstracts of 56th SEG Mtg., Houson, pp. 473–476

GLOSSARY

Aeolotropic *(See Anisotropic)*
This term is used by some British authors.

Anelastic (Non elastic).
In anelastic media, stress is related both to strain and to time derivatives of strain or to strain history (this includes non-elastic effects such as viscoelasticity or plasticity). Energy is spent whenever the stress field is altered. Removal of the stresses does not bring a deformed body back to its initial state. Because of differential attenuation, propagation through an anelastic wedge produces inhomogeneous waves.

Anisotropic
A medium is anisotropic for a given property when the magnitude of a quantity characteristic of this property depends on the direction in which it is measured. We are concerned here with anisotropy of the elastic behaviour which results in anisotropy of wave propagation velocity and of wave attenuation. In isotropic media, all directions are equivalent as far as the relations between

stress and strain components are concerned. The elastic moduli and elastic coefficients of isotropic materials are thus independent of direction. Two of them are enough for describing the elastic behaviour of matter. In anisotropic media, on the contrary, the deformations depend not only on the value of the stress components but also on their orientation with respect to some characteristic directions in the media. Well-known to physicists are the anisotropy and the symmetries of crystals. Geophysicists are confronted with natural media and these have measurable anisotropy with regard to the properties of elastic waves. Particular media are known to exist in which the elastic properties depend only on the angle between a given direction and the direction along which the observation is made. In a plane perpendicular to this symmetry direction, the material behaves as isotropic. This case is described as one of transverse isotropy. A prominent feature of anisotropic media is that they generally allow propagation of only three polarized waves per direction. One of these waves is quasi-longitudinal, the two others are quasi-transverse. Exceptions occur along symmetry axes.

Birefringence

Property of a medium, the anisotropy of which creates two transmitted transverse waves out of one incident one. Birefringence is a well-known optical property of some crystals, of calcite for instance: when reading a text through a slab of this mineral, twin images are observed. In seismology, the phenomenon occurs also. It produces *S*-wave splitting. One incident *S*-wave penetrating into an anisotropic medium is separated into two quasi-transverse waves that travel in that medium, usually along different polarizations, with different velocities and different polarizations.

Conversion

The term refers to the classical situation in which a wave impinging on an interface between two elastic (or anelastic) media generates waves that exhibit a mode of vibration different from that of the incident wave. Assuming the incident waves to be *S* or *P*, waves of the same type (*S* or *P*) and converted waves of the other type (*P* or *S*) are reflected and are transmitted. The situation differs from that of birefringence, where two quasi-*S* waves are generated out of one *S*, or quasi-*S* wave.

Elastic

An elastic medium is one which, after being submitted to a stress field, goes back to its initial state as soon as the forces are removed. The stress at each point and at each instant depends only on the strain at this point and at this time. The medium has no memory. No energy is dissipated when the stress varies. All the energy stored in a strained volume is returned to the external environment as soon as the stress field is cut off. In contrast, anelastic media, when strained, transform some of the available elastic energy into heat. As this energy is lost for propagation, the waves are attenuated in excess of the amount due to geometrical spreading and to the effect of boundaries.

Elastic coefficients

Quantities appearing in the stress-strain relation which expresses Hooke's law in its generalized form. For small deformations of an elastic medium, the strain tensor is related to the stress tensor by a linear equation. The 4×4 tensor which, acting on the stress tensor, gives the strain tensor has as its 81 elements the elastic coefficients of the material, of which at most 21 are independent. The dimension of these coefficients is one of stress. They are therefore expressed in gigapascals (GPa). Elastic coefficients should not be mistaken for elastic moduli, the latter being quantities that can directly be obtained as the result of a simple physical experiment (one gets Young's modulus by stretching a specimen, the rigidity when exerting shearing efforts on it, and the compressibility when submitting it to a pressure). Moduli and coefficients are related by linear equations.

Energy velocity

The velocity with which wave energy flows. In isotropic media, energy and phase of body waves propagate with the same velocity. In anisotropic materials, energy usually travels in a direction different from that of phase, and with a different velocity. Energy velocity is sometimes

called group velocity. The idea of group velocity has to do with the propagation of a signal that undergoes dispersion, for instance in a wave guide. If the spectrum is narrow, the signal will look like a wave packet and the group velocity is that of the envelope. Since the velocity of energy transport in anisotropic elastic and boundless media in no way depends on frequency, the concept of wave groups is misleading and the term "energy velocity" should be preferred.

Heterogeneous medium

A medium that is not homogeneous because its properties vary from point to point. It may be isotropic or anisotropic. The heterogeneous nature of a medium is related to wavelength. Commonly, the scale of the heterogeneities is small or comparable to wavelength. If this is not the case, each heterogeneity is individualized by the wave as a particular homogeneous medium.

Homogeneous medium

A medium that exhibits constant properties throughout. It may be isotropic or anisotropic. Clearly, media that would be homogeneous at all frequencies are abstractions suitable for the establishment of theory, but impossible to find in Nature.

Homogeneous wave

A wave, the amplitude of which is constant on a given surface with constant phase. Of course, the amplitude may vary when the wave propagates. Different amplitudes correspond to successive wave surfaces, but the wave amplitude is constant on each of the surfaces (consider spherical waves for instance). Just like plane waves, homogeneous waves virtually cannot be observed in the real world, but they are a handy tool for first-approximation reasoning.

Hooke's law

Hooke's law, in its conventional form, describes the behaviour of elastic media. It states that each component of the stress tensor is a linear combination of the components of the strain tensor. Using tensor calculus, the law is written $\sigma_{ij} = c_{ijkl}\varepsilon_{kl}$, where σ_{ij} and ε_{kl} are respectively the stress and strain tensors, and c_{ijkl} is the elasticity tensor. The c's are elastic coefficients with dimensions of pressure. As the stress and strain tensors are second rank, they have $3^2 = 9$ components. The elasticity tensor is a fourth rank tensor and has $3^3 = 81$ components. In the most general case, 21 of these components are independent. If the medium is endowed with symmetry properties, the number of independent components is reduced. A medium that would have the symmetry of monoclinic crystals would have 13 independent elastic coefficients, one with that of the orthorhombic system 9, and one with that of the hexagonal system 5. An isotropic medium has its elastic behaviour fully described when two elastic coefficients are specified. Hooke's law undergoes a generalization when linear viscoelastic media are considered. The linear combination of strain tensor components is replaced by a convolution of time functions describing the impulse reponse of the medium with time functions describing the strain. Performing a Fourier transform on the viscoelastic equation, one obtains for each frequency a linear relation between the tensors of the Fourier components of stress and of strain. This relation has the same form as Hooke's law for elastic media, but the elastic coefficients are then complex quantities.

Inhomogeneous wave

A wave, the amplitude of which is not constant along a surface with equal phase. Besides surfaces with constant phase, surfaces with constant amplitude can therefore be defined that travel along with the disturbance.

Isotropic

An isotropic medium for a given property is one in which all directions are equivalent for this property. It may be homogeneous or heterogeneous (inhomogeneous). Natural media are hardly ever isotropic, with the exception of water layers.

Longitudinal wave

A body wave in which the particle motion at a given point is directed perpendicularly to the wave surface at that point.

***P*-wave**

A body wave, the particle motion of which derives from a scalar potential. The curl of the particle motion vector is therefore zero at all points and at all instants. Physically, this means that the wave only produces a volume change. This is why *P*-waves are also called irrotational or dilatational. A homogeneous *P*-wave has its particle motion perpendicular to the wave surface: it is rectilinear and longitudinal. For this reason, all *P*-waves are — sometimes incorrectly — called longitudinal waves.

Phase velocity

The velocity with which a given feature of a signal travels. This definition assumes some degree of stability of the wavelet shape during its propagation. If the signal is quasi-sinusoidal, one usually picks a peak or a trough. If the spectrum is wide, more distinctive features such as kinks or secondary peaks may be used. In anisotropic media, energy and phase generally do not travel with the same velocity and in the same direction, but they are frequency-independent. In wave guides, phase and group velocities are usually different and they vary with frequency.

Poisson's ratio

The ratio of the relative increase in diameter of a cylindrical sample to the relative shortening that results from application of a compressive axial stress. This ratio is therefore a dimensionless quantity. Strictly speaking, it can be defined only for samples of material. However, knowing V_P and V_S of a layer, one can compute the Poisson's ratio of *in situ* rocks.

The range of variation of Poisson's ratio extends from – 0.2 to 0.5. Negative values may correspond to samples of anisotropic material. Low values are indicative of rather loose material, such as those found in LVL's. The upper limit, 0.5, corresponds to liquids.

Polarization

Quality of a wave, the particle motion of which is constrained to take place in a given plane, or on a given curve. If the curve is a straight line, the wave is said to be linearly polarized. If it is an ellipse or a circle, it is elliptically or circularly polarized. When the motion occurs in a direction perpendicular to the wave surface, it is said to be longitudinal. If the particle trajectory is located in the plane tangent to the wave surface, the polarization is transverse. In anisotropic media, waves are generally polarized either quasi-longitudinally or quasi-transversally.

Ray

The trajectory of energy transported by a wave. In isotropic media, rays are orthogonal to the wave surfaces. In anisotropic media, they usually are not. Rays cannot be defined when considering certain phenomena, such as diffraction, conical waves, diffusion. Their use ought to be restricted to propagation in non-diffusing material and to reflection on and refraction by smooth interfaces (smooth means that the radius of curvature of interface irregularities is much larger than the wavelengths of interest).

***S*-wave**

A wave, the particle motion of which is the curl of a vector potential. For this reason, *S*-waves are also called rotational waves. The divergence of the particle motion vector is therefore zero at all points and at all instants. Physically, this means that the medium locally experiences shape modifications without any volume change. Therefore, *S*-waves are also called equivoluminal or distortional. A homogeneous *S*-wave travelling in an isotropic medium has its particle motion contained in a plane tangent to the wave surface. It is transverse and this is the reason why all *S*-waves are — sometimes incorrectly — called transverse waves. When referred to the surface of the ground, a transverse wave is called *SH* when its particle motion is rectilinear and horizontal, *SV* when it is rectilinear and contained in a vertical plane. As a generalization, when an *S*-wave

arrives at the interface between two media, it is often called *SH* if particle motion is perpendicular to the plane defined by the incident ray and the normal to the interface, and *SV* when contained in that plane.

Shear- or rigidity modulus

The ratio of shearing stress to angular shearing strain. Shear modulus μ is one of the two Lamé's constants that define the behaviour of an isotropic elastic solid. It is equal to ϱV_S^2, where ϱ is density and V_S is shear wave velocity. In an elastic fluid, such as water (neglecting its viscosity), no shearing stress can exist, $\mu = 0$ and no *S*-waves can propagate.

Shear strain

A state of deformation in which, at least locally, parallel planes in the material are shifted along themselves, with their distance remaining constant. The deformation is equivoluminal.

Shear wave splitting *(see Birefringence)*

The phenomenon by which a single *S*-wave, upon entering an anisotropic medium, generates two quasi *S*-waves that usually travel with different velocities.

Symmetry

The symmetry characteristics of a medium are an expression of the fact that, at a given point, its properties are not altered when one performs certain symmetry transformations. For instance, if a stack of thin beds with plane parallel interfaces is rotated by any angle around an axis perpendicular to the bedding, the elastic properties referred to a given fixed coordinate system remain invariant. Conversely, if the medium is given and the coordinate system is rotated around the same axis, the tensor of the elastic coefficients must remain unchanged. The number of independent coefficients is reduced by these symmetry properties below that number (21) which is determined by general elastic and thermodynamic considerations. The maximum reduction is that which corresponds to isotropy. All directions are equivalent in an isotropic solid and there are only two independent elastic coefficients. Neumann's principle states that the whole elastic behaviour of an anisotropic medium must have the same symmetries. At any given point, the sets of directions that have symmetry characteristics identical to those of the material are equivalent as far as wave propagation is concerned. The velocities of waves travelling along such equivalent directions are equal. Particle motion polarization exhibits the same symmetry properties. It follows that the polarization of waves propagating along a symmetry axis or along a direction lying in a symmetry plane is easily determined. The directions of symmetry axes and planes therefore constitute the natural frame of reference that has to be taken into account when studying an anisotropic medium.

Tomography

A process by which waves are sent to travel in various directions through a body to be investigated, and the properties of the material are estimated from cumulative effects observed on the waves that propagated through it. X-ray absorption tomogrphy is extensively used in medical exploration. Seismic tomography and ocean acoustical tomography make use of elastic waves in order to estimate material properties in a number of elementary volumes inside the illuminated region. Some methods use time or amplitude information only, others time and amplitude.

Transversely isotropic medium

A medium, the anisotropy of which depends only on the angle of the observation direction with a given direction characteristic of the material. Perpendicularly to this given direction, properties are orientation-independent. This is why the material may be described as transversely isotropic. Examples are geological series composed of stacks of parallel layers that are thin with respect to wavelength, or rocks with thin parallel liquid inclusions.

Transverse wave

A wave that causes particles to move in planes tangent to surface waves.

Viscoelastic (linear)

A linear viscoelastic medium is one in which strain has a linear dependence on stress and on its time derivatives and integrals. Strain and stress components are related by means of convolution equations. The four-by-four tensor of the elastic coefficients is replaced by a four-by-four matrix of time functions. When Fourier-transformed, the equation again takes the general form of a conventional Hooke's law. The elasticity tensor is then made up of Fourier components of the time functions. As these coefficients are complex, complex quantities are substituted for the usual elastic coefficients. As a result, wave velocities are also complex. This corresponds to physical observation. The various frequency components of the wave function are attenuated and phase-shifted by different amounts because of partial conversion of energy into heat. Pulses will change shape, even when travelling as plane waves.

Wave surface

A surface with constant phase. This is a surface on which the phase of harmonic components of the wave function is constant. At any point the phase-velocity vector is normal to the wave surface.

Wavefront

A surface which separates two regions of space, one of which is still undisturbed, the other one already being subjected to wave agitation. It may also be called a surface of kinematic discontinuity, as particle motion acceleration is discontinuous when crossing a wavefront.

Wavelength

The wavelength of a sinusoidal wave is the distance between two wave surfaces on which the displacements have a phase difference of 2π (or a time lag of one period).

S-HULLÁMOK ÉS A SZEIZMIKUS ANIZOTRÓPIA

Gérard GRAU

Ha a *P*-hullám felvételek gyengék, *S*-hullámokat használva esetleg jobb szelvényeket készíthetünk. Sokszor az *S*-hullám szelvények előnyösen kiegészítik a *P*-hullám méréseket, ha a litológia meghatározása a cél, vagy ha a fényes foltok okát akarjuk ellenőrizni. Az *S*-hullámok — a változatos polarizációs hatások miatt — több információt tudnak nyújtani az egyes földtani képződményekről, mintha kizárólag *P*-hullámokat észlelünk. A polarizációs hatások gondos vizsgálatával felfedezhető a kőzetek repedezettsége, amely az olajipari mérnökök számára igen lényeges információ. A cikk bevezető a transzverzális hullámok és az üledékes kőzetek anizotrópiájának in-situ tanulmányozásáról, értelmezéséről és a szénhidrogén kutatásban való alkalmazásáról tartott tanfolyam anyagához. Célja, hogy összefoglalja a főbb fizikai elveket, a jelenlegi szeizmikus gyakorlatot és a tervezett kutatási irányokat.

ПОПЕРЕЧНЫЕ ВОЛНЫ И СЕЙСМИЧЕСКАЯ АНИЗОТРОПИЯ

Жерар ГРО

Если записи продольных волн слишком слабы, может быть, удастся получить разрезы более высокого качества с использованием поперечных волн. Разрезы по поперечным волнам зачастую удачно дополняют измерения продольных волн, если задача заключается в определении литологических особенностей горных пород или же в выяснении причин появления светлых пятен. По определенным геологическим образованиям — в связи с разнообразными поляризационными эффектами — поперечными волнами часто обеспечивается больше информации, нежели при регистрации одних лишь продольных волн. При скрупулезном изучении поляризационных эффектов можно выявить трещиноватость горных пород, что представляет собой весьма важную информацию для инженеров-промысловиков. Настоящая статья представляет собой введение к курсу изучения поперечных волн и анизотропии осадочных пород в массиве, интерпретации и применения в поисках и разведке нефти и газа. Ее задача заключается в обобщении главнейших физических принципов, практики современной сейсморазведки и основные направления исследований.

GEOPHYSICAL TRANSACTIONS 1988
Vol. 34. No. 1. pp. 45—58

POLARIZATION AND ANISOTROPY

Klaus HELBIG*

In anisotropic elastic media there exist for each direction of the wave normal three waves with, in general, different velocities of propagation and mutually perpendicular (spatially fixed) displacement vectors. If two of the velocities coincide the corresponding displacement vectors are constrained to a plane. For moderate anisotropy (e.g. in all known geological media) the fastest of the three waves has a nearly longitudinal displacement, the other two are nearly transverse. In general, the ray, the wave normal and the displacement vector have different directions. The deviation of the (nearly) longitudinal ray and the corresponding displacement vector from the normal are 'similar', i.e. they have the same zeros and the same algebraic sign, thus the angle between displacement and ray is normally small. For the other two waves similar statements do not hold. 'Anisotropy effects' are mostly greater for the nearly transverse waves. In particular, the two nearly transverse waves can travel with different velocity resulting in 'shear-wave splitting'.

If the cause of the anisotropy is known, the magnitude of the anisotropy effects – such as shear-wave splitting – can be interpreted in terms of the strength of the cause, i.e. the volume density of flat aligned cracks. A qualitative interpretation is straightforward, for quantitative interpretation one might have to correct the observed polarization for changes at transmission through intervening interfaces and for deviating raypaths of the two nearly transverse waves.

Keywords: anisotropic materials, birefringence, polarization, S-waves, SH-waves, SV-waves

1. Introduction

The velocity of a plane elastic wave with given direction of the normal can be regarded to be closely related to an eigenvalue of a real-valued, symmetric 3 by 3 matrix, the Christoffel matrix (compare (A1), where the slowness $n = 1/V$ has been used instead of the velocity V). The elements of this matrix are combinations of elastic constants and direction cosines, and the elements on the main diagonal have the structure $(a^2 + b^2 + c^2 - \varrho V^2)$. Such a matrix has, in general, three eigenvalues ϱV^2. There are thus, in each direction, three velocities (and the velocities in opposite directions are identical).

2. Polarization with respect to the wave normal

For any given wave normal n there are three waves (represented by elements of plane waves) travelling with different phase velocities *(Fig. 1)*. The phase velocities are indicated by the projections on the normal. The displace-

* Department of Exploration Geophysics, Institute for Earth Sciences, Rijksuniversiteit Utrecht, 3508 TA Utrecht, The Netherlands
Manuscript received: 5 October, 1987

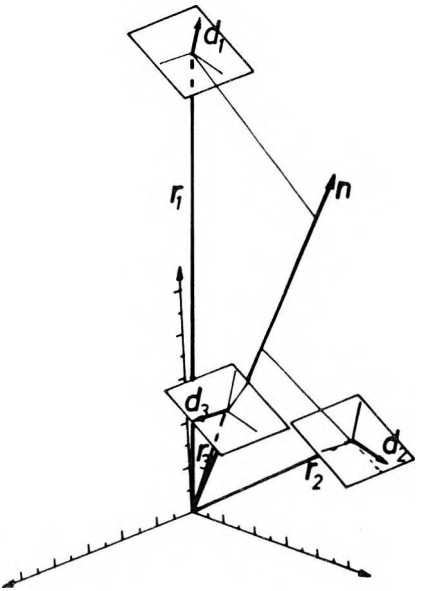

Fig. 1. Phase velocity and displacement vectors in the three-dimensional space
r_1, r_2, r_3 — rays; d_1, d_2, d_3 — displacements

1. ábra. Fázissebességek és elmozdulás-vektorok háromdimenziós térben
r_1, r_2, r_3 — sugarak; d_1, d_2, d_3 — elmozdulások

Рис. 1. Скорости фаз и векторы смещений в трехмерном пространстве:
r_1, r_2, r_3 — лучи; d_1, d_2, d_3 — смещения.

ments d_1, d_2 and d_3 belonging to the three waves are mutually perpendicular, but are not necessarily lined up with either the normal or the ray. The fastest of the three waves generally has nearly longitudinal displacement, the other two nearly transverse displacements.

If in any direction of propagation two of the eigenvalues coincide, the two corresponding eigenvectors no longer have fixed directions. However, they are constrained to the plane that is orthogonal to the third eigenvector, the plane of polarization. Two arbitrary base vectors can be chosen (without loss of generality orthogonal to each other) in this plane to describe any polarization vector *(Fig. 2)*.

In general, none of the three polarization vectors is parallel to the wave normal. Directions where that is the case are called longitudinal directions. Obviously, in a longitudinal direction the two 'other' polarizations are purely transverse since the plane of polarization coincides with the plane of equal phase.

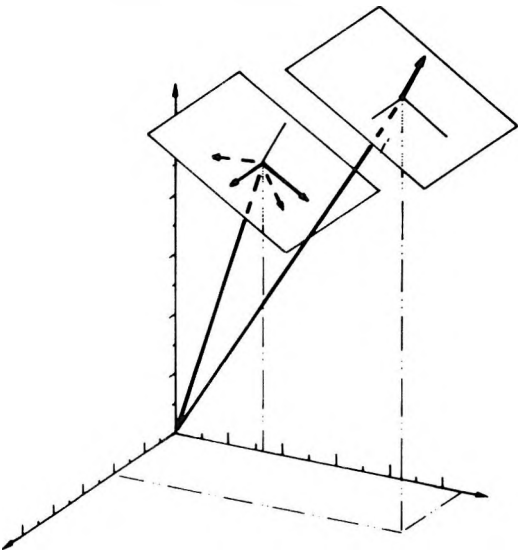

Fig. 2. Two pairs of mutually perpendicular vectors. Note that the plane surface elements are the 'planes of polarization' (and not elements of the wave plane as in Fig. 1)

2. ábra. Két pár kölcsönösen merőleges vektor. A sík felületi elemek a „polarizációs síkok" (és nem a hullámsík elemei, mint az 1. ábrán)

Рис. 2. Две пары взаимно-перпендикулярных векторов. Плоские участки поверхности являются «плоскостями поляризации» (в отличие от участков волновой плоскости, как на рис. 1).

3. Polarization with respect to the ray

In general, the direction of the ray — the direction of energy transport — deviates from the direction of the wave normal (compare Fig. 1). At least in the cases that interest us — moderate anisotropy of not too complicated a type — the (nearly) longitudinal ray deviates from the direction of the wave normal in the same direction as the (nearly) longitudinal displacement, and for directions deviating not too much from directions of symmetry one of the (nearly) transverse rays often deviates in the opposite direction (for a proof of this statement see the Appendix). Thus at least under the stated conditions the maximum observable polarization anomaly (i.e. the largest deviation of the displacement vector from the nominal displacement direction parallel or orthogonal to the ray) is larger for one of the (nearly) transverse waves than for the (nearly) longitudinal wave (see, e.g. *Fig. 3*). This agrees with the qualitative statement that the propagation of (nearly) transverse waves is, in general, more strongly affected by anisotropy than the propagation of (nearly) longitudinal waves. For other conditions — strong anisotropy of a simple type and more

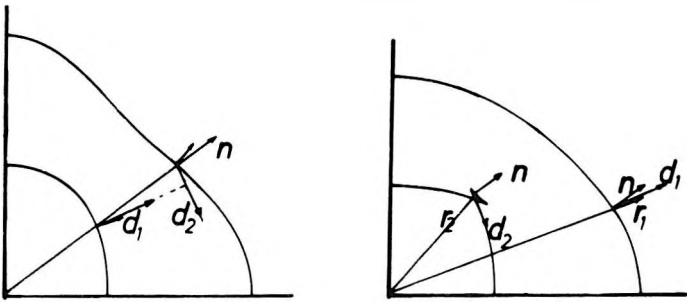

Fig. 3. Intersection of the slowness surface (left) and the wave surface (right) of a transversely isotropic medium with a coordinate plane for the quasi *P* and quasi *S* sheets. d_1 and d_2 — displacement vectors corresponding to a common normal. For the *qP* sheet displacement *d* and ray *r* lie to the same side of the wave normal *n*. For the *qS* sheet the deviations are in opposite directions

3. ábra. Transzverzálisan izotrop közeg lassúsági felületének (baloldalt) és hullám felületének (jobboldalt) metszése a koordinátasíkkal, kvázi *P* és kvázi *S* polarizációs síkot feltételezve. d_1 és d_2 egy közös normálishoz tartozó elmozdulásvektorok. A *qP* sík esetén a *d* elmozdulás és *r* sugár az *n* hullámnormális azonos oldalán fekszik, a *qS* sík esetén az eltérések ellentétes irányban vannak

Рис. 3. Пересечение поверхности медлительности попересно изотропной среды (слева) и поверхности волны (справа) с координатной плоскостью в предположении, что поляризационными плоскостями являются квази-продольные и кавзи-поперечные волны. d_1 и d_2 — векторы смещения, соответствующие одной и той же общей нормали. При плоскости *qP* смещение *d* и луч *r* лежит на одной и той же стороне нормали *n* к волне, а при плоскости *qS* расхождения наблюдаются в обе стороны.

complicated types of anisotropy — the above statements either have to be modified or have not been checked.

Since the deviations of the longitudinal displacement vector and the ray from the wave normal have the same sign, it follows that in longitudinal directions, the directions of the longitudinal ray and the wave normal coincide. A similar statement for trasverse waves does not hold: there are directions where the (quasi-)transverse ray has the direction of the wave normal, but the corresponding displacement is, in general, not purely transverse (see the Appendix and *Fig. 4*).

4. Polarization of shear waves in isotropic media

In isotropic media all directions are longitudinal directions, and in all directions the smaller two of the three eigenvalues coincide. In isotropic elastic media one thus always has a longitudinal wave and one transverse wave of arbitrary direction of polarization. As said before, two arbitrary base vectors for the transverse displacement may be chosen. However, that is completely true only under homogeneous conditions: at any interface (and also at the free surface) all stresses must be continuous. It is thus advisable to choose one of

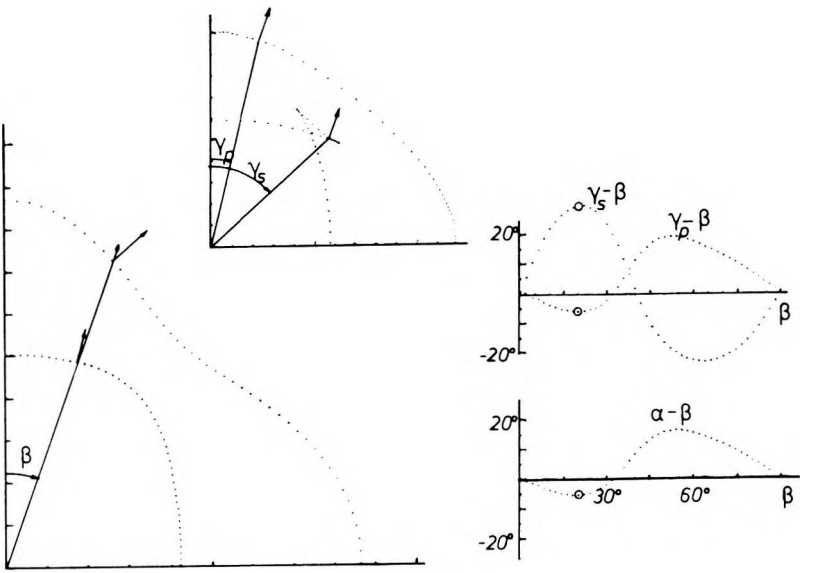

Fig. 4. Left: slowness and wave surface. Top right: deviation of *qP*- and *qS*-ray from the normal, bottom: deviation of the displacement vectors from the nominal direction (the normal). Note the similarity of the deviation of the *qP* ray with the deviation of the displacements [after HELBIG 1966]

4. ábra. Bal oldal: lassúság- és hullámfelület. Jobb oldalt fent: a *qP* és *qS* sugarak eltérése a normálistól, lent: az elmozdulásvektorok eltérése a névleges iránytól (a normálistól). Figyelemre méltó a *qP* sugár és az elmozdulások eltérésének hasonlósága [HELBIG 1966]

Рис. 4. Слева: медлительность и поверхность волны; справа вверху: отклонение лучей *qP* и *qS* от нормали, внизу: отклонение векторов смещений от номинального направления (от нормали). Заслуживает внимания подобие луча *qP* и разницы смещений [по HELBIG 1966].

the base vectors parallel to the line of intersection of the plane of polarization and the interface *(Fig. 5)*. The corresponding transverse displacement then lies in the interface, and the continuity of stresses is particularly simple since only shear tractions in the chosen direction are acting.

If the displacements are referred to a horizontal interface (e.g. the free surface), the corresponding wave type is called the *SH*-wave (i.e. the horizontally polarized shear wave). The main advantage of this choice of base vector is that an incident *SH*-wave generates only secondary (reflected and transmitted) waves of the same type. The polarization vector of the 'other' shear wave (the second base vector) lies in a vertical plane containing the ray and the wave normal. The corresponding wave is called the *SV*-wave (i.e. the shear wave with the polarization vector in the vertical plane). At the interface (or the free surface) normal and tangential displacements and tractions occur, and the continuity can be satisfied only with secondary waves of *SV*- and *P*-type.

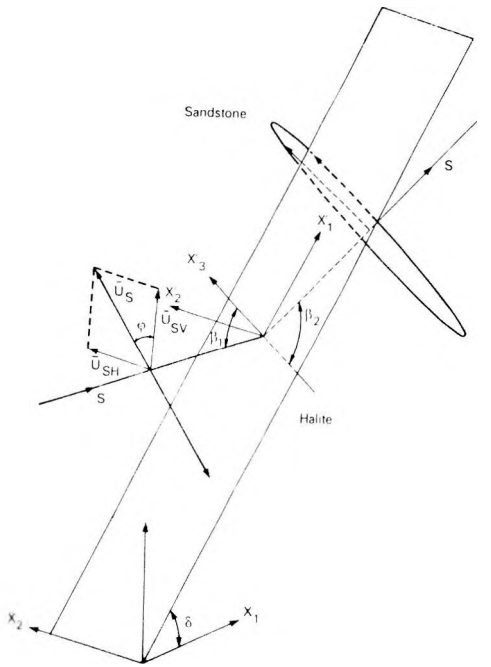

Fig. 5. Choice of a local coordinate system (x'_1, x'_2, x'_3) at an interface. It has been assumed that the angle of incidence is so large that two reflected compressional waves can be generated. This leads to a phase shift of the transmitted *SV*-component and thus to elliptical polarization [from Douma and Helbig 1987]

5. ábra. Helyi koordinátarendszer (x'_1, x'_2, x'_3) kiválasztása egy határfelületen. Feltételezzük, hogy a beesési szög olyan nagy, hogy két reflektált kompressziós hullám generálható. Ez az áthaladó *SV*-komponens fázistolásához, és így elliptikus polarizációhoz vezet [Helbig és Douma 1987]

Рис. 5. Выбор местной системы координат (x'_1, x'_2, x'_3) на поверхности раздела. Предполагается, что угол вхождения настолько велик, что возникают две преломленные волны сжатия. Это приводит к смещению по фазе проходящей компоненты *SV* и, таким образом, к эллиптической поляризации [Helbig–Douma 1987].

At an arbitrarily dipping interface one should correctly speak of *ST*- and *SN*-waves (with tangential and normal displacements, respectively). However, that is rarely done: one continues to call the waves corresponding to the two base vectors *SH*- and *SV*-waves (with respect to the interface).

The differences in the continuity conditions for *SH*- and *SV*-waves result in different transmission and reflection coefficients. Thus the angle between the displacement vector of an arbitrarily polarized shear wave (i.e. neither pure *SH* nor pure *SV* polarization) and the vertical plane changes at each interface (Fig. 5). Generally, the change at a single interface is small, but after transmission through several interfaces of different attitude the changes might accu-

mulate [DOUMA and HELBIG 1987]. An important consequence of the equality of the two smaller eigenvalues in isotropic media is that kinematically the two shear waves are identical. In particular, the two signals travel along precisely the same path, and one can thus speak of one signal with its direction of polarization.

5. Polarization in anisotropic media

Let us now consider the wave propagation through a set of anisotropic media separated by interfaces of arbitrary attitude. In a medium of not too complicated anisotropy (i.e. for hexagonal symmetry) one can still speak of *SH*- and *SV*-waves. However, one now has to be careful whether this is done with respect to the free surface or with respect to the inherent coordinate system of the anisotropic medium. The problem is simple only if the axis of symmetry is vertical. For a horizontal axis the problem becomes complicated, and for an obliquely tilted axis there seems to be no way to reconcile the two points of view. Then it might be better to distinguish the two (nearly) transverse waves in a different way, e.g. by indices 2 and 3 (depending on the order of the corresponding eigenvalues). This works locally, but globally there would still be some confusion since the order of the eignevalues changes where the slowness surfaces intersect.

The aspects of anisotropy that interest us here are:

a) The base vectors are 'preordained' by the internal structure of the medium;

b) The two (quasi-) shear waves travel with different velocities. Thus there will be a separation of the two signals after sufficient path length (called 'shear-wave splitting');

c) Since the two shear waves are not kinematically indentical, the two ray paths corresponding to the two (quasi-) shear waves are different. In principle, the two rays might even have sampled different parts of the subsurface. For the correct (forward) description of ray paths and arrival times one can make use of the generalization of Snell's law *(Fig. 6)* and the geometrical properties of the slowness surface. The slowness vectors of all waves participating in a reflection/refraction process have their endpoints on a common normal to the interface. The rays have the direction of the normals to the slowness surfaces;

d) Under general conditions — arbitrary type of anisotropy, interfaces with arbitrary attitude — each of the three incident waves can cause three transmitted and three reflected waves. Under such conditions inversion can be extremely difficult, and even the forward modelling of amplitudes becomes a complicated task.

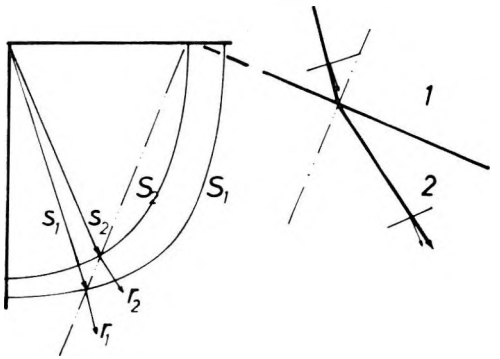

Fig. 6. Snell's law for anisotropic media [after HELBIG 1965]

6. ábra. A Snellius–Descartes törvény anizotrop közegre [HELBIG 1965 nyomán]

Рис. 6. Закон Снеллия–Декарта для анизотропной среды [по HELBIG 1965].

6. Evaluation of shear-wave splitting

Shear-wave splitting can be used to determine the orientation and intensity of the cause of anisotropy, e.g. oriented cracks due to tectonic stress [CRAMPIN 1985a, b]. A qualitative evaluation is straightforward: the azimuthal variation of the magnitude of the split and the orientation of the 'preordained' polarization inside the anisotropic medium indicate the orientation, the magnitude of the split in the maximum direction indicates the cumulative intensity of cracking over that part of the path that lies inside the anisotropic (i.e. cracked) medium.

Quantitative evaluation is another matter. The direction of the polarization observed in a borehole during an offset VSP survey or at the free surface is not necessarily the same as that inside the anisotropic medium but must be corrected for changes at intervening interfaces (including phase shifts if one of the waves has undergone overcritical reflection, see Fig. 5 and DOUMA and HELBIG 1987). At the free surface the superposition of the reflected waves has to be taken into account. Since the raypaths inside the anisotropic medium coincide only under special conditions at entry and exit, the 'magnitude of split' has to be corrected for different path lengths. In extreme cases the two raypaths might have travelled through different parts of the anisotropic medium so the degree of splitting is not diagnostic for the difference in shear velocities of different polarization at any particular location. Such corrections can be complicated for structurally complex situations.

The cautionary remarks at the end are not meant to downgrade the ideas put forward in the workshop, but to underline the exciting challenge we are facing.

Acknowledgement

I thank Michael Schoenberg of the Schlumberger Doll Laboratory in Ridgefield for many fruitful discussions and for his share in the determination of the orthorhombic slowness surface in Fig. A1.

APPENDIX

Displacements and rays in the planes of symmetry of orthorhombic media

The system of equations governing the propagation of plane waves in an orthorhombic medium is

$$\begin{bmatrix} c_{11}n_1^2 + c_{66}n_2^2 + c_{55}n_3^2 - 1 & A_{12}n_1n_2 & A_{13}n_1n_3 \\ A_{12}n_1n_2 & c_{66}n_1^2 + c_{22}n_2^2 + c_{44}n_3^2 - 1 & A_{23}n_2n_3 \\ A_{13}n_1n_3 & A_{23}n_2n_3 & c_{55}n_1^2 + c_{44}n_2^2 + c_{33}n_3^2 - 1 \end{bmatrix} \begin{bmatrix} \alpha_1 \\ \alpha_2 \\ \alpha_3 \end{bmatrix} = 0, \quad \text{(A1)}$$

where the c_{IJ} are the elastic constants divided by the density ϱ, the α_I are the direction cosines of the displacement vector, the n_I are the components of the slowness vector (magnitude $1/V$ and direction of the wave normal), $Q = 9-I-J$, $P = 9-I-K$, $M = 9-J-K$, $\{I, J, K\} = \{1, 2, 3\}$, $I \neq J \neq K$, and $A_{IJ} = (c_{IJ} + c_{QQ})$. Since $n_I = n \cos \beta_I$ (where β_i are the direction cosines of the wave normal), the parameters of (A1) are functions of the direction of propagation. An example where the direction is changed over one octant is shown in *Fig. A1*.

In a plane of symmetry the system decouples into two sets. One describes the elliptical curve of intersection of the plane with the slowness sheet corresponding to displacements perpendicular to the plane. For instance, in the *IJ*-plane this elliptical curve of intersection belongs to displacements in the *K*-direction:

$$\begin{bmatrix} c_{II}n_I^2 + c_{QQ}n_J^2 - 1 & A_{IJ}n_In_J & 0 \\ A_{IJ}n_In_J & c_{QQ}n_I^2 + c_{JJ}n_J^2 - 1 & 0 \\ 0 & 0 & c_{PP}n_1^2 + c_{MM}n_J^2 - 1 \end{bmatrix} \begin{bmatrix} \alpha_I \\ \alpha_J \\ \alpha_K \end{bmatrix} = 0 \quad \text{(A1a)}$$

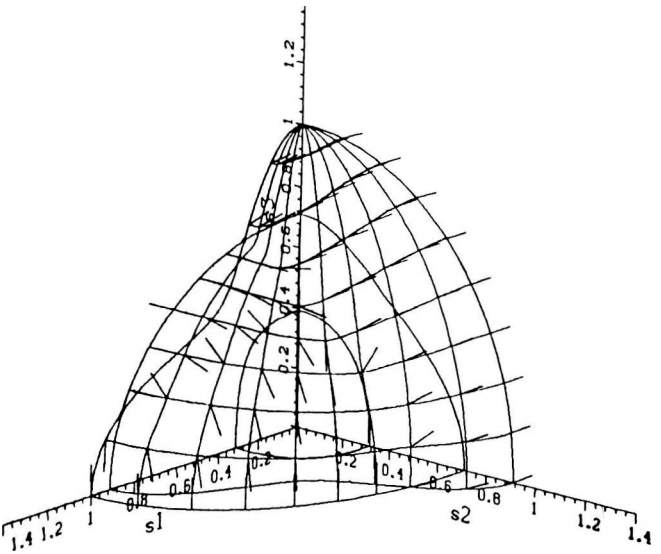

Fig. A1. Slowness surface and displacement vectors for an orthorhombic medium. Note: the outer two (qS) sheets belong to one doubly connected continuous surface
[from unpublished work by SCHOENBERG and HELBIG]

A1. ábra Lassúsági felületek és elmozdulásvektorok ortorombikus közegre. Megjegyezzük, hogy a külső két (qS) felületelem egyetlen kettősen kapcsolódó folytonos felülethez tartozik
[SCHOENBERG és HELBIG nem közreadott munkájából]

Рис. A1. Поверхности медлительности и векторы смещения в орторомбической среде. Примечание: внешние две ячейки поверхности (qS) относятся к одной и той же непрерывной поверхности с двойной связью
[из неопубликованной работы SCHOENBERG–HELBIG].

With $A = A_{IJ}$, $\tan\alpha = \alpha_I/\alpha_J$ and $\tan\beta = n_I/n_J$, one has from the first two equations

$$\tan\beta\tan\alpha = -\frac{An_I^2}{c_{II}n_I^2 + c_{QQ}n_J^2 - 1} = -\frac{c_{QQ}n_I^2 + c_{JJ}n_J^2 - 1}{An_J^2} = w \qquad \text{(A2)}$$

and

$$-\frac{\tan\beta}{\tan\alpha} = \frac{c_{II}n_I^2 + c_{QQ}n_J^2 - 1}{An_J^2} = \frac{An_I^2}{c_{QQ}n_I^2 + c_{JJ}n_J^2 - 1} = w \qquad \text{(A2a)}$$

Since $\tan\left(\alpha + \frac{\pi}{2}\right) = \frac{-1}{\tan\alpha}$, the two equations (A2) and (A2a) are related in the following way: if (A2) refers for a certain w to a (nearly) longitudinal wave, (A2a) for the same w refers to the corresponding (nearly) transverse wave [and vice versa, see HELBIG 1966].

The two equations can be solved for n_I^2 and n_J^2 resulting in

$$\left.\begin{aligned} n_I^2 &= \frac{Cw + Aw^2}{Ac_{JJ} + (Bc_{JJ} + Cc_{II} - E^2)w + Ac_{II}w^2} \\ n_J^2 &= \frac{A + Bw}{Ac_{JJ} + (Bc_{JJ} + Cc_{II} - E^2)w + Ac_{II}w^2} \end{aligned}\right\} \tag{A3}$$

$$\left.\begin{aligned} n_I^2 &= \frac{Cw + Aw^2}{Ac_{QQ} + (Bc_{QQ} + Cc_{QQ} + E^2)w + Ac_{QQ}w^2} \\ n_J^2 &= \frac{A + Bw}{Ac_{QQ} + (Bc_{QQ} + Cc_{QQ} + E^2)w + Ac_{QQ}w^2} \end{aligned}\right\} \tag{A4}$$

$$\tan^2\beta = \frac{Cw + Aw^2}{A + Bw} \qquad \tan^2\alpha = \frac{Aw + Bw^2}{C + Aw} \qquad \tan\beta/\tan\alpha = \frac{A + Bw}{C + Aw} \tag{A5}$$

with $B = c_{II} - c_{QQ}$, $C = c_{JJ} - c_{QQ}$, and $E^2 = BC - A^2$. E^2 has the dimension of a squared (normalized) elastic constant but may be negative.

Equation (A3) refers to (nearly) longitudinal waves and (A4) to (nearly) transverse waves if $0 \leqq w \leqq \infty$. It follows from the last equation (A5) that the assignment is interchanged on replacement of w by

$$\tilde{w} = -\frac{C + Aw}{A + Bw}$$

This replacement is possible iff $E^2 \neq 0$. The exception is treated at the end.

The ray has the direction of the normal to the slowness surface, i.e.

$$\tan\gamma = -\frac{\mathrm{d}n_J/\mathrm{d}w}{\mathrm{d}n_I/\mathrm{d}w} = -\tan\beta\,\frac{\mathrm{d}n_J^2/\mathrm{d}w}{\mathrm{d}n_I^2/\mathrm{d}w},$$

thus

$$\begin{aligned} \frac{\tan\gamma}{\tan\beta} &= \frac{\dfrac{Cc_{QQ} + A^2}{Ac_{JJ}} + 2\dfrac{C_{II}}{c_{JJ}}w + \dfrac{Bc_{II}}{Ac_{JJ}}w^2}{\dfrac{C}{A} + 2w + \dfrac{Bc_{QQ} + A^2}{Ac_{JJ}}} = \\ &= 1 + \frac{1}{Ac_{JJ}}\,\frac{(A^2 - C^2) + 2A(B - C)w + (B^2 - A^2)w^2}{\dfrac{C}{A} + 2w + \dfrac{Bc_{QQ} + A^2}{Ac_{JJ}}} \end{aligned} \tag{A6}$$

With $w_1 = \tilde{w}(-1) = \dfrac{C - A}{B - A}$ and $w_2 = \tilde{w}(1) = -\dfrac{C + A}{B + A}$ one has for (nearly) longitudinal waves for $B \neq A$:

$$\left.\begin{aligned} \frac{\tan\gamma-\tan\beta}{\tan\beta} &= (B^2-A^2)\,\frac{(w-w_1)(w-w_2)}{Cc_{JJ}+2Ac_{JJ}w+Bc_{QQ}w^2} \\ \text{and}\qquad \frac{\tan\alpha-\tan\beta}{\tan\beta} &= (B-A)\,\frac{(w-w_1)}{C+Aw} \end{aligned}\right\} \qquad \text{(A7)}$$

and thus

$$\frac{\tan\gamma-\tan\beta}{\tan\alpha-\tan\beta} = (B+A)\,\frac{(w-w_2)(C+Aw)}{Cc_{JJ}+2Ac_{JJ}w+Bc_{QQ}w^2} \qquad \text{(A8)}$$

and for $B=A$:

$$\frac{\tan\gamma-\tan\beta}{\tan\beta} = \frac{A-C}{2c_{JJ}}\,\frac{w-w_2}{\dfrac{C}{A}+2w+\dfrac{c_{II}}{c_{JJ}}w^2} \quad \text{and} \quad \frac{\tan\alpha-\tan\beta}{\tan\beta} = \frac{A-C}{C+Aw} \qquad \text{(A9)}$$

and thus

$$\frac{\tan\gamma-\tan\beta}{\tan\alpha-\tan\beta} = \frac{C+Aw}{c_{JJ}}\,\frac{w-w_2}{\dfrac{C}{A}+2w+\dfrac{c_{II}}{c_{JJ}}w^2} \qquad \text{(A10)}$$

Provided that $A>0$, all terms in (A8) and (A10) are positive, and thus the displacement vector and the ray of the (nearly) longitudinal wave deviate from the direction of the normal in the same direction. From (A7) one has:

For any direction where the (nearly) longitudinal displacement is strictly longitudinal, the corresponding ray is parallel to the wave normal.

For (nearly) transverse waves the expression corresponding to (A7) is

$$\frac{\tan\gamma_s-\tan\beta}{\tan\beta} = -\frac{E^2}{c_{QQ}}\,\frac{(w-1)(w+1)}{C+2Aw+\left(B+\dfrac{E^2}{c_{QQ}}\right)w^2} \qquad \text{(A11)}$$

The deviation of the displacement vector from the 'nominal' direction is the same as for the (nearly) longitudinal wave given in the second equality in (A7). The deviations of directions of the displacement and (nearly) transverse ray thus vanish at different angles. The only exception occurs for $w_1=1$, i.e. for $B=C$. In this case both deviations vanish for $\beta=\dfrac{\pi}{4}$. For $E^2=BC-A^2=0$ the (nearly) longitudinal wave surface and slowness surface are ellipsoids, while the corresponding surfaces of the (nearly) transverse wave are spheres [RUDZKI 1912]. The direction of the (nearly) transverse ray thus coincides – for all directions – with the wave normal. For the directions of (nearly) longitudinal displacement and ray one has

$$\tan\alpha = \frac{B}{A}\tan\beta \quad \text{and} \quad \tan\gamma = \frac{c_{II}}{c_{JJ}}\tan\beta. \tag{A12}$$

Transversely isotropic media are a special case. If the 3-axis is the rotational axis of symmetry, the standard notation is obtained by the choice $I=1$, $K=2$, $J=3$, $Q=4$, $P=6$ and $M=5$ ($=4$ for reasons of rotational symmetry).

REFERENCES

CRAMPIN S. 1985a: Evaluation of anisotropy by shear wave splitting. Geophysics **50,** 1, pp. 142–152

CRAMPIN S. 1985b: Evidence for aligned cracks in the Earth's crust. First Break **3,** 3, pp. 12–20

DOUMA J. and HELBIG K. 1987: What can the polarization of shear waves tell us? First Break **5,** 3, pp. 95–104

HELBIG K. 1965: Die Indexfläche als Hilfsmittel für strahlengeometrische Konstruktionen bei der Interpretation seismischer Beobachtungen, insbesondere bei anisotropem Untergrund. Bayrische Akademie der Wissenschaften, Mathematisch-Naturwissenschaftliche Klasse, Abhandlungen, Neue Folge, Heft 122, 100 p.

HELBIG K. 1966: A graphical method for the construction of rays and traveltimes in spherically layered media, Part 2: Anisotropic case, theoretical considerations. Bulletin of the Seismological Society of America **56,** pp. 527–559.

RUDZKI M. P. 1912: Parametrische Darstellung der elastischen Welle in anisotropen Medien. Anzeiger der Akademie der Wissenschaften zu Krakau, Jgg. 1911, pp. 503–536

POLARIZÁCIÓ ÉS ANIZOTRÓPIA

Klaus HELBIG

Anizotrop rugalmas közegben a hullámnormális minden irányához három hullám tartozik, általában különböző terjedési sebességgel és kölcsönösen merőleges (térben rögzített) elmozdulásvektorral. Ha a sebességek közül kettő megegyezik, a megfelelő elmozdulásvektorok síkra korlátozódnak. Közepes anizotrópiára (pl. minden földtani közegben) a három hullám közül a leggyorsabbnak közel longitudinális az elmozdulása, a másik kettő pedig közel transzverzális. A sugár, a hullám normálisa és az elmozdulásvektor általában különböző irányú. A közel longitudinális sugár és a megfelelő elmozdulásvektor eltérése a normálistól „hasonló", azaz például nullpontjaik és algebrai előjelük azonos, így az elmozdulás és a sugár közötti szög általában kicsi. A másik két hullámra hasonló megállapítások nem érvényesek. Az anizotrópia általában erősebben hat a közel transzverzális hullámokra. Különösen a két közel transzverzális hullám terjedési sebessége tér el, ami „nyíróhullám hasadást" (kettős törést) eredményez.

Ha az anizotrópia oka ismert, akkor az anizotrópia hatások – mint pl. a nyíróhullám hasadás – nagysága a kiváltó ok nagyságával korrelálható (pl. irányított repedések térfogatsűrűsége). A minőségi értelmezés egyértelmű, a mennyiségi értelmezés még bizonytalan, a hullámterjedés során határfelületeken való áthaladáskor polarizáció változás léphet fel. Ezt, továbbá a két közel transzverzális hullám sugárútjainak elhajlását korrekcióba kell venni.

ПОЛЯРИЗАЦИЯ И АНИЗОТРОПИЯ

Клаус ГЕЛЬБИГ

В анизотропной упругой среде всем направлениям нормалей к волнам соответствуют три волны, в общем случае с различными скоростями распространения и со взаимно-перпендикулярными (закрепленными в пространстве) векторами смещений. Если из скоростей две совпадут, то соответствующие вектора смещений будут находиться в плоскости. При анизотропии средней величины (например, во всех геологических средах) из трех волн смещение наиболее быстрой — почти продольное, а двух других — поперечное. Луч, нормаль к волне и вектор смещения обычно направлены по-разному. Отклонение примерно продольного луча от соответствующего вектора смещения — «подобное», то-есть, например, их нулевые точки и алгебраические знаки совпадают, так что угол, образованный смещением и лучом, обычно мал. Подобные выводы несостоятельны в отношении двух других волн. Анизотропией обычно оказывается более сильное влияние на поперечные волны. Особенно отличаются друг от друга скорости распространения двух приблизительно поперечных волн, что приводит к «рачщеплению волн скалывания» (к двойному преломлению).

При известной причине анизотропии эффекты, связанные с анизотропней, как например рачщепление поперечных волн, коррелируются по своей величине с величиной вызывающей их появление причины (например, с объемной частотой ориентированных трещин). Качественная интерпретация однозначна, количественная же пока не надежна, ибо при распространении волн сквозь поверхности раздела может иметь место изменение поляризации. Оно, равно как и отклонение лучевых путей обоих примерно поперечных волн, должно быть учтено в поправках.

GEOPHYSICAL TRANSACTIONS 1988
Vol. 34. No. 1. pp. 59—81

STRESS-INDUCED ANISOTROPY IN ELASTIC MEDIA

Ludwig ENGELHARD*

The linear Hooke's law for elastic media represents in general the first order approximation of a nonlinear stress–strain relation for small stresses and strains. If also second order expressions are considered, the influence of static stresses on the propagation of elastic waves will be included in the wave equation. These effects are discussed in view of applications to seismic work. The microscopic origin of stress-induced anisotropy is reviewed. The stress-field due to the overburden pressure is responsible for a stress-induced transverse isotropy, while horizontal tectonic stresses additionally generate azimuthal anisotropy, leading to a splitting (birefringence, double refraction) of vertically propagating shear waves. Inherent and stress-induced anisotropy can be distinguished from their different symmetry properties.

Keywords: stress-induced anisotropy, shear-wave splitting, birefringence, nonlinear elasticity, Murnaghan constants

1. Introduction

Stress-induced anisotropy in solid materials is well known in optics. This anisotropy leads to a splitting of the electromagnetic (transverse) waves into two components that travel at different velocities in the medium: This is termed birefringence or double refraction. Both wave components show a time delay against each other after they have passed through the medium, leading to distinct interference phenomena which can be used for stress analysis in engineering modelling [see e.g. MEUTH 1973, BLÜML et al. 1982]. Similarily, during the past decade, the application of stress-induced elastic anisotropy, appearing as birefringence of elastic transverse waves ("shear wave splitting") has found growing interest for testing materials with regard to internal stresses by ultrasonic shear waves [e.g.: HSU 1974, BLINKA and SACHSE 1976, KINO et al. 1979, SCHNEIDER and GOEBBELS 1982].

In addition, increasing consideration has been given to the study of stress-induced elastic anisotropy by seismic waves both for understanding the origins of anisotropy in general and for the intention of deriving the tectonic the origins of anisotropy in general and for the intention of deriving the tectonic stress field from seismic measurements. A first attempt to formulate a rigorous and general theory on wave propagation in an elastic medium under stress was made by BIOT [1940], but it was HUGHES and KELLY [1953] who derived expressions in closed form from the stringent framework given by MURNAGHAN

* Institut für Geophysik und Meteorologie der Technischen Universität, Mendelssohnstraße 3, D–3300 Braunschweig, Federal Republic of Germany
Manuscript received: 14 September, 1987

[1951] for the theory of elasticity in the case of finite deformations. On this basis many other authors treated their study of waves in prestressed solids, e.g. WALTON [1974], BONAFEDE et al. [1978], BACH and ASKEGAARD [1979]. Reference is also made to SEEGER and MANN [1959] and SEEGER and BUCK [1960] and, for collateral reading to the fundamental article of HUGHES and KELLY [1953]. TRUESDELL and NOLL [1965] present expressions for the velocities in the medium under stress in a different notation, but these can be transformed into those of HUGHES and KELLY [1953] in terms of the Murnaghan constants (see Appendix B). Corresponding considerations on stress-induced anisotropy of elastic wave propagation were made by TOLSTOY [1982] and NORRIS [1983]; they regard implicitly the (finite) strain caused by the static stress in terms of a generally nonlinear elasticity and superimpose the small strains of the elastic wave in terms of *linear* elasticity.

The application of stress-induced anisotropy for stress evaluation is still in its initial phase. AGGSON [1978] proposed a sonic tool for borehole measurements of the tectonic stress by observation of the interference between the *SV*- and *SH*(tangential)-wave, caused by shear-wave splitting. The analysis of shear wave *(SH)* vertical seismic profiles by consideration of the change of the state of polarization as well as by cepstral analysis for tectonic stress estimation has been studied by TÖNNIES [1986]. ZOBACK [1985] proposed that the horizontal polarization of tube-waves recorded on vertical seismic profiles may be used to measure the tectonic stress.

2. Phenomenological structure of stress-induced anisotropy

In this contribution, let us neglect any inherent (intrinsic) anisotropy of the medium. Thus, we consider a homogeneous medium which is isotropic if there are no stresses applied. Since we wish to consider the influence of high static stresses (overburden pressure, tectonic stress) on the propagation of elastic waves, we can no longer use the linear Hooke's law as a stress–strain relation. Instead, the strength of the static stress field makes it necessary to take into account the nonlinear elasticity of the medium. Up to the quadratic order, we have to deal with a stress–strain relation of the following form, in symbolic notation:

$$\sigma = (\lambda, \mu)\varepsilon + (l, m, n)\varepsilon^2 \tag{1}$$

where σ indicates the tensor (of second rank) of stress, ε the tensor (of second rank) of strain, (λ, μ) represents the tensor (of fourth rank) of the elastic moduli for linear elasticity, which, for a homogeneous and isotropic medium, consists of only two independent parameters, the Lamé moduli λ and μ, in this notation. Correspondingly, (l, m, n) indicates a tensor of elastic moduli of the sixth rank, describing the quadratic component in the stress–strain relation; for a medium which is homogeneous and isotropic in the stress-free state, it contains three independent parameters, which are the Murnaghan constants l, m, n in this notation [MURNAGHAN 1951]. A different choice of notation is presented in

Appendices A and B. Thus Hooke's law, which is the linear approximation of a generally nonlinear elastic stress–strain relation, is extended to the quadratic order and three further elastic constants – the Murnaghan constants – are involved for a homogeneous and initially isotropic medium. We will use the term *elastic* for a medium described by a nonlinear stress–strain relation in order to express that we assume no elastic hysteresis to be present, the latter property usually being ascribed as *anelastic*. Occasionally the term *hyperelastic* is used for the nonlinear medium without hysteresis [TRUESDELL 1961] if the stress–strain relation can be derived from an energy function — as is the case in our problem (see Appendix B).

Furthermore, in the frame of a nonlinear theory of elasticity, we must take into account that the strain tensor ε is also nonlinearily related to the displacement vector **u**, which is neglected in linear elasticity:

$$\varepsilon_{ik} = \frac{1}{2}\left(\frac{\partial u_i}{\partial x_k} + \frac{\partial u_k}{\partial x_i}\right) + \frac{1}{2}\,\frac{\partial u_j}{\partial x_i}\cdot\frac{\partial u_j}{\partial x_k} \tag{2}$$

where u_n represents the component n of the displacement vector **u** and x_m is the mth coordinate. In equation (2) and in the following, we make use of a summation convention requiring that all expressions must be summed up from one to three over that index which appears twicefold within the expression. As a consequence of the nonlinearity in equation (2), the Lamé moduli of linear elasticity will also appear in addition to the Murnaghan constants in nonlinear terms in the wave equation for the displacement **u**. The wave equation for the displacement **u** is derived in the usual way, starting from Newton's law (summation convention on index k!):

$$\varrho\,\frac{\partial^2 u_i}{\partial t^2} = \frac{\partial \sigma_{ik}}{\partial x_k} \tag{3}$$

where ϱ is the mass density.

Inserting the nonlinear stress–strain relation (equation (1)) as well as the nonlinear relation of strain and displacement (equation (2)) we get the following wave equation in symbolic notation:

$$\varrho_o\,\frac{\partial^2 \mathbf{u}}{\partial t^2} = (\lambda, \mu)\,\frac{\partial^2 \mathbf{u}}{\partial x^2} + (\lambda, \mu, l, m, n)\,\frac{\partial \mathbf{u}}{\partial x}\cdot\frac{\partial^2 \mathbf{u}}{\partial x^2} + \frac{\partial \sigma_{ik}^{static}}{\partial x_k} \tag{4}$$

In this *symbolic* formulation, the derivatives $\frac{\partial \mathbf{u}}{\partial x}$ and $\frac{\partial^2 \mathbf{u}}{\partial x^2}$ represent any of the vectorial derivatives curl, div, grad div and curl curl, as they occur in the equation, ϱ_o indicates the density of the medium in the undeformed state.

$\frac{\partial \sigma_{ik}^{static}}{\partial x_k}$ represents the divergence of the static portion of the total stress field acting on the medium. In geophysics, this includes tectonic and gravity forces.

If now the total displacement $\mathbf{u}$ is regarded as consisting of a static part $\mathbf{u}_{static}$ and of a wave part $\mathbf{u}_{wave}$

$$\mathbf{u} = \mathbf{u}_{static} + \mathbf{u}_{wave} \tag{5}$$

we see immediately that the wave equation can no longer be split — as in the case of linear elasticity — into separate equations for only the static displacement and only the wave displacement. The reason is the existence of nonlinear expressions in the wave equation (4), which also comprises mixed terms of the form

$$\frac{\partial \mathbf{u}_{static}}{\partial x} \cdot \frac{\partial^2 \mathbf{u}_{wave}}{\partial x^2} .$$

Such mixed terms express a coupling of the wave propagation with the static stress field.

The static displacement is time independent by definition, viz:

$$\frac{\partial \mathbf{u}_{static}}{\partial t} = 0 \tag{6}$$

and hence, using the partition of the displacement in equation (5), we derive from equation (4) the following form of the wave equation in the lowest order of nonlinearity:

$$\begin{aligned} \varrho_0 \frac{\partial^2 \mathbf{u}_{wave}}{\partial t^2} = & \left[(\lambda, \mu) + (\lambda, \mu, l, m, n) \frac{\partial \mathbf{u}_{static}}{\partial x} \right] \cdot \frac{\partial^2 \mathbf{u}_{static}}{\partial x^2} + \frac{\partial \sigma_{ik}^{static}}{\partial x_k} + \\ & + \left[(\lambda, \mu) + (\lambda, \mu, l, m, n) \frac{\partial \mathbf{u}_{static}}{\partial x} \right] \cdot \frac{\partial^2 \mathbf{u}_{wave}}{\partial x^2} + \\ & + \left[\text{terms of the form } \frac{\partial \mathbf{u}_{wave}}{\partial x} \cdot \frac{\partial^2 \mathbf{u}_{wave}}{\partial x^2} \text{ that are neglected} \right] \end{aligned} \tag{7}$$

Although this equation is nonlinear in the total displacement (and also in the static displacement), it is, in this order of approximation, linear in that portion of the displacement which is caused by the wave. I will therefore term this approximation "quasilinear".

In this quasilinear approximation, the wave equation, equation (7), is formally separable into an equation for the static displacement and an equation for the wave displacement, if we formally introduce a new, stress dependent tensor of elastic moduli by

$$(\lambda^*, \mu^*) = \left[(\lambda, \mu) + (\lambda, \mu, l, m, n) \frac{\partial \mathbf{u}_{static}}{\partial x} \right]$$

This tensor of stress dependent moduli (λ^*, μ^*) contains in general more than two independent parameters and it formulates the anisotropy of the medium as a function of the static stress. The wave propagation then is *formally* described in terms of linear elasticity. This is the reason why linear elasticity works so well for the elastic wave propagation in the Earth, if only pressure dependent wave velocities and occasionally anisotropy are allowed. In simplified words, we may regard a general nonlinear stress–strain relation (see *Fig. 1*) and introduce "new" stress dependent moduli, thus expressing the curvature of the stress–strain curve. The wave propagation is then governed in terms of linear elasticity by the slope of the tangent, $(\lambda^*, \mu^*) = \dfrac{d\sigma}{d\varepsilon}$, to the stress–strain curve at the value of the static load. In this treatise, however, we will prefer the explicit formulation of nonlinear elasticity in terms of stress-independent elastic moduli. The inhomogeneous wave equation (7) can be solved in two steps:

a) In the absence of a seismic wave

$$\mathbf{u}_{wave} = 0$$

a nonlinear equation holds for the static displacement alone, depending on the static stress field σ^{static};

b) Once the static displacement $\mathbf{u}_{static}$ is derived as a function of static stress, this solution can be inserted into the entire wave equation (7) and a linear wave equation for $\mathbf{u}_{wave}$ will be left.

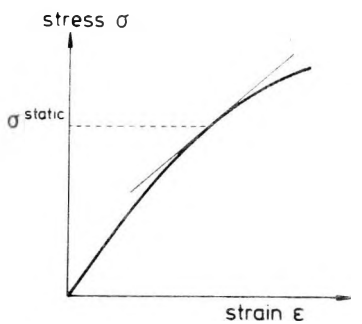

Fig. 1. Nonlinear stress–strain curve with tangent modulus $d\sigma/d\varepsilon$ at a load σ^{static}

1. ábra. Nem lineáris feszültség–alakváltozás függvény a $d\sigma/d\varepsilon$ tangens modulussal, σ^{static} terhelésnél

Рис. 1. Нелинейная функция напряжение–деформация с тангенсовым модулем $d\sigma/d\varepsilon$ при нагрузке σ^{static}

The solution of this problem was given by HUGHES and KELLY [1953] for three typical conditions:

1) For pure hydrostatic (lithostatic) pressure p (isotropic stress)

$$\varrho_0 V_P^2 = (\lambda + 2\mu) - \frac{p}{3K}[10\mu + 7\lambda + 6l + 4m] \tag{8a}$$

$$\varrho_0 V_S^2 = \mu - \frac{p}{3K}\left[3(\lambda + 2\mu) + 3m - \frac{1}{2}n\right] \tag{8b}$$

where V_P, V_S are the compressional and shear-wave velocities, respectively, and K is the bulk modulus

$$K = \lambda + \frac{2}{3}\mu \tag{9}$$

Equations (8a) and (8b) represent a description of the pressure dependence of the wave velocities in terms of the pressure independent Lamé and Murnaghan constants;

2) For axial compressive stress σ parallel to the direction of wave propagation

$$\varrho_0 V_P^2 = (\lambda + 2\mu) - \frac{\sigma}{3K}\left[\frac{\mu+\lambda}{\mu}(10\mu + 4\lambda + 4m) + \lambda + 2l\right] \tag{10a}$$

$$\varrho_0 V_S^2 = \mu - \frac{\sigma}{3K}\left[4(\mu+\lambda) + \frac{\lambda}{4\mu}\cdot n + m\right] \tag{10b}$$

3) For axial compressive stress perpendicular to the direction of wave propagation

$$\varrho_0 V_P^2 = (\lambda + 2\mu) - \frac{\sigma}{3K}\left[2l - \frac{2\lambda}{\mu}(2\mu + \lambda + m)\right] \tag{11a}$$

$$\varrho_0 V_{S_\perp}^2 = \mu - \frac{\sigma}{3K}\left[m - 2\lambda - \frac{\mu+\lambda}{2\mu}\cdot n\right] \tag{11b}$$

$$\varrho_0 V_{S_\parallel}^2 = \mu - \frac{\sigma}{3K}\left[(\lambda + 2\mu) + m + \frac{\lambda}{4\mu}\cdot n\right] \tag{11c}$$

where the symbols $\perp$ and $\parallel$ indicate if the polarization of the shear wave is perpendicular or parallel, respectively, to the stress.

Hence, the medium becomes anisotropic, as soon as the stress field is not isotropic. In this order of approximation, the corrections describing the influence of the stress field on the wave propagation are linear in the stress. Therefore, the solutions given in equations (8), (10), and (11) can be additively superposed in order to apply to the general case.

3. Geophysical relevance of stress-induced anisotropy

We will not treat in this contribution the geophysical consequences of anisotropy in general, but present instead discussions on special cases of stress-induced anisotropy. For general reading on wave propagation in anisotropic media, irrespectively of its origin, the reader is referred to the other contributions in this volume and e.g. to HELBIG [1981], CRAMPIN [1981], HELBIG [1983], CRAMPIN [1984a, b, c], CRAMPIN et al. [1984], HELBIG [1984], CRAMPIN [1985] and for the more practical aspects see e.g. TODD et al. [1973], WINTERSTEIN [1986], HAKE [1986] and THOMSEN [1986].

3.1 Transverse stress-induced isotropy

Suppose there are no horizontal tectonic stresses, then, in a homogeneous and originally isotropic formation, the overburden pressure generates a non-lithostatic (anisotropic) stress field at depth (see e.g. p. 108 of TURCOTTE and SCHUBERT [1982], or JAEGER and COOK [1976], p. 113 and p. 369):

$$\begin{aligned} \sigma_{zz} &= \varrho g z = S_V \text{ (overburden pressure)} \\ \sigma_{xx} = \sigma_{yy} &= \frac{\lambda}{\lambda + 2\mu} \varrho g z = \frac{\nu}{1-\nu} \varrho g z = S_H \end{aligned} \tag{12}$$

where z is the depth, σ_{zz} and σ_{xx}, σ_{yy} are the principal stresses in the vertical and horizontal directions, respectively, for which also the notation S_V for the vertical and S_H for the horizontal stress may be used. The stresses are defined as positive in this treatise if they are compressive. ν is Poisson's ratio. The ratio

$$\frac{S_H}{S_V} = \frac{\nu}{1-\nu} \tag{13}$$

is independent of depth. For a Poisson ratio of $\nu = 1/4$ the ratio S_H/S_V becomes $1/3$. The pressure p, being the isotropic part of the stress field, is given by

$$p = \frac{1}{3}(\sigma_{xx} + \sigma_{yy} + \sigma_{zz}) = \frac{1}{3}(2S_H + S_V) = \frac{1}{3} \varrho g z \frac{1+\nu}{1-\nu} \tag{14}$$

while the deviatoric stresses S'_V and S'_H are

$$\begin{aligned} S'_V &= S_V - p = \frac{2}{3} \varrho g z \frac{1-2\nu}{1-\nu} \\ S'_H &= S_H - p = -\frac{1}{3} \varrho g z \frac{1-2\nu}{1-\nu} \end{aligned} \tag{15}$$

and hence

$$\begin{aligned} \frac{S'_H}{S'_V} &= -\frac{1}{2} \\ S'_V - S'_H &= \varrho g z \frac{1-2\nu}{1-\nu} \end{aligned} \tag{16}$$

While pressure p leads, according to equations (8) to an isotropic change of the velocities, depending on the magnitude of the Lamé and Murnaghan elastic constants as well as on the sign of the Murnaghan constants, the deviatoric stress components lead to transverse isotropy according to equations (10) and (11). For the P-wave, the vertical velocity follows from equation (10a) for σ being S'_V, plus the pressure dependent part of equation (8a) for p. Correspondingly, the horizontal P-wave velocity follows from S'_V being inserted in equation

(11a) plus p being inserted in equation (8a). Similarily, but in a more complicated way, the stress-induced transverse (azimuthal) isotropy affects the shear wave. For the vertical shear-wave velocity, equation (10b) – with σ being S'_V plus equation (8b) with p according to equation (14) – must be taken. For the horizontal shear-wave velocity, equation (11b) or (11c) – depending on whether it is an *SH*- or *SV*-polarized shear wave, with σ being S'_V plus the pressure dependence from equation (8b) – is valid. Thus, a general polarization direction leads to a splitting of the horizontally propagating shear wave into two components (*SH* and *SV*) that travel at different velocities (double refraction, birefringence).

For a general direction of wave propagation, care must be taken that the stress-dependent expressions in equations (10) and (11) transform as components of a tensor of second rank. Shear-wave splitting will occur whenever the shear wave is not purely *SH* polarized and propagates in a non-vertical direction. Thus, for a homogeneous layer, anisotropy in the form of transverse isotropy will always be present from stress-induced anisotropy. This contributes to other sources of transverse isotropy like lithological and stratigraphic (fine layering) anisotropy. WINTERSTEIN [1986] demonstrates impressively how seriously transverse isotropy influences the stacking velocities. His conclusion that these effects contain information on lithology can be specified for the stress-induced part of transverse isotropy in the remark that the Murnaghan constants may be regarded as lithological parameters.

3.2 Azimuthal anisotropy

We assume now, in addition to the stress field which is generated by the overburden pressure, a horizontal tectonic (axial, compressive deviatoric) stress S'_t. If the tectonic axial stress alone would be present, not in addition to the vertical deviatoric stress, it would induce a transverse isotropy with a horizontal axis of symmetry. In the general case, for the *P*-wave, the anisotropy must be described for the vertical direction of propagation by equation (11a), with S'_t being inserted for σ, plus the stress-dependent part of equation (10a), with σ being S'_V, and with the pressure influence of equation (8a). The horizontal *P*-wave velocity follows correspondingly from equation (11a), with the perpendicular tensorial component of the horizontal tectonic stress S'_t plus S'_V, inserted for σ, plus the parallel tensorial component of S'_t for σ in equation (10a), and with the pressure influence of equation (8a).

The situation becomes even more complicated for shear waves. Therefore, for simplicity, let us regard the case of a vertically travelling shear wave *(SH)*, as it occurs in practice for shear-wave vertical seismic profiles *(VSP)* or for nearly vertical rays in shear-wave reflection seismics. The tectonic stress S'_t is then perpendicular to the propagation of the wave. In addition to the pressure influence in equation (8b) and the influence of the vertical deviatoric stress S'_V

in equation (10b), the tectonic stress in equations (11b) and (11c), respectively, gives different velocities, depending on whether the tectonic stress lies in the plane of polarization or perpendicular to it. Thus, a shear wave of an arbitrary orientation of its polarization direction will split into a parallel and a perpendicular component, which travel at different velocities.

As a result, from the time delay between both components, an originally linearly polarized shear wave becomes elliptically polarized after the passage of a finite path length; the general relation between time delay of orthogonally polarized waves and the state of polarization may be found, for example in monographs on optics, like BORN and WOLF [1980]. For a transient shear-wave signal, as seismic wavelets are, with a beginning and an end, the faster travelling component determines the polarization of the beginning of the recorded signal, while its end is determined by the slow wave component. In the main phase of the recorded signal, the composition of both components generally leads to elliptical polarization. Thus, we need only to know which is the parallel and which is the perpendicular component, respectively, the slow or the fast shear wave, in order to derive the orientation of the tectonic stress from polarization studies; in general (see below) it is the component polarized parallel to the stress that travels faster. In *Figure 2* such a change of the state of polarization over the duration of the recorded wavelet is demonstrated in a sequence of synthetically generated hodographs for the stress assumed to act with an angle of 30° with respect to the x-axis in a mathematically positive sense [after TÖNNIES 1986]. The plane of polarization of the source is rotated in steps of 10 degrees. The source signal is a Ricker wavelet of 25 Hz dominant frequency, and a time delay of 40 ms is assumed between both components. Furthermore, the spectrum of the composed wavelet will periodically be modulated by an interference structure caused by the interference of the two components of the wave from their time delay (cf. Appendix C). AGGSON [1978] has proposed that the frequency interval between these maxima and minima be used to estimate the strength of the tectonic stress field from shear-wave borehole logging and TÖNNIES [1986] has given synthetic examples for such evaluation by cepstral analysis.

Quantitatively, we derive for the time delay Δt between the parallel and perpendicular to the stress polarized shear wave:

$$\Delta t = \frac{\Delta z}{V_\parallel} - \frac{\Delta z}{V_\perp} = \frac{\Delta z}{V_\parallel \cdot V_\perp} \frac{V_\perp^2 - V_\parallel^2}{V_\perp + V_\parallel} \tag{17}$$

where Δz is the length of the travel path. By use of equations (11b) and (11c):

$$\Delta t = \frac{\Delta z}{V_\parallel \cdot V_\perp} \frac{\mu}{\varrho_0} \frac{1}{V_\perp + V_\parallel} \frac{4\mu + n}{4\mu^2} \sigma \tag{18}$$

σ being the axial stress perpendicular to the propagation direction (equal to S_t' for the tectonic origin of this stress). Furthermore,

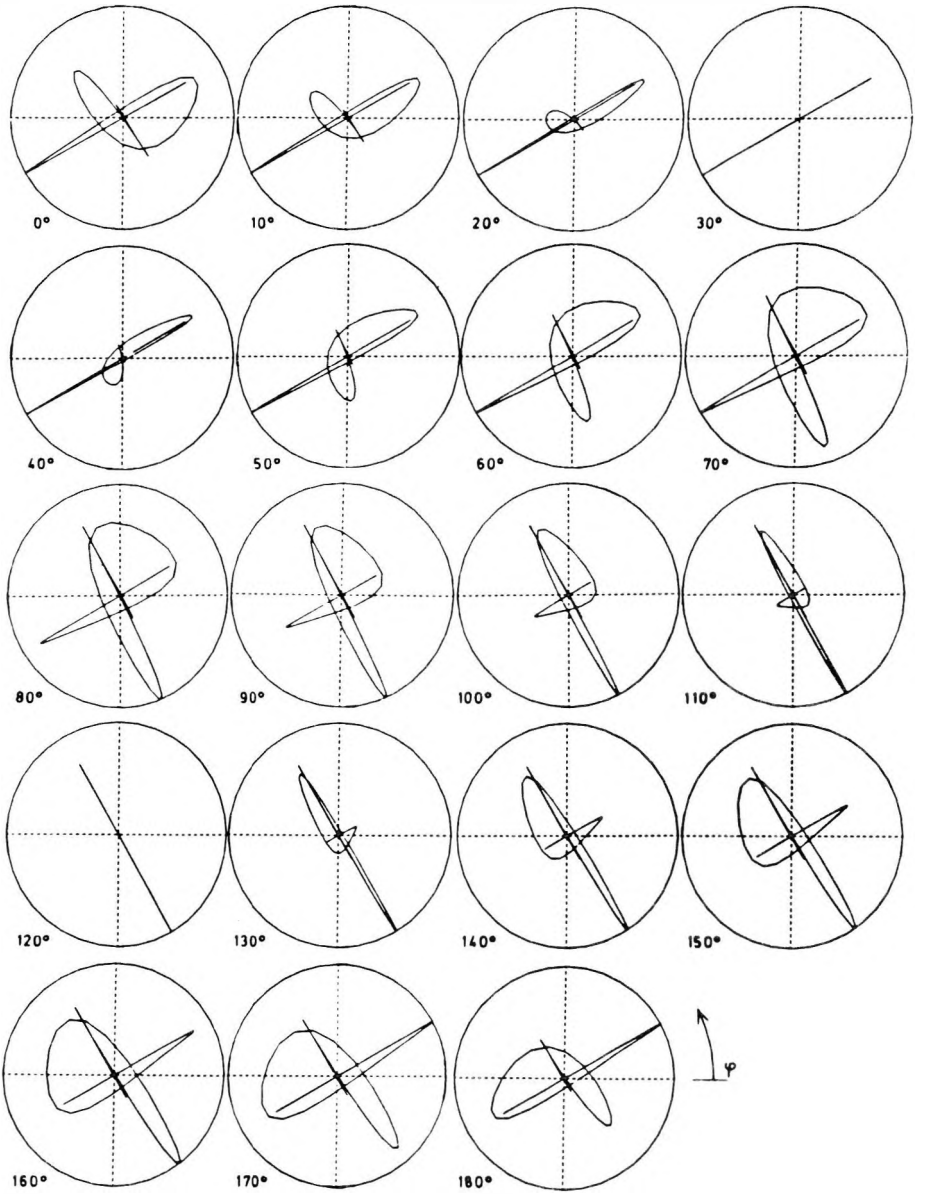

Fig. 2. Variation of the form of the hodograph as a function of the azimuth of the polarization of the source. The axis of the tectonic stress is assumed to be oriented at 30° with respect to the *x*-axis [after TÖNNIES 1986]

2. ábra. A hodográf alakváltozásai a hullámforrás polarizációs azimutja függvényében. Feltételezzük, hogy a tektonikai feszültség tengelye az *x* tengellyel 30°-os szöget zár be [TÖNNIES 1986 nyomán]

Рис. 2. Изменения годографа в зависимости от азимута поляризации источника волн. Предполагается, что ось тектонических напряжений составляет угол 30° с осью *x* [по TÖNNIES 1986].

$$\frac{\mu}{\varrho_0} = V_{S0}^2 \tag{19}$$

where V_{S0} is the (isotropic) shear-wave velocity in the medium without stress. In this order of approximation, which includes only expressions that are linear in stress, we estimate in equation (18)

$$\begin{aligned} V_\perp + V_\parallel &\approx 2V_{S0} \\ V_\parallel \cdot V_\perp &\approx V_{S0}^2 \end{aligned} \tag{20}$$

We then have for the time delay Δt:

$$\Delta t = \alpha_s \frac{\Delta z}{V_{S0}} \sigma \tag{21}$$

where α_s is termed the "constant of stress induced birefringence".

$$\alpha_s = \frac{4\mu + n}{8\mu^2} \tag{22}$$

V_{S0} in equation (21) may be taken in practice as the geometric or arithmetic mean velocity, according to equations (20). Since

$$t_0 = \frac{\Delta z}{V_{S0}} \tag{23}$$

is the mean travel time of the shear waves, we can rearrange equation (21) in the form

$$\frac{\Delta t}{t_0} = \alpha_s \sigma \tag{24}$$

3.3 Order of magnitude of stress-induced anisotropy

The magnitude of the stress-induced anisotropy is determined by the strength of the axial stresses and by the magnitude of the Lamé and Murnaghan elastic constants. While the Murnaghan constants are known for a variety of "laboratory materials", like pure metals or synthetic materials, only very few measurements of these constants for minerals and rocks are reported in the literature. In *Figure 3*, the measurements on granite, presented by AGGSON [1978], show the stress-induced shear-wave splitting to be of remarkable order of magnitude. This diagram allows one to estimate the constant of stress-induced birefringence α_s for this sample of granite; the difference between the velocities at zero stress indicates the presence of inherent anisotropy in this rock sample. WALTON [1974] presented a set of Lamé and Murnaghan constants for Barre granite, and TÖNNIES [1986] derived another set for Barre granite from the data of NUR and SIMMONS [1969]. These data, together with corresponding sets of elastic moduli of some other materials for comparison, are presented in *Table I*. While the Murnaghan constants for metals are in general of the order

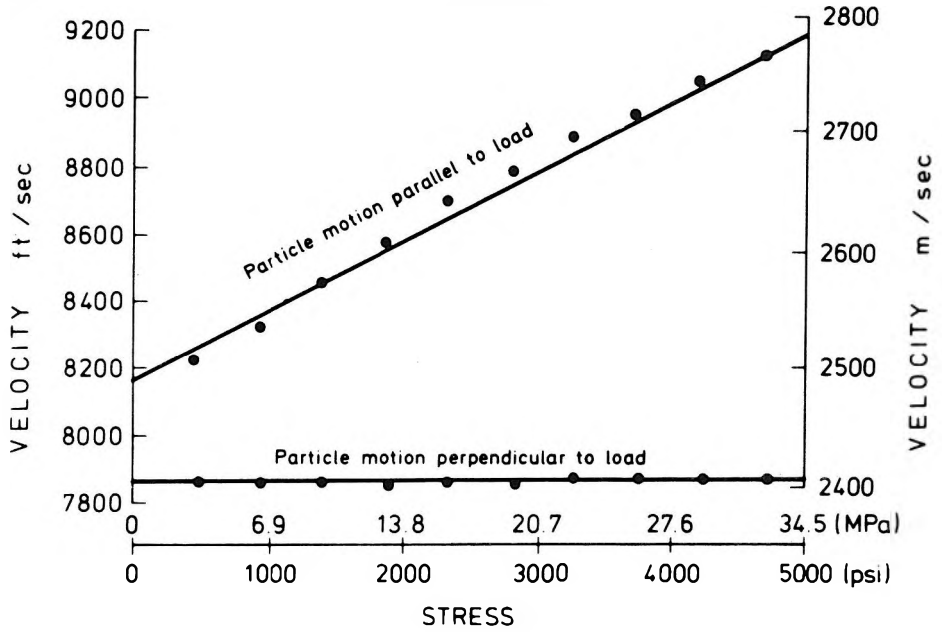

Fig. 3. Measurement of stress-induced shear-wave splitting in granite [after AGGSON 1978]

3. ábra. A feszültség által kiváltott nyiróhullám kettős-törés mérése gránitban [AGGSON 1978 nyomán]

Рис. 3. Измерение двупреломления поперечных волн, вызванных напряжениями, в гранитах [по AGGSON 1978].

of five to ten times the magnitude of the Lamé constants, they seem to be far greater in rocks. This may be caused by the micro-heterogeneity in the interior of rocks (see section 4). The negative sign of α_s for most of the materials indicates that the shear wave polarized parallel to the stress travels faster.

Thus, for granite, we estimate the order of magnitude of shear-wave splitting induced by stress to be

$$\alpha_s = -2.3 \text{ (dry)} \ldots -4.8 \text{ (wet) GPa}^{-1}$$

The axial tectonic stress may typically be of the order of some ten MPa, hence from Eq. (24)

$$\frac{\Delta t}{t_0} \approx -0.05$$

This means that the time delay between both shear-wave components will be of the order of 20 ms for a mean shear-wave travel time of $t_0 = 400$ ms, which may correspond to a travel path length of about 1000m in granite. The time delay expressed in terms of the phase delay $\Delta\varphi$ between both shear-wave components turns out to be

Material		λ in GPa	μ in GPa	l in GPa	m in GPa	n in GPa	ϱ_0 in g/cm^3	α_S in GPa^{-1}
Barre-granite (dry)	1)	1.16	18.38	−3600	−6540	−6300	2.650	$-2303 \cdot 10^{-3}$
Barre-granite (wet)	2)	29.7	25.3	−4800	−8400	−25000	2.66	$-4862 \cdot 10^{-3}$
Granite	3)							$-4495 \cdot 10^{-3}$
Stone—Mountain-granite	4)	4.0	15.4				2.614	
Polystyrene	5)	2.89	1.38	−19	−13	−10	1.056	$-293 \cdot 10^{-3}$
Pyrex-glass	5)	13.5	27.5	+14	+92	+420		$+88 \cdot 10^{-3}$
Armco-iron	5)	110	82	−348	−1030	+1100		$+27 \cdot 10^{-3}$
Iron	6)	113	81	−167	−755	−1490		$-22 \cdot 10^{-3}$
Copper	6)	105	47	−157	−608	−1560		$-78 \cdot 10^{-3}$
Steel	7)	115.8	79.8	−248	−623	−714		$-8 \cdot 10^{-3}$

1) TÖNNIES [1986], based on NUR and SIMMONS [1969]
2) WALTON [1974]
3) AGGSON [1978]
4) LANDOLT—BÖRNSTEIN [1982], p. 42 (included in this compilation to demonstrate the large variations that the same type of rock may exhibit in its elastic properties)
5) HUGHES and KELLY [1953]
6) SEEGER and BUCK [1960]
7) EGLE and BRAY [1976]

Table I. Lamé and Murnaghan constants and the constant of stress-induced shear-wave birefringence for some materials

I. táblázat. A Lamé és Murnaghan állandók, valamint a feszültség által keltett nyíróhullám kettős-törés konstansa néhány anyagra

Таблица I. Константы Ламэ и Мурнагана, а также константа двупреломления поперечной волны, вызванной напряжением, для некоторых веществ.

$$\Delta\varphi = \frac{\Delta t}{T} 2\pi = \frac{t_0}{T} 2\pi \, \alpha_s \, \sigma \tag{25}$$

where T is the period of the shear wave. Hence, the phase delay $\Delta\varphi$ becomes 2π if t_0/T equals about 20 (for the values that have been assumed above). Thus, for a wavelet of a dominant frequency of 20 Hz, a phase delay of 2π occurs if t_0 is about 1000 ms. Remember that a linearly polarized wave becomes circularly polarized for a phase delay of $\Delta\varphi = \pi/2$ if both orthogonal components are of equal magnitude [for details, see BORN and WOLF 1980]. All the other effects of stress-induced anisotropy, as discussed above, may be of the same order of magnitude. Note that the deviatoric vertical stress S'_V, according to equation (15), is of the order of 10 MPa at a depth of 1000 m for $\varrho = 2.6 \cdot 10^3$ kg/m^3 (granite) and a Poisson number of $\nu = 1/4$, and increases linearly with depth. The data presented in Table I also confirm that it was necessary, for the derivation of a theory of stress-induced anisotropy, to deal not only with the nonlinear relation of the strain and displacement (equation (2)), but also with the nonlinear stress–strain relation (equation (1)). In fact, in the stress-dependent expressions of equations (8), (10) and (11) the terms of the Murnaghan constants become the overwhelming parts compared with those of the Lamé moduli.

4. Further remarks on the nature of stress-induced anisotropy

Nothing is said in the frame of this theory about the petrophysical origin of stress-induced anisotropy on a microscopic scale ("microscopic" with respect to the wavelength), because our description is purely phenomenological. Several causes may contribute, whereas in any given formation one of the phenomena will be expected to be dominant. In preference, the oriented closure and/or oriented generation of microcracks by stress is mainly discussed in the literature [NUR and SIMMONS 1969, TODD et al. 1973, CRAMPIN et al. 1980, CRAMPIN and MCGONIGLE 1981, CRAMPIN et al. 1984, CRAMPIN and ATKINSON 1985, ROBERTS and CRAMPIN 1986, BROOKS et al. 1987]. But we also think of such sources of stress-induced anisotropy like the change of the shape of pores (e.g. spherical pores become ellipsoidal under stress), the change of the contact between the individual grains in a preferred direction, the elastic differential rotation of nonspherical grains if they are embedded in a matrix of different elastic properties, and the change of structure of the crystal lattice in the grains. The last phenomenon dominates in the studies of stress-induced anisotropy in solid-state physics, e.g. BIRCH [1947], SEEGER and MANN [1959], SEEGER and BUCK [1960], BATEMAN et al. [1961], THURSTON [1965] and, is a main part, in acoustoelastic imaging of internal stress fields by ultrasonic shear-wave birefringence. All the other phenomena mentioned above account for the material heterogeneity. These dominate in natural rocks and thus the excess of Murnaghan's constants for rocks in relation to homogeneous materials may be explained. Obviously, the Murnaghan elastic constants express the readiness of the material to close or generate cracks, to change the shape of the pores, to change the contact of the grains, the ability of elongated grains to rotate and the facility to change the structure of the crystal lattice.

In view of the prospect of deriving information on the stress field in the Earth from the observation of stress-induced anisotropy, the distinction between inherent and stress-induced anisotropy is of major importance. In ultrasonic experiments MAHADEVAN [1966] found the inherent shear-wave birefringence to depend on the frequency whereas the stress-induced part proved to be frequency independent. SCHNEIDER et al. [1985], who have analysed this effect in more detail, successfully applied a procedure on this basis to separate both portions of anisotropy. It seems questionable whether similar effects occur in seismics, but careful studies should be executed in the future. In general, the separation of stress-induced and inherent anisotropy is possible by taking advantage of the difference in symmetry of the medium, expressed in different symmetry properties of the modulus tensor c_{ijkl} [THURSTON 1974, p. 227, KING and FORTUNKO 1983, THOMPSON et al. 1984, NIKITIN and CHESNOKOV 1984]. This tensor of elastic moduli itself depends on the stress to account for the nonlinearity of the stress–strain relation (this is, in the first order expansion of c_{ijkl} with respect to the stress, fully equivalent to the formulation of equation (1), see KING and FORTUNKO [1983]). It turns out, that

$$\varrho(V_{ij}^2 - V_{ji}^2) = \begin{cases} \sigma_{ii} - \sigma_{jj} & \text{for stress-induced anisotropy} \\ 0 & \text{for inherent anisotropy} \end{cases} \tag{26}$$

where V_{ij} is the velocity of a shear-wave propagating in the i direction and polarized in the j direction. Equation (26), indicates the lower symmetry of stress-induced anisotropy compared with inherent anisotropy. Furthermore it implies as a consequence that the abbreviated Voigt notation for the modulus tensor, as used by many authors to describe anisotropy [e.g. THOMSEN 1986], cannot be used for stress-induced anisotropy [THURSTON 1974]. Hence, it follows from equation (26) that the stresses can also be derived from shear-wave anisotropy observations in the presence of inherent anisotropy if the material is traversed by rays in orthogonal directions and correspondingly mutually exchanged polarization directions; this is easier to achieve in the laboratory with ultrasonic experiments than in seismics. In seismic work, one may observe shear-wave anisotropy from a steep ray and from oblique rays under different azimuths and polarization directions and use equations (10) and (11) in tensorial rotated form, corresponding to the directions of the ray and of the polarization.

Anisotropy depending on the stress field has also been observed in the subcrustal lithosphere and in the upper mantle [e.g. CRAMPIN 1977, ANDO et al. 1980, ANDO and ISHIKAWA 1982, ANDO et al. 1983, FUCHS 1983, FUKAO 1984, SHEARER and ORCUTT 1986]. Two models for the origin of this anisotropy have been subject to discussion, the crack alignment model and the olivine alignment model [ANDO et al. 1983]. While in the crack alignment model magma filled cracks in a preferred direction are assumed, in the olivine alignment model, which is now widely favoured [CRAMPIN et al. 1984], the orientation of olivine crystallites—which themselves show a crystalline anisotropy—by flow processes is supposed [FUCHS 1983, CHRISTENSEN 1984, ARTYUSHKOV 1984, SHEARER and ORCUTT 1986, SAYERS 1987]. Although this type of anisotropy is *stress*-influenced, hence allowing for stress analysis in these depths, it is due to rheology, that is not based on elasticity as described by equation (1) but that accounts also for the flow [see e.g. FUCHS 1983]. In view of this it does not strictly belong to the class of stress-induced anisotropy, whereas flow-induced anisotropy seems to characterize this type of anisotropy more precisely.

5. Conclusions

The study of stress-induced anisotropy from seismic observations is not only of importance for the analysis of the Earth's stress field but also for lithological information in the sense of WINTERSTEIN [1986], from the estimation of third-order (Murnaghan) elastic moduli. Laboratory measurements of the Murnaghan elastic moduli for a variety of sedimentary and crystalline rocks are now urgently required to estimate the order of magnitude of the stress-induced anisotropy in more detail than is done in this treatise in section 3.3, and to get an idea of its lithological span of variability. On the other hand, more observa-

tional data under controlled conditions, like shear-wave vertical seismic profiles (VSP) using 3-component geophones in the borehole, are needed. Care must be taken that the polarization direction of the shear-wave source is neither parallel nor perpendicular to the tectonic stress otherwise no shear-wave splitting would occur; thus, in general, at least two polarization orientations, forming an angle of 45° to each other, should be chosen.

In shear-wave polarization studies, furthermore, attention must be paid to changes of the state of polarization due to other origins, such as from transmission and reflection at dipping interfaces [DOUMA and HELBIG 1987] or from the effect of the free surface [EVANS 1984].

The linear increase with depth of the vertical deviatoric stress S'_V (cf. equation (15)) suggests that stress-induced transverse isotropy may play a significant role in the lithosphere. This assumption is consistent with the model of DZIEWONSKI and ANDERSON [1981] and ANDERSON and DZIEWONSKI [1982] for a general transverse isotropy in the lithosphere.

At last, the author wishes to draw attention to higher order elastic effects, which influence the frequency of a seismic wave. In equation (7), we have neglected terms that describe an interaction of the propagating wave with itself. These terms involve nonlinear spectral mixing leading to the generation of harmonic frequencies. A theory in closed form like that for the quasilinear approximation has not yet been published. If such effects would become noticeable in seismic work, depending once more on the magnitude of the Murnaghan elastic moduli, they would influence spectral studies as, for example, seismic attenuation determinations. Observational indications, on the other hand, have been reported by AGNEW [1981] and by BERESNEV et al. [1986].

APPENDIX A
Murnaghan's elastic moduli in Eulerian and Lagrangian coordinates

In a theory of finite elastic deformations, attention must be paid to a strict and persistent definition of the variables, since initial coordinates and final coordinates are no longer interchangeable. The choice of the initial coordinates as independent variables is called "Lagrangian formulation", while the choice of final coordinates as independent variables is termed "Eulerian formulation" [HUGHES and KELLY 1953]. Care must be taken if use is made of the literature, whether Eulerian or Lagrangian coordinates are used since the set of third order elastic moduli is different in both formulations. In general, however, the Lagrangian description is preferably used in the literature—as it is in this contribution. SEEGER and MANN [1959] presented the relations that allow the conversion between both representations. If l, m, n are Murnaghan's moduli in Lagrangian formulation and l', m', n' are those as defined in Eulerian formulation, then the following interrelations hold:

$$
\begin{aligned}
l &= -2(3\lambda + 4\mu) + 3l' + m' \\
m &= -2\mu - \frac{1}{2} m' \\
n &= -12\mu + n'
\end{aligned}
\tag{A-1}
$$

$$
\begin{aligned}
l' &= 2(\lambda + 2\mu) + \frac{1}{3}(l + 2m) \\
m' &= -4\mu - 2m \\
n' &= 12\mu + n
\end{aligned}
\tag{A-2}
$$

APPENDIX B
Other than Murnaghan notation of elastic third order moduli

The elastic energy density in Lagrangian representation $\varphi(\varepsilon_{ik})$, where ε_{ik} are the components of the strain tensor, reads in the formulation according to MURNAGHAN [1951]:

$$
\varphi = -p_0 I_1 + \frac{\lambda + 2\mu}{2} I_1^2 - 2\mu I_2 + \frac{l + 2m}{3} I_1^3 - 2m I_1 I_2 + n I_3 \tag{B-1}
$$

p_0 is the initial (hydrostatic/lithostatic) pressure, λ and μ are the Lamé-, and l, m, n the Murnaghan elastic moduli, and I_1, I_2, I_3 the first, second, and third tensorial invariants:

$$
\begin{aligned}
I_1 &= \varepsilon_{ii} = \mathrm{Tr}\,(\varepsilon_{ik}) \\
I_2 &= \det \begin{pmatrix} \varepsilon_{11} & \varepsilon_{12} \\ \varepsilon_{21} & \varepsilon_{22} \end{pmatrix} + \det \begin{pmatrix} \varepsilon_{22} & \varepsilon_{23} \\ \varepsilon_{32} & \varepsilon_{33} \end{pmatrix} + \det \begin{pmatrix} \varepsilon_{33} & \varepsilon_{31} \\ \varepsilon_{13} & \varepsilon_{11} \end{pmatrix} \\
I_3 &= \det\,(\varepsilon_{ik})
\end{aligned}
\tag{B-2}
$$

Recall the summation convention as defined in Section 2, following equation (2), also for the following. The stress–strain relation in initial coordinates is given by (cf. SEEGER and MANN [1959]):

$$
\sigma_{ik} = \mathbf{J}_{ij} \frac{\partial \varphi}{\partial \varepsilon_{jk}} \tag{B-3}
$$

where the Jacobian matrix $\mathbf{J}_{ij}$, connecting the final coordinates x_i' with the initial coordinates x_j is

$$
\mathbf{J}_{ij} = \frac{\partial x_i'}{\partial x_j} = \delta_{ij} + \frac{\partial u_i}{\partial x_j} \tag{B-4}
$$

where the u_i are the components of the displacement vector.

TRUESDELL and NOLL [1965] use in their treatise the following formulation of the elastic energy density for vanishing initial pressure p_0 (their equation (93.1)):

$$\varphi = \frac{\lambda+2\mu}{2} I_1^2 - 2\mu I_2 + \mu\beta_1 I_1^3 + \mu\beta_2 I_1 I_2 + \mu\beta_3 I_3 \tag{B-5}$$

Therefore, from comparison with equation (B–1), this notation can be converted into Murnaghan's expression by

$$\begin{aligned} \mu\beta_1 &= l + 2m \\ \mu\beta_2 &= -2m \\ \mu\beta_3 &= n \end{aligned} \tag{B-6}$$

On the other hand, these authors compare the stress–strain relation, following from (B–5), with an expression which they define as the second-order stress–strain relation for general elastic materials (their equation (66.3)), and they derive that

$$\begin{aligned} \alpha_3 &= -\alpha_1 + 3\beta_1 + \beta_2 \\ \alpha_4 &= \beta_2 + \beta_3 \\ \alpha_5 &= 2\alpha_1 - 2 - \beta_2 - \beta_3 \\ \alpha_6 &= 4 + \beta_3 \end{aligned} \tag{B-7}$$

where α_i are the elastic constants as introduced in a second-order expansion of the stress with respect to the strain. Substituting Murnaghan's constants from (B–6) into (B–7), and α_1 being λ/μ, we derive:

$$\begin{aligned} \mu\alpha_3 &= -\lambda + l \\ \mu\alpha_4 &= -2m + n \\ \mu\alpha_5 &= 2\lambda - 2\mu + 2m - n \\ \mu\alpha_6 &= 4\mu + n \end{aligned} \tag{B-8}$$

This result, however, is inconsistent with the conversion they themselves give on p. 230 of their work.

If, on the other hand, these conversions (B–8) are inserted into their own expressions for the velocities in their notation, then using α_i, one gets exactly the velocities as given by HUGHES and KELLY [1953], see equations (8), (10), and (11). Hence, we conclude that the conversion in the form (B–8) and not the conversion of TRUESDELL and NOLL [1965], p. 230, for α_i into Murnaghan constants is valid [TÖNNIES 1986].

APPENDIX C
Structure of the spectral interference pattern for a double-refracted shear wave

Consider, for simplicity, the case of a vertical seismic profile (VSP), where a horizontally polarized shear-wave travels in the vertical direction. Since the orientation of the horizontal tectonic stress will not be known in general, we assume the angle of the polarization direction with respect to the direction of the tectonic stress to be α. By the double refraction in the medium the shear wave splits into components polarized parallel and perpendicular with respect to the stress:

$$\begin{aligned} s_{\parallel}(t) &= s_0(t) \cdot \cos \alpha \\ s_{\perp}(t) &= s_0(t) \cdot \sin \alpha \end{aligned} \tag{C–1}$$

where s_0 is the source wavelet in the time domain.

The orientation of a horizontal geophone at depth will generally not be under control, although it may be known, for example, from a compass signal. Let β be the angle of the geophone orientation against the stress direction, then the signal s_G, recorded by the geophone, will be

$$s_G(t) = s_{\parallel}(t) \cos \beta + s_{\perp}(t+\delta) \sin \beta \tag{C–2}$$

where δ is the time delay (positive or negative) between both shear-wave components, caused by the birefringence. Together with equation (C–1) follows the equation

$$s_G(t) = a s_0(t) + b s_0(t+\delta) \tag{C–3}$$

where

$$\begin{aligned} a &= \cos \alpha \cos \beta \\ b &= \sin \alpha \sin \beta. \end{aligned} \tag{C–4}$$

By Fourier transformation, we derive for the spectrum of the geophone signal:

$$S_G(\omega) = S_0(\omega) [a + b e^{i\omega\delta}] \tag{C–5}$$

where $S_0(\omega)$ is the source spectrum. The expression within the brackets represents the spectral interference pattern, superposed upon the source spectrum. For the power spectrum of the geophone signal we get

$$|S_G(\omega)|^2 = |S_0(\omega)|^2 [a^2 + b^2 + 2ab \cos(\omega\delta)]. \tag{C–6}$$

The power spectrum of the interference pattern is schematically depicted in *Fig. 4*. Its amplitude, and thus its sensitivity for detection from experimental data, obviously depends on the product ab, which is maximal for $\alpha = \beta = \pi/4 : (ab)_{max} = 1/4$. Depending on the signs of a and b, respectively, the

interference can also begin with a minimum at zero frequency. Since the spectral modulation by the interference is periodic, a cepstral analysis is appropriate for analysing the modulation quefrency, i.e. to derive the time delay δ.

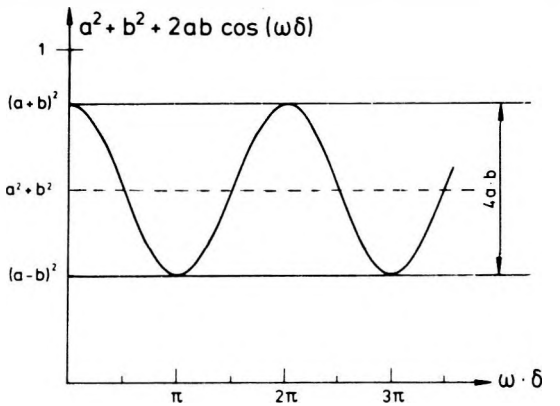

Fig. 4. Power spectrum of the interference pattern

4. ábra. Az interferencia kép teljesítményspektruma

Рис. 4. Спектр мощности интерференционной картины.

REFERENCES

AGGSON J. R. 1978: The potential application of ultrasonic spectroscopy to underground site characterization. Preprint of the 48th annual meeting of the SEG, San Francisco

AGNEW D. C. 1981: Nonlinearity in rock: Evidence from Earth tides. J. Geophys. Res. **86,** B5, pp. 3969–3978

ANDERSON D. L., DZIEWONSKI A. M. 1982: Upper mantle anisotropy: Evidence from free oscillations. Geophys. J. Roy. Astron. Soc. **69,** 2, pp. 383–404

ANDO M., ISHIKAWA Y., WADA H. 1980: *S*-wave anisotropy in the upper mantle under a volcanic area in Japan. Nature **286,** 5768, pp. 43–46

ANDO M., ISHIKAWA Y. 1982: Observations of shear-wave velocity polarization anisotropy beneath Honshu, Japan: Two masses with different polarizations in the upper mantle. J. Phys. Earth **30,** 2, pp. 191–199

ANDO M., ISHIKAWA Y., YAMAZAKI F. 1983: Shear-wave polarization anisotropy in the upper mantle beneath Honshu, Japan. J. Geophys. Res. **88,** B7, pp. 5850–5864

ARTYUSHKOV E. V. 1984: On the origin of the seismic anisotropy of the lithosphere. Geophys. J. Roy. Astron. Soc. **76,** 1, pp. 173–178

BACH F., ASKEGAARD V. 1979: General stress-velocity expressions in acoustoelasticity. Exper. Mechanics **19,** pp. 69–75

BATEMAN T., MASON W. P., MCSKIMMIN H. J. 1961: Third-order elastic moduli of germanium. J. Appl. Phys. **32,** 5, pp. 928–936

BERESNEV I. A., KARRYEV B. S., KHAVROSHKIN O. B., NIKOLAEV A. V., SOLOVIEV V. S., TSIPLAKOV V. V. 1986: Experimental investigations of the nonlinear seismic effects. Preprint, prepared for publication (Institute of Physics of the Earth, USSR Academy of Sciences)

BIOT M. A. 1940: The influence of initial stress on elastic waves. J. Appl. Phys. **11,** pp. 522–530

BIRCH F. 1947: Finite elastic strain of cubic crystals. Phys. Rev. **71,** 1, pp. 809–824

BLINKA J., SACHSE W. 1976: Application of ultra-sonic-pulse-spectroscopy measurements to experimental stress analysis. Exp. Mech. **16,** pp. 448–453

BLÜML P., HOSP E., RITTER R., SIMON B. 1982: Optische Verfahren in der experimentellen Spannungsanalyse. VDI-Berichte **439,** pp. 97–121

BONAFEDE M., BOSCHI E., SABADINI R. 1978: Some effects of elastic prestress within the Earth. Nuovo Cim. **1C,** 2, pp. 97–109

BORN M., WOLF E. 1980: Principles of optics. Sixth edition. Pergamon Press, Oxford, New York, etc.

BROOKS S. G., CHROSTON P. N., BOOTH D. C. 1987: Extensive-dilatancy anisotropy (EDA) inferred from observations of crustal shear waves generated by a refraction experiment in northern Scandinavia. Geophys. J. Roy. Astron. Soc. **90,** 1, pp. 225–232

CHRISTENSEN N. I. 1984: The magnitude, symmetry and origin of upper mantle anisotropy based on fabric analyses of ultramafic tectonites. Geophys. J. Roy. Astron. Soc. **76,** 1, pp. 89–111

CRAMPIN S. 1977: A review of the effects of anisotropic layering on the propagation of seismic waves. Geophys. J. Roy. Astron. Soc. **49,** 1, pp. 9–27

CRAMPIN S., EVANS R., ÜÇER B., DOYLE M., DAVIS J. P., YEGORKINA G. V., MILLER A. 1980: Observations of dilatancy-induced polarization anomalies and earthquake prediction. Nature **286,** 5776, pp. 874–977

CRAMPIN S. 1981: A review of wave motion in anisotropic and cracked elastic-media. Wave Motion **3,** pp. 343–391

CRAMPIN S., MCGONIGLE R. 1981: The variation of delays in stress-induced anisotropic polarization anomalies. Geophys. J. Roy. Astron. Soc. **64,** 1, pp. 115–131

CRAMPIN S. 1984a: An introduction to wave propagation in anisotropic media. Geophys. J. Roy. Astron. Soc. **76,** 1, pp. 17–28

CRAMPIN S. 1984b: Anisotropy in exploration seismics. First Break **2,** 3, pp. 19–21

CRAMPIN S. 1984c: Effective anisotropic elastic constants for wave propagation through cracked solids. Geophys. J. Roy. Astron. Soc. **76,** 1, pp. 135–145

CRAMPIN S., CHESNOKOV E. M., HIPKIN R. A. 1984: Seismic anisotropy — the state of the art. First Break **2,** 3, pp. 9–18

CRAMPIN S. 1985: Evaluation of anisotropy by shear-wave splitting. Geophysics **50,** 1, pp. 142–152

CRAMPIN S., ATKINSON B. K. 1985: Microcracks in the Earth's crust. First Break **3,** 3, pp. 16–20

DOUMA J., HELBIG K. 1987: What can the polarization of shear waves tell us? First Break **5,** 3, pp. 95–104

DZIEWONSKI A. M., ANDERSON D. L. 1981: Preliminary reference Earth model. Phys. Earth and Planet. Inter. **25,** 4, pp. 297–356

EGLE D. M., BRAY D. E. 1976: Measurement of acoustoelastic and third-order elastic constants for rail steel. J. Acoust. Soc. **60,** 3, pp. 741–744

EVANS R. 1984: Effects of the free surface on shear wavetrains. Geophys. J. Roy. Astron. Soc. **76,** 1, pp. 165–172

FUCHS K. 1983: Recently formed elastic anisotropy and petrological models for the continental subcrustal lithosphere in southern Germany. Phys. Earth and Planetary Inter. **31,** 2, pp. 93–118

FUKAO Y. 1984: Evidence from core-reflected shear waves for anisotropy in the Earth's mantle. Nature **309,** 5970, pp. 695–698

HAKE H. 1986: Slant stacking and its significance for anisotropy. Geophys. Prosp. **34,** 4, pp. 595–608

HELBIG K. 1981: Systematic classification of layer-induced transverse isotropy. Geophys. Prosp. **29,** 4, pp. 550–577

HELBIG K. 1983: Elliptical anisotropy — its significance and meaning. Geophysics **48,** 7, pp. 825–832

HELBIG K. 1984: Transverse isotropy in exploration seismics. Geophys. J. Roy. Astron. Soc. **76,** 1, pp. 79–88

HSU N. N. 1974: Acoustical birefringence and the use of ultrasonic waves for experimental stress analysis. Exp. Mech. **14,** pp. 169–176

HUGHES D. S., KELLY J. L. 1953: Second-order elastic deformation of solids. Phys. rev. **92,** 5, pp. 1145–1149

JAEGER J. C., COOK N. G. W. 1976: Fundamentals of rock mechanics. Second Edition. J. Wiley, London, New York

KING R. B., FORTUNKO C. M. 1983: Determination of in-plane residual stress states in plates using horizontally polarized shear waves. J. Appl. Phys. **54,** 6, pp. 3027–3035

KINO G. S., HUNTER J. B., JOHNSON G. C., SELFRIDGE A. R., BARNETT D. M., HERMANN G., STEELE C. R. 1979: Acoustoelastic imaging of stress fields. J. Appl. Phys. **50, 4,** pp. 2607–2613

LANDOLT-BÖRNSTEIN 1982: Numerical data and functional relationships in science and technology. Group V, Vol. 1(b): Physical properties of rocks (Angenheister G. ed.), Springer, Berlin

MAHADEVAN P. 1966: Effect of frequency on texture-induced ultrasonic wave birefringence in metals. Nature **211,** 5049, pp. 621–622

MEUTH H.-O. 1973: Werkstoffprüfung — Lebensdauer durch Zerstörung. Bild d. Wiss. **10,** pp. 42–52

MURNAGHAN F. D. 1951: Finite deformation of an elastic solid. J. Wiley, New York

NIKITIN L. V., CHESNOKOV E. M. 1984: Wave propagation in elastic media with stress-induced anisotropy. Geophys. J. Roy. Astron. Soc. **76,** 1, pp. 129–133

NORRIS A. N. 1983: Propagation of plane waves in a pre-stressed medium. J. Acoust. Soc. Am. **74,** 5, pp. 1642–1643

NUR A., SIMMONS G. 1969: Stress-induced velocity anisotropy in rock: an experimental study. J. Geophys. Res. **74,** 27, pp. 6667–6674

ROBERTS G., CRAMPIN S. 1986: Shear-wave polarizations in a hot-dry-rock geothermal reservoir: anisotropic effects of fractures. Int. J. Rock. Mech. Min. Sci. & Geomech. Abstr. **23, 4,** pp. 291–302

SAYERS C. M. 1987: Elastic wave anisotropy in the upper mantle. Geophys. J. Roy. Astron. Soc. **88,** 2, pp. 417–424

SCHNEIDER E., GOEBBELS K. 1982: Zerstörungsfreie Bestimmung von (Eigen-) Spannungen mit linear-polarisierten Ultraschallwellen. VDI-Berichte 439, pp. 91–96

SCHNEIDER E., HIRSEKORN S., GOEBBELS K. 1985: Zerstörungsfreie Bestimmung von Volumenspannungen in Bauteilen mit Walztextur durch Ultraschall-Verfahren. VDI-Berichte 552, pp. 253–264

SEEGER A., MANN E. 1959: Anwendung der nichtlinearen Elastizitätstheorie auf Fehlstellen in Kristallen. Z. Naturforschg. **14a,** pp. 154–164

SEEGER A., BUCK O. 1960: Die Ermittelung der elastischen Konstanten höherer Ordnung. Z. Naturforschg. **15a,** pp. 1056–1067

SHEARER P. M., ORCUTT J. A.: 1986: Compressional and shear wave anisotropy in the oceanic lithosphere — the Ngendei seismic refraction experiment. Geophys. J. Roy. Astron. Soc. **87,** 3, pp. 967–1003

THOMPSON R. B., SMITH J. F., LEE S. S. 1984: Microstructure-independent acoustoelastic measurement of stress. Appl. Phys. Lett. **44,** 3, pp. 296–298

THOMSEN L. 1986: Weak elastic anisotropy. Geophysics **51,** 10, pp. 1954–1966

THURSTON R. N. 1965: Effective coefficients for wave propagation in crystals under stress. J. Acoust. Soc. Amer. **37,** 2, pp. 348–356

THURSTON R. N. 1974: Waves in solids. Encyclopedia of Physics — Handbuch der Physik (Flügge S. ed.) Vol. VIa/4, Springer, Berlin

TODD T., SIMMONS G., BALDRIDGE W. S. 1973: Acoustic double refraction in low-porosity rocks. Bull. Seismol. Soc. Amer. **63,** 6/I, pp. 2007–2020

TOLSTOY I. 1982: On elastic waves in prestressed solids. J. Geophys. Res. **87,** B8, pp. 6823–6827

TÖNNIES V. C. 1986: Spannungsinduzierte Anisotropie — Untersuchungen zur Spannungsanalyse mit seismischen Verfahren. Diplomarbeit. Institut für Geophysik und Meteorologie der technischen Universität, D-3300 Braunschweig, F. R. G.

TRUESDELL C. 1961: General and exact theory of waves in finite elastic strain. In: Truesdell C. (ed.), Arch. Rational Mech. Anal. **8,** pp. 263–296, Springer, Berlin

TRUESDELL C., NOLL W. 1965: Non-linear field theories of mechanics. Encyclopedia of Physics — Handbuch der Physik (Flügge S., ed.) Vol. III/3, Springer, Berlin

TURCOTTE D. L., SCHUBERT G. 1982: Geodynamics. J. Wiley, New York, Chichester, etc.
WALTON K. 1974: The seismological effects of elastic pre-straining within the Earth. Geophys. J. Roy. Astron. Soc. **36**, 3, pp. 651–677
WINTERSTEIN D. F. 1986: Anisotropy effects in *P*-wave and *SH*-wave stacking velocities contain information on lithology. Geophysics **51**, 3, pp. 661–672
ZOBACK M. D. 1985: Recent developments of deep crustal stress measurement methods. Abstracts of the 2nd International Symposium on Observation of the Continental Crust through Drilling (of the Inter-Union Commission on the Lithosphere Coordinating Committee "Continental Drilling", organized as 4th Alfred-Wegener Conference), October 4–6, Seeheim, F.R.G.

FESZÜLTSÉG ÁLTAL KIVÁLTOTT ANIZOTRÓPIA RUGALMAS KÖZEGBEN

Ludwig ENGELHARD

A rugalmas közegekre vonatkozó lineáris Hook törvény általánosságban a nemlineáris terhelés–alakváltozás összefüggés első rendű közelítésének tekinthető, kis feszültségekre és alakváltozásokra. Ha másodrendű tagokat is figyelembe veszünk, akkor a hullámegyenlet tartalmazza a statikus feszültségek hatását a rugalmas hullámok terjedésére. Ezeket a hatásokat tárgyalja a cikk, szeizmikus szemszögből. A feszültség által okozott anizotrópia mikroszkopikus eredetéről áttekintést ad. A fedő terhelés okozta feszültségtér indukált transzverzális izotrópiát hoz létre, a horizontális tektonikai feszültségek pedig iránytól függő anizotrópiát idéznek elő, amely a vertikálisan terjedő nyiróhullámok kettős töréséhez vezet. Az eredendő és a terhelés által indukált anizotrópia megkülönböztethető az eltérő szimmetria tulajdonságok alapján.

АНИЗОТРОПИЯ, ВЫЗВАННАЯ НАПРЯЖЕНИЯМИ В УПРУГОЙ СРЕДЕ

Людвиг ЭНГЕЛЬХАРД

Линейный закон Гука, описывающий упругие среды, в общем может рассматриваться в качестве первого приближения зависимости деформации от нелинейных нагрузок, действительного при малых напряжениях и деформациях. Если учесть и члены второго порядка, то в полученном волновом уравнении будет содержаться и влияние статических нагрузок на распространение упругих волн. В статье рассматриваются именно эти соотношения с упором на сейсморазведку. Дается обзор микроскопического происхождения анизотропии, вызванной напряжениями. Полем напряжений, возникающим из-за нагрузок со стороны кровли, обуславливается поперечная изотропность, в то время как горизонтальными тектоническими напряжениями вызывается азимутальная анизотропия, приводящая к двойному преломлению поперечных волн распространяющихся в вертикальном направлении. Первичная и вызванная нагрузками анизотропия может различаться по неодинаковым особенностям симметрии.

GEOPHYSICAL TRANSACTIONS 1988
Vol. 34. No. 1. pp. 83—99

THE GEOLOGICAL AND INDUSTRIAL IMPLICATIONS OF EXTENSIVE-DILATANCY ANISOTROPY*

Stuart CRAMPIN**

Extensive-dilatancy anisotropy (EDA) is the hypothesized distribution of stress-aligned fluid-filled microcracks pervading most rocks in the Earth's crust. The geometry of the EDA cracks and the aligning stress-field can be monitored by analysing the waveforms of shear waves propagating through the rockmass. The ability to estimate some of the parameters of the crack and stress geometry by analysing shear-wave particle displacements has widespread implications.

Keywords: anisotropy, dilatancy, microcracks, *S*-waves, birefringence, shear-wave splitting, earthquake prediction

1. Introduction

An anisotropic solid contains an internal structure such as aligned crystals or aligned cracks so that the elastic behaviour varies with direction. This contrasts with a uniform isotropic solid where the properties are the same in all directions. Such anisotropy in rocks in the Earth would have two major effects on seismic wave propagation. Firstly the velocities of both *P*-waves (with longitudinal particle motion) and shear waves (with transverse motion) vary with the direction of propagation. Second, on entering a region of anisotropy, shear waves split into the two (or more) phases with fixed velocities and fixed polarizations that propagate in that particular direction through the anisotropy.

Until recently, most seismic investigations in the Earth's crust were confined to *P*-waves recorded on vertical-component instruments. It was found that layers and blocks of isotropic rock can model *P*-wave arrival times with considerable accuracy. The fact that many rocks are crystalline and anisotropic on a small scale was interpreted as indicating that the orientation of the anisotropy was sufficiently random at larger scales that the comparatively long-wavelength seismic waves sample only the average (isotropic) properties of the rockmass [EWING et al. 1957]. In addition, it is difficult to recognize smooth variations of *P*-wave or shear-wave velocities unless arrival times can be observed over a wide range of directions in a single homogeneous layer, and this is seldom possible in the usually complicated crustal structure. Thus shear-wave splitting is likely to be the most reliable indicator of anisotropy in the crust. It is only in the last three or four years that digital recording and analysis technology has

* The paper is a reprint of *Nature* Vol. 328. No. 6130 (Aug. 1987), pp. 491—496, with the permission of the Editor

** British Geological Survey, Murchison House, West Mains Road, Edinburgh EH9 3LA, UK

advanced sufficiently for shear-wave splitting to be easily recorded and identified in short-period shear waves.

Shear-wave splitting, also known as birefringence and double refraction, is diagnostic of some form of effective anisotropy along the raypath [CRAMPIN 1978, 1981]. Following the recognition that such behaviour would be expected in propagation through aligned microcracks, it was suggested [CRAMPIN 1978] that it might be possible to monitor earthquake dilatancy by analysing shear waves recorded above small earthquakes. (Dilatancy is the increase in volume as microcracks open before failure in rock specimens subjected to laboratory stresses greater than half the eventual fracture strength of the intact sample [BRACE et al. 1966]).

2. Observational evidence

To try to detect such shear-wave splitting, closely spaced networks of three-component seismometers were deployed above a swarm of small earthquakes near the North Anatolian Fault (NAF) in Turkey. These Turkish Dilatancy Projects operated for a few months in 1979 (TDP1), a few months in 1980 (TDP2), and for six months in 1984 (TDP3 — currently being analysed). Shear-wave splitting was indentified [CRAMPIN et al. 1980, BOOTH et al. 1985, CRAMPIN et al. 1985] in all shear wavetrains recorded within the shear-wave window at the surface (the shear-wave window is defined by an angle of incidence less than the critical angle $\sin^{-1} Vs/Vp$ — approximately 35° for Poisson's ratio of 0.25 [EVANS 1984, BOOTH and CRAMPIN 1985]). The shear waves were scattered (this is now recognized as being caused principally by interactions with the irregular surface topography) but displayed remarkably consistent alignment of the shear-wave polarizations. The polarizations of the leading (faster) split shear waves were parallel to the direction of maximum horizontal compression along that particular section of the NAF [CRAMPIN and BOOTH 1985]. The parallel orientations and several other features of the records are consistent with propagation through the effective anisotropy of uniform distributions of parallel vertical water-filled microcracks striking perpendicular to the (horizontal) minimum compressional stress [CRAMPIN and BOOTH 1985]. The seismograms indicate anisotropy (the crack distribution) throughout the region surrounding the swarm not just near the stress-concentrations immediately adjacent to the focus [CRAMPIN and BOOTH 1985].

Shear-wave splitting above small earthquakes and parallel polarizations have now been widely observed in many places around the world *(Table I)*, and there are no counter examples where short-period shear waves recorded subsurface or within the shear-wave window at the surface do not show evidence of shear-wave splitting. Particularly important observations are that temporal variations in the shear-wave splitting have been recognized in two seismic gaps where large earthquakes are expected [PEACOCK et al. 1988, CHEN et al. 1986]. Shear-

wave splitting has also been observed: above acoustic events in geothermal experiments [KANESHIMA et al. 1986, ROBERTS and CRAMPIN 1986]; in shear-wave vertical-seismic-profiles (VSPs) in a geothermal reservoir [MAJER et al. 1985, DALEY et al. 1986], in sedimentary basins [CRAMPIN and BUSH 1986, CRAMPIN, BUSH et al. 1986, JOHNSTON 1986, BECKER and PERELBERG 1986], and elsewhere [LEARY and LI 1986, LI et al. 1986]; and in most shear-wave reflection surveys made for exploration and production purposes in hydrocarbon reservoirs [ALFORD 1986, WILLIS et al. 1986]. The polarizations of the shear waves in the geothermal reservoir [MAJER et al. 1985, DALEY et al. 1986] are directly related to visible macro-fractures, and the oil company reflection surveys and VSPs interpreted as indicating the orientation of subsurface fractures [JOHNSTON 1986, BECKER and PERELBERG 1986, ALFORD 1986, WILLIS et al. 1986].

Table I. Seismic observations of seismic anisotropy in the crust

I. táblázat A kéregbeli szeizmikus anizotrópia megfigyelései szeizmikus módszerekkel

Таблица I. Наблюдение за сейсмической анизотропией земной коры сейсмическими методами.

Location	Rock type	Earthquake mechanisms	Shear-wave alignments		References
			Station	Network	
Shear-wave splitting above small earthquakes:					
North Anatolian Fault, Turkey	Sediments, metamorphic	Strike-slip	Parallel	Parallel	CRAMPIN et al. 1980, BOOTH et al. 1985, CRAMPIN and BOOTH 1985
Peter the First Range, USSR	Poorly consolidated sediments	Thrust	Parallel	Parallel	CRAMPIN, BOOTH et al. 1986
North Wales, UK	Granite, slate, metamorphic	Strike-slip	Parallel	Various	PEACOCK 1985
Kinki District, Japan	Granite, slate, sediments	Strike-slip	Parallel (granite, sedi-ments), scattered (slate)	Parallel (granite, sedi-ments), scattered (slate)	KANESHIMA et al. 1987
Kyushu, Japan	Various	Normal	Parallel	Various	KANESHIMA et al. 1986
Quebec, Canada	Sediments	Strike-slip	Parallel	Parallel	BUCHBINDER 1985
Anza, California, USA	Various	Strike-slip	Parallel	Various	PEACOCK et al.

Table I. continued

Shear-wave splitting above shallow events in geothermal reservoirs:

Takinoue, Japan	Metamorphic	–	Parallel	Parallel	Kaneshima et al. 1986
Cornwall, UK	Granite	–	Parallel	Parallel	Roberts and Crampin 1986

Shear-wave splitting in VSPs:

Paris Basin, France	Sandstone, shale	–	*	*	Crampin and Bush 1986
Texas, USA	Austin chalk	–	*	–	Johnston 1986, Becker and Perelberg 1986
Four sites in California	Various	–	*	–	Li et al. 1986, Leary and Li 1986, Majer et al. 1985, Daley et al. 1986

Shear-wave splitting in reflection surveys:

Twelve sites across North America	Various	–	*	–	Alford 1986, Willis et al. 1986

Velocity anisotropy in refracted *P*-waves:

Mount Hood, Oregon, USA	Metamorphic	–	–	–	Crampin et al. 1986

* Impulsive shear wave arrivals from earthquakes usually possess easily identifiable polarizations. Emergent harmonic arrivals from shear-wave vibrators can only be interpreted accurately by modelling with synthetic seismograms.

3. Shear-wave splitting

The many complications of the shear wavetrain were attributed in the past to scattering at (unspecified) heterogeneities. Recent observations of shear-wave splitting and the remarkable parallelism of the polarizations clearly indicate an internal structure (anisotropy) and not a random distribution of scatterers. Any single observation of shear-wave splitting can usually be simulated by propaga-

tion through a combination of isotropic discontinuities. However, the almost universal presence of shear-wave splitting and the uniform alignment of the leading shear waves normal to the direction of minimum compressional stress cannot be explained by any realistic combination of isotropic structures [CRAMPIN et al. 1984, CRAMPIN 1985a], and the uniformity of the observations in Table I suggests that some form of effective anisotropy is present in most crustal rocks.

In seeking the cause of this seismic anisotropy, three phenomena appear to be critical:

(a) the almost universal presence of anisotropy in many types of rocks at many depths and in many geological and tectonic environments [CRAMPIN and BOOTH 1985, ROBERTS and CRAMPIN 1986, ALFORD 1986, WILLIS et al. 1986];
(b) the uniformity of the alignment of the polarization of the leading split shear waves [BOOTH et al. 1985, CRAMPIN, BOOTH et al. 1986, PEACOCK et al. 1988, ROBERTS and CRAMPIN 1986] normal to the current minimum horizontal compression; and
(c) the temporal variations of the behaviour of shear-wave splitting in seismic gaps [PEACOCK et al. 1988, CHEN et al. 1986].

The explanation for these phenomena must be sought among the five major causes of seismic anisotropy in the Earth identified in a recent review [CRAMPIN, CHESNOKOV et al. 1984].

Aligned crystals. Crystals may be aligned by stress by creep and re-crystallization. This can only occur at temperatures greater than those usually found in the relatively cool upper crust where splitting is observed [BOOTH et al. 1985, CRAMPIN, BOOTH et al. 1986, ROBERTS and CRAMPIN 1986]. Splitting also occurs in poorly consolidated and contorted sedimentary sequences where uniformly aligned crystals are unlikely to be present [CRAMPIN, BOOTH et al. 1986].

Lithologic anisotropy caused by a fabric such as aligned grains. Any lithologic anisotropy is likely to be confined to particular rock strata, will show little time variation, and cannot satisfy (a), (b) and (c) above.

Long-wavelength anisotropy such as that caused by periodic thin layers. Again, such anisotropy is likely to be limited in space and fixed in time, and cannot satisfy the three critical observations.

Direct stress-induced anisotropy. Direct stress-induced anisotropy only becomes significant when the stress becomes a large proportion of the eventual fracture strength. This could be important at stress concentrations very close to the extremities of faults, but the stress in stable areas where splitting has also been observed is probably several orders of magnitude too small to cause observable effects [DAHLEN 1972]. In any case, rock physics experiments demonstrate that rocks deform by dilatancy (opening of microcracks) before direct stress-induced anisotropy becomes significant [BRACE et al. 1966].

Crack-induced anisotropy caused by aligned cracks and microcracks. The next sections argue that cracks and particularly microcracks are universally present in the crust, are aligned by the current stress-field and, most important, have configurations which can be easily modified by changes in stress on a short enough time-scale to cause the observed temporal variations.

4. Extensive-dilatancy anisotropy

Distributions of stress-aligned fluid-filled microcracks must be expected in the crust [FYFE et al. 1978]. Every sedimentary rock retains water in its interstices after deposition, and the long enduring regional stress-fields will tend to align the pore space normal to the minimum compressional stress by such processes as subcritical crack-growth [ATKINSON 1984]. This will not result in perfectly flat parallel microcracks but it may cause sufficient flattening of the pore space to be anisotropic to shear waves as the observed anisotropy is relatively weak. Such effects have been demonstrated in rock physics experiments [RAI and HANSON 1986] (but at larger stresses in order to obtain results at an acceptable time scale). Similarly, prograde metamorphic processes release chemically bound water from most igneous rocks [FYFE et al. 1978] and the only mechanism for such water to be released is by hydraulic fracture [FYFE et al. 1978] at high pore-fluid pressures into inter- and intra-granular microcracks which will again be aligned normal to the minimum compressional stress. Thus distributions of cracks and (principally) microcracks must exist within the in situ rockmass, and although their geometry can be modified by stress, they are not directly stress-induced. This phenomenon of stress-aligned cracks, originally recognized above earthquake foci, is known as extensive-dilatancy anisotropy (EDA) [CRAMPIN, EVANS et al. 1984], and has now been recognized throughout much of the crust [CRAMPIN 1985a, CRAMPIN and ATKINSON 1985]. Typical observations of shear-wave splitting suggest a maximum differential velocity-anisotropy of about 4% yielding a crack density of $Na^3/V = 0.04$ where N is the number of cracks of radius a in a volume V. This is equivalent to a crack of diameter 0.7 in each unit cube.

One of the fundamental difficulties of testing this hypothesis of EDA cracks is that in situ microcracks in the crust are essentially inaccessible to physical examination. *Table II* lists twenty largely independent phenomena controlling the behaviour of (isolated) fluid-filled microcracks at depth in the crust [CRAMPIN 1985a, CRAMPIN and ATKINSON 1985]. The effects of almost all of these phenomena are directly or indirectly controlled by stress. This means that whenever we approach in situ microcracks by drilling, mining, or excavating, the rock is disturbed by partial de-stressing, and a new stress anomaly imposed. Since isolated fluid-filled microcracks are probably a comparatively mobile phenomenon in the crust, the in situ microcrack geometry is usually destroyed. Even well logs, which may appear to be examining in situ conditions, are sampling material which has the original stress-field severely modified and the in situ microcrack geometry is disturbed within a metre or two of the wellbore. In situ microcracks are likely to leave residual traces in the rock, but because EDA cracks are frequently isolated microcracks in igneous and metamorphic rocks and are pores with (usually) weak preferred orientations in sedimentary rocks, there are also considerable difficulties in examining traces of EDA in the rock physics laboratory. Extrapolating from conditions in the rock physics laboratory to in situ conditions requires extreme caution and, as Table II

suggests, requires a multi-variable extrapolation over many orders of magnitude, only a few of which can be monitored at any one time in the laboratory. This inaccessibility means that seismic shear waves are the principal technique for monitoring crack properties in situ and the exact configuration of EDA cracks can only be estimated.

Since the wavelengths of shear waves are many times the likely crack dimensions, shear waves can give us little information about the crack dimensions. However, the dimensions of EDA cracks are likely to span several orders of magnitude. In intact igneous and metamorphic rocks, the dimensions may vary from submicrometre to a few tens of micrometres and are initially isolated with few connections to other cracks. In sedimentary rocks, the EDA cracks may be larger, up to 1 or 2 mm in some rocks, and may be merely the oriented portion of a randomly oriented pore-space of much greater porosity. In fractured beds the crack dimensions may be several metres. We use the term "EDA cracks" to include this wide range of phenomena. All EDA cracks are likely to have high pore-fluid pressures equalling the lithostatic stress but possible very low porosities particularly in igneous and metamorphic rocks.

Table II. Phenomena controlling the behaviour of in situ cracks

II. táblázat. A repedések in situ viselkedését befolyásoló jelenségek

Таблица II. Явления, контролирующие поведение трещин в массиве.

External conditions:

(1) Lithostatic stress
(2) Deviatoric stress
(3) Temperature
(4) Properties of rockmass

Internal conditions:

(5) Pore-fluid pressure
(6) Compressibilty of pore-fluid
(7) Viscosity of pore-fluid
(8) Debris in crack void
(9) Vapour/liquid ratio in pore-fluid
(10) Properties of pore-fluid under high temperatures and pressures

Dynamic conditions:

(11) Rate of strain
(12) Rate of crack healing
(13) Rate of crack growth

Crack parameters:

(14) Orientation
(15) Dimensions
(16) Aspect ratio
(17) Distribution
(18) Smoothness of crack faces
(19) Connectedness (degree of isolation)
(20) Geometry (parallel, biplanar, etc.)

Shear waves are very sensitive to the interaction with the free surface and although the general character of the patterns of polarization can be modelled with synthetic seismograms [CRAMPIN and BOOTH 1985], exact matching of observations and synthetics at the surface is unlikely to be possible except in exceptionally simple structures. This means that subsurface recordings in VSPs

are going to be particularly important for determining the properties of EDA cracks.

The only set of three-component shear-wave VSPs to modelled by synthetics at this time (in the sedimentary sequences of the Paris Basin) [CRAMPIN and BUSH 1986, CRAMPIN, BUSH et al. 1986] provides the first quantitative evaluation of EDA cracks. The detailed waveforms of shear waves recorded downwell from shear-wave vibrators from a wide range of offsets on the surface are well-matched by synthetic seismograms of shear-waves propagating through a very simple two-layered model containing a weak distribution of parallel liquid-filled microcracks (crack densities of 0.03 and 0.01 respectively). The microcracks strike parallel to the direction of horizontal compressional stress [CRAMPIN and BUSH 1986, CRAMPIN, BUSH et al. 1986].

A similar quantitative evaluation was also obtained from azimuthal velocity variations of *P*-waves in a refraction survey around Mount Hood, Oregon [KOHLER et al. 1982]. The velocity variations were interpreted in terms of fluid-filled microcracks, which because of the high heat-flow around Mount Hood may indicate the presence of fluid-filled microcracks throughout most of the crust [CRAMPIN, MCGONIGLE et al. 1986]. It should be noted that such *P*-wave studies are limited to studies of horizontally propagating head-waves, and are unlikely to be repeated very frequently as the survey around Mount Hood was exceptionally comprehensive with hundreds of source to geophone paths in a comparatively small area.

Originally proposed as existing only around earthquake foci [CRAMPIN, EVANS et al. 1984], there is now a large amount of evidence (Table I) that suggest that EDA cracks exist in many (perhaps most) rocks in the crust [CRAMPIN 1985b, CRAMPIN and ATKINSON 1985], and shear-wave splitting as an indicator of subsurface fracture alignments is now being investigated by the hydrocarbon industry [CRAMPIN and BUSH 1986, CRAMPIN, BUSH et al. 1986, JOHNSTON 1986, BECKER and PERELBERG 1986, ALFORD 1986, WILLIS et al. 1986]. Seismic evidence in the papers cited in Table I suggest that most rocks in at least the upper 10 to 20 km of the brittle crust contain EDA cracks. The cracks are typically aligned vertically and perpendicular to the (usually horizontal) minimum compressional stress. Recognition that distributions of EDA cracks exist in most rocks is, I suggest, a fundamental advance in our understanding of the physical state of in situ rock which has many geological and industrial implications [CRAMPIN 1985b, CRAMPIN and ATKINSON 1985].

5. Geological implications

The presence of fluids at all levels in the Earth's crust is well established [FYFE et al. 1978], although the mechanism by which fluids are retained at necessarily high pore-fluid pressures at depths in the crust has not previously been specified. FYFE et al. suggest, for example, that most fluids are retained in cracks (veins) and fractures, and the implication that metamorphic hydraulic

fracture releases connate water from most grains into (initially isolated) microcracks throughout the rockmass is not followed through. The evidence referred to above suggests that many rocks in the crust contain an internal structure of fluid-filled EDA microcracks aligned by the contemporary regional stress field. EDA cracks provide a mechanism for the presence of fluids in the crust, and are, I suggest, the primary cause of a wide variety of previously unrelated phenomena:

High pore-fluid pressures necessary for fault movements. Many tectonic processes, particularly thrust faulting, require high pore-fluid pressures to reduce the normal stresses sufficiently to allow slippage to occur. Fluids from even low porosity EDA cracks will be concentrated and channelled by subcritical crack-growth at high-stress concentrations into regions of higher dilatancy near the eventual fault zone. The fault planes will be lubricated, frictional forces reduced, and slippage may occur.

Flexibility of crustal plates. The presence of EDA cracks allows large crustal plates and blocks to deform to accomodate small changes of strain imposed by plate tectonics and fault movements. This tends to reduce earthquake activity so that relatively aseismic areas may exist within plates and blocks moving over the surface of a non-spherical mantle and undergoing deformation around their margins.

Main driving mechanism for earthquake precursors. Modifications and manipulations of EDA cracks by stress changes are the common driving mechanisms for the large variety of precursors that are intermittently observed before earthquakes. Since EDA cracks are necessarily aligned and their effects anisotropic, each precursory phenomenon will depend on the geometry of the particular earthquake stress-field, the geological structure, and the geometry of the recording sites [CRAMPIN 1978]. Thus, the search for particular precursors may be difficult and lead to inpredictable results.

Relative P- and S-wave attenuation. The theoretical attenuation due to scattering at crack margins of shear-waves propagating through liquid-filled cracks is greater than the theoretical attenuation of *P*-waves by more than three times (sometimes much more, depending on direction) [CRAMPIN 1984]. This is approximately the relative attenuation observed in the Earth. The attenuation caused by propagation through liquid-filled cracks is not well understood. Although the effects of scattering at crack margins are too small, the introduction of a small gas bubble or turbulent flow could increase the attenuation by orders of magnitude. Thus EDA cracks are certainly one of the causes for the greater shear-wave attenuation in the Earth, and the variation of attenuation with azimuth and incidence angle is the reason for some of the inconsistencies in observations of attenuation in the crust. It is worth noting that because distributions of microcracks change the effective elastic constants of the matrix, the microcracks may affect a wide range of seismic wavelengths.

Relative terrestrial and lunar attenuation. The marked difference in attenuation between the Earth and the Moon is usually attributed to the lack of evaporites on the Moon [GOINS et al. 1981]. In the Earth's crust (and by implication,

the mantle, since isolated inclusions of melt or other fluids in the mantle are also not going to be easily closed by lithostatic stress), the attenuation is principally the result of scattering by fluid-filled EDA cracks. In the Moon, where there are no pore-fluid pressures to keep cracks open, cracks will be closed or absent and there will be little attenuation.

High conductivity deep in the crust. The electrical conductivity at all levels in the crust is anomalously high by several orders of magnitude relative to dry rocks in the laboratory [SHANKLAND and ANDER 1983], and may vary with azimuth by an order of magnitude. The high conductivity and the variation with azimuth are the result of aligned fluid-filled EDA cracks both at shallow depths, as measured by well logs, and at deeper depths (down to 20 km) as determined by large-aperture long-period measurements at the surface.

6. Earthquake prediction research

The variety of precursors, which are sporadically observed before earthquakes, are usually ascribed to the indirect effects of the variation of stress. The most direct effects of changes of stress are modifications of the configurations of the EDA cracks in the stressed rockmass. Since the behaviour of shear waves is controlled by three-dimensional variations in the crack geometry, it is probable that analyses of shear-wave splitting could lead to direct determinations of changes in the crack configuration and hence stress changes, and thus offer a technique for earthquake prediction. No larger event has yet been "captured" within any of the small number of existing three-component seismometer networks and no definite changes in the configuration of EDA cracks has yet been recognized, although some possible temporal changes may have been identified (see the paragraph referring to aspect ratio below).

There are several ways in which changes of stress may alter the configuration of EDA cracks:

Changes in the orientation of the cracks. Changes in the direction of stress are likely to alter the orientation of EDA cracks. This would result in changes in the shear-wave polarizations, which are the most easily identifiable and stable parameters of shear-wave splitting. However, stress changes before an earthquake are usually confined to modifying the magnitude of the stress but preserving the same principal axes. This would not alter crack orientations and there would be no change in shear-wave polarizations. BOOTH et al. [1985] and CRAMPIN and BOOTH [1985] observed possible changes in the polarization direction near one of the TDP sites in Turkey between 1979 and 1980, and suggested that it might have been caused by local stress polarization anomalies. However, the same polarizations are seen to persist in TDP3 and the anomalies are now thought to be caused by the interactions of the shear-wave arrivals with the very steep local topography.

Changes in crack density. Increasing stress is likely to increase crack densities by promoting crack growth (by subcritical crack growth [ATKINSON 1984])

rather than by opening new cracks, which occurs only at high stress [BRACE et al. 1966]. Increasing crack density would increase the differential shear-wave anisotropy and increase the time delay between the split shear waves. This should be recognizable if exactly repeatable sources of shear waves can be monitored with the same instrumental networks (see below).

Changes of crack aspect-ratio. The direct elastic effect of increasing stress on a rock containing EDA cracks is likely to increase the aspect ratio (similar to the increasing conventional high-stress dilatancy in rock specimens subject to uniaxial compression). This would have most effect on modifying the time delays between shear-waves propagating at between 40° and 80° to the crack normal [CRAMPIN et al. 1986, CRAMPIN and BUSH 1986]. PEACOCK et al. [1988] have reported temporal changes in shear-wave splitting at a seismic station near the Anza seismic gap in California that could be interpreted as stress-induced increases of the aspect ratio of EDA cracks during the build-up of stress before the expected large earthquake. If this is the first observation of a precursory variation in shear-wave splitting, it could be a very important breakthrough in earthquake prediction research.

Changes of pore-fluid content. The dilatancy-diffusion theory of earthquake precursors suggested that changes of stress could cause fluids to drain from dilated cracks modifying wave propagation through the cracked rock [AGGARWAL et al. 1973]. It is suggested here that this phenomenon is unlikely to occur for small often-isolated EDA cracks except at high stress concentrations in a limited volume in the immediate vicinity of a fault (but see the next paragraph). The limited volume is likely to be too small to affect shear waves significantly.

Changes of pore-fluid pressure. Changing the dimensions of cracks by crack growth or changing aspect-ratio is likely to alter the pore-fluid pressure (at least temporarily). Significant increases of aspect-ratio may lead to under-saturation and the introduction of small vapour-filled bubbles into the cracks. Variations of pore-fluid pressure and particularly the introduction of small bubbles have little direct effect of seismic velocities and are unlikely to be easily recognized in patterns of particle displacement. The largest effect of the introduction of bubbles will be to increase attenuation. Attenuation, however, is difficult to monitor from earthquake sources, but changes in attenuation should be easily recognized if experiments can be repeated with identical sources (see below).

The principal effect of changes in aspect ratio, the parameter most likely to be modified by changes of stress, is that the time delay between the split shear waves will be modified. Since shear waves have severe interactions with the free surface [EVANS 1984, BOOTH and CRAMPIN 1985], and small earthquakes have unrepeatable source radiation [EVANS et al. 1985], it is unlikely that time delays can be accurately monitored using surface recordings of natural events. However, three-component VSPs using repeated shear-wave sources are likely to be very sensitive to even small changes in time delays, and repeated shear-wave VSPs is the preferred technique for monitoring small changes in the stress field and hence for predicting earthquakes.

Shear-wave VSPs would also allow changes in attenuation to be monitored.

Many of the changes discussed above, particularly increases in aspect ratio, are expected to modify the shear-wave attenuation. This has received little attention in the past because all existing investigations have used earthquake sources which are too arbitrary to enable attenuation to be monitored.

Since modifying EDA cracks is the most direct effect of changes of stress before earthquakes, and since analyzing EDA cracks is the only way that the essentially anisotropic nature of all stress-induced effects can be explored, monitoring shear-wave splitting with shear-wave VSPs could be a very promising technique for earthquake prediction research.

7. Industrial implications

Cracks and stress are frequently crucially important in drilling, mining, or excavating, and the ability to monitor the geometry of cracks and stress by analysis of, particularly, shear-wave VSPs has a number of possibly very important applications. The following list is not exhaustive.

Predicting orientations of hydraulic fractures. The orientations of stress-aligned EDA cracks, which may be estimated by analysing the waveforms of shear waves, predict the orientations of any subsequent hydraulic fractures. This has been demonstrated at the hot-dry-rock geothermal experiment in Cornwall [ROBERTS and CRAMPIN 1986]. The polarizations of shear waves recorded at the surface from a very small acoustic event, stimulated when testing the hydraulic equipment, had the same polarizations as those from larger events when the fracture system was established and both were oriented parallel to the strike of the major hydraulic fractures [ROBERTS and CRAMPIN 1986]. This demonstrates that the internal structure of aligned EDA cracks in the rockmass existed before the structure of major hydraulic fractures was established, and that both crack geometries had the same anisotropic symmetry. Modelling the detailed waveforms of the shear waves with synthetic seismograms [CRAMPIN, BUSH et al. 1986] demonstrates that three-component shear-wave VSPs are likely to be a more accurate technique for estimating crack and stress orientations than monitoring recordings made at the surface.

Estimating internal structure of hydrocarbon reservoirs. The analysis of shear-wave VSPs provide direct geophysical information about the in situ reservoir rock, which can be related to preferred directions of flow and other properties of the reservoir. Detailed modelling of shear waveforms in three-component shear-wave VSPs [CRAMPIN and BUSH 1986, CRAMPIN, BUSH et al. 1986] yields accurate estimates of the internal structure throughout the rockmass surrounding the well, not just in the immediate vicinity of the well hole which may be anomalous. This is a new source of directly interpretable information which could be important for the appraisal and evaluation of hydrocarbon reservoirs and for optimizing production strategies for secondary and tertiary recovery.

Investigating the geometry of fractures in geothermal reservoirs. Shear waveforms, particularly in VSPs, can yield estimates of orientations of in situ microcracks and macrofractures in both wet and hot-dry-rock geothermal reservoirs [ROBERTS and CRAMPIN 1986, MAJER et al. 1985], although at present none have been fully interpreted. Recording the wavetrains of acoustic events on three-component geophones downwell in the centre of the cracked reservoir is likely to be particularly informative, since the behaviour of the wavetrains is controlled by the separations of the major hydraulic fractures and the penetration of the cooling cracks normal to the major crack faces.

Investigating nuclear waste depositories in solid rock. Estimating the orientations of EDA cracks by VSPs before nuclear waste disposal in a repository in intact rock (possibly clay) will indicate the orientations of eventual thermal-expansion or leakage cracks and allow the position of the depository to be optimized. Similarly, repeated VSPs after deposition shoud allow the extent of the cracking to be monitored.

Investigating rockbursts in mines. Rockbursts are explosive breakouts of walls or roofs which occur in some mines and may cause extensive loss of life and equipment. Shear-wave splitting caused by EDA cracks has been observed in mines [NICOLAYSEN 1987, YOUNG in press]. Investigating such cracks by monitoring shear waves is likely to demonstrate the detailed stress variations prior to rockbursts. The particular importance to earthquake and rockburst prediction research is that the source of rock bursts can be dissected after the event so that the relics of the crack behaviour at the source can be examined [NICOLAYSEN 1987]. This could lead to important advances in understanding source processes.

Estimating slope stability. EDA cracks appear to exist in all types of rock from poorly consolidated sediments [CRAMPIN, BOOTH et al. 1986] to hard igneous rock [BOOTH et al. 1985, KANESHIMA et al. 1987]. EDA cracks in unstable slopes are likely to display larger crack densities (probably by crack growth rather than by new cracks opening) and larger aspect ratios as the instability increases. Such changes in crack configurations could be monitored by analysing shear waves in repeated cross-hole or VSP experiments using shear-wave sources.

Estimating overburden fractures in open-cast mining. It is necessary to obtain estimates of overburden fracture density in order to optimize the use of expensive mining equipment in open-cast mining [YOUNG and HILL 1986]. Recording shear waves with three-component geophones in cross-hole shooting, or VSPs appropriate, should yield detailed estimates of crack geometry and crack density.

8. Discussion

The previous sections suggest some of the possible implications and applications of monitoring EDA cracks with shear waves. Estimating the internal structure (fracture orientations) of reservoirs is already being investigated by the

hydrocarbon industry [JOHNSTON 1986, BECKER and PERELBERG 1986, ALFORD 1986, WILLIS et al. 1986]. Since shear wavetrains contain three or four times more information about the structure along the raypath and the source than the equivalent *P*-wavetrain [CRAMPIN 1985b], it is clear that monitoring shear waves has great potential for many earth science investigations.

One of the major reasons why EDA cracks have not been recognized earlier is that the majority of short-period seismic investigations in the Earth's crust have been restricted in the past to analysis of *P*-wave arrival-times for which single-component vertical seismometers provide adequate recordings. Thin liquid-filled cracks have very little effect on *P*-wave propagation [CRAMPIN 1978, 1981, 1984] and the isotropic *P*-wave velocity models, that have been so enormously successful in describing the shallow Earth structure, are generally valid. The internal structure of aligned EDA cracks only becomes apparent if shear-wave splitting is recorded by three-component digital recorders so that polarization diagrams can be monitored. As yet there are comparatively few suitable recordings in either earthquake or exploration seismology, although the number is rapidly increasing now that the importance of anisotropy has been recognized.

It appears that the presence of EDA microcracks and the ability to monitor crack and stress geometry with shear waves opens new ways of examining in situ rocks (and possibly other solids) that is likely to have important implications and applications over a very wide field. The modelling of three-component shear waves in VSPs in the Paris Basin [CRAMPIN and BUSH 1986, CRAMPIN, BUSH et al. 1986] is the first time that the detailed waveforms of short-period shear waves have been successfully modelled by synthetic seismograms. Since shear waves contain so much more information than *P*-waves [CRAMPIN 1985b], the developments reviewed here are potentially very significant.

Acknowledgements

I thank David C. Booth for his comments on the manuscript. The work was supported by the Natural Environment Research Council (NERC) with some indirect support from the United States Geological Survey (USGS).

REFERENCES

AGGARWAL Y. P., SYKES L. R., ARMBRUSTER J., SBAR M. L. 1973: Premonitory changes in seismic velocities and prediction of earthquakes. Nature **241**, 5385, pp. 101–104

ALFORD R. M. 1986: Shear data in the presence of azimuthal anisotropy. Expanded Abstracts, 56th Ann. Int. SEG Meeting, Houston, pp. 476–479

ATKINSON B. K. 1984: Subcritical crack growth in geological materials. J. Geophys. Res. **89**, 86, pp. 4077–4114

BECKER D. F. and PERELBERG A. I. 1986: Seismic detection of subsurface fractures. Expanded Abstracts, 56th Ann. Int. SEG Meeting, Houston, pp. 466–468

BOOTH D. C. and CRAMPIN S. 1985: Shear-wave polarization on a curved wave front at an isotropic free surface. Geophys. J. R. Astr. Soc. **83**, 1, pp. 31–45

BOOTH D. C., CRAMPIN S., EVANS R., ROBERTS G. 1985: Shear-wave polarization near the North Anatolian Fault—I. Evidence for anisotropy-induced shear-wave splitting. Geophys. J. R. Astr. Soc. **83,** 1, pp. 61–73

BRACE W. F., PAULDING B. W., SCHOLTZ C. 1966: Dilatancy in the Fracture of Crystalline Rocks. J. Geophys. Res. **71,** 16, pp. 3939–3953

BUCHBINDER G. G. R. 1985: Shear-wave splitting and anisotropy in the Charlevoix seismic zone. Quebec. Geophys. Res. Lett. **121,** pp. 425–428

CHEN T.-C., BOOTH D. C., CRAMPIN S. 1986: Temporal variations in shear-wave splitting: observations near the North Anatolian Fault 1979–1984. EOS **67,** 44, p. 1117

CRAMPIN S. 1978: Seismic-wave propagation through a cracked solid: polarization as a possible dilatancy diagnostic. Geophys. J. R. Astr. Soc. **53,** 3, pp. 467–496

CRAMPIN S. 1981: A review of wave motion in anisotropic and cracked elastic media. Wave Motion **3,** pp. 343–391

CRAMPIN S. 1984: Effective anisotropic elastic constants for wave propagation through cracked solids. Geophys. J. R. Astr. Soc. **76,** 1, pp. 135–145

CRAMPIN S. 1985a: Evidence for aligned cracks in the Earth's crust. First Break **3,** 3, pp. 12–15

CRAMPIN S. 1985b: Evaluation of anisotropy by shear-wave splitting. Geophysics **50,** 1, pp. 142–152

CRAMPIN S., EVANS R., ÜÇER S. B., DOYLE M., DAVIS J. P., YEGORKINA G. V., MILLER A. 1980: Observations of dilatancy-induced polarization anomalies and earthquake prediction. Nature **286,** 5776, pp. 874–877

CRAMPIN S., EVANS R., ATKINSON B. K. 1984: Earthquake prediction: a new physical basis. Geophys. J. R. Astr. Soc. **76,** 1, pp. 147–156

CRAMPIN S., CHESNOKOV E. M., HIPKIN R. G. 1984: Seismic anisotropy — the state of the art: II. Geophys. J. R. Astr. Soc. **76,** 1, pp. 1–16

CRAMPIN S., EVANS R., ÜCER S. B. 1985: Analysis of records of local earthquakes: the Turkish Dilatancy Projects (TDP1 and TDP2). Geophys. J. R. Astr. Soc. **83,** 1, pp. 1–16

CRAMPIN S. and BOOTH D. C. 1985: Shear-wave polarizations near the North Anatolian Fault — II. Interpretation in terms of crack-induced anisotropy. Geophys. J. R. Astr. Soc. **83,** 1, pp. 75–92

CRAMPIN S. and ATKINSON B. K. 1985: Microcracks in the Earth's crust. First Break **3,** 3, pp. 16–20

CRAMPIN S., BOOTH D. C., KRASNOVA M. A., CHESNOKOV E. M., MAXIMOV A. B., TARASOV N. T. 1986: Shear-wave polarizations in the Peter the First Range indicating crack-induced anisotropy in a thrust-fault regime. Geophys. J. R. Astr. Soc. **84,** 2, pp. 401–412

CRAMPIN S. and BUSH I. 1986: Shear-waves revealed: extensive-dilatancy anisotropy confirmed. Expanded Abstracts, 56th Ann. Int. SEG Meeting, Houston, pp. 481–484

CRAMPIN S., MCGONIGLE R., ANDO M. 1986: Extensive-dilatancy anisotropy beneath Mount Hood, Oregon and the effect of aspect ratio on seismic velocities through aligned cracks. J. Geophys. Res. **91,** B12, pp. 12703–12710

CRAMPIN S., BUSH I., NAVILLE C., TAYLOR D. B. 1986: Estimating the internal structure of reservoirs with shear-wave VSPs. The Leading Edge, **5,** 11, pp. 35–39

DAHLEN F. A. 1972: Bull. Seism. Soc. Am., **62,** pp. 1183–1193

DALEY T. M., MAJER E. L., MCEVILLY T. V. 1986: Analysis of Shearwave and P-wave Data at the Salton Sea Scientific Drilling Program. EOS **67,** 44, p. 1116

EVANS R. 1984: Effects of the free surface on shear wavetrains. Geophys. J. R. Astr. Soc. **76,** 1, pp. 165–172

EVANS R., ASUDEH I., CRAMPIN S., ÜÇER S. B. 1985: Tectonics of the Marmara Sea region of Turkey: new evidence from micro-earthquake fault plane solutions. Geophys. J. R. Astr. Soc. **83,** 1, pp. 47–60

EWING W. M., JARDETZKY W. S., PRESS F. 1957: Elastic waves in layered media. McGraw—Hill Book Co. Inc., New York, 380 p.

FYFE W. S., PRICE N. J., THOMPSON A. B. 1978: Fluids in the Earth's crust. Their significance in metamorphic, tectonic and chemical transport processes. Elsevier, Amsterdam, 383 p.

GOINS N. R., DAINTY A. M., TOKSÖZ M. N. 1981: Seismic energy release of the Moon. J. Geophys. Res. **86,** B1, pp. 378–388

JOHNSTON D. H. 1986: VSP detection of fracture-induced velocity anisotropy. Expanded abstracts, 56th Ann. Int. SEG Meeting, Houston, 1986. pp. 464–466

KANESHIMA S., ITO H., MITSUHIKO S. 1986: Abstracts, Second Int. Work. Seismic Anisotropy, Moscow, 1986, p. 127, 128

KANESHIMA S., ANDO M., CRAMPIN S. 1987: Shear-wave splitting above small earthquakes in the Kinki district of Japan. Phys. Earth. Planet. Int., **45,** 1, pp. 45–58

KOHLER W. M., HEALY J. H., WEGENER S. S. 1982: Upper Crustal Structure of the Mount Hood, Oregon, region as revealed by time term analysis. J. Geophys. Res. **87,** B1, pp. 339–355

LEARY P. C. and LI Y.-G. 1986: VSP fracture study of Mojave Desert hydrofracture borehole. EOS **67,** 44, p. 1116

LI Y.-G., LEARY P. C., AKI K. 1986: Seismic ray tracing for VSP observations in inhomogeneous aligned fractured rock at Oroville, CA. EOS, **67,** 44, p. 1117

MAJER E. L., MCEVILLY T. V., EASTWOOD F. S. 1985: Fracture mapping using shear wave vertical seismic profiling. EOS **66,** p. 950

NICOLAYSEN L. O. 1987: Shear wave splitting identified from rock bursts in Western Deep Levels Gold Mine, South Africa (personal communication)

PEACOCK S. 1985: Shear wave polarizations: IV. Aftershocks of the North Wales earthquake of July 1984. Geophys. J. R. Astr. Soc. **81,** 1, p. 341

PEACOCK S., CRAMPIN S., BOOTH D. C., FLETCHER J. B. 1988: Shear-wave splitting in the Anza seismic gap, Southern California: temporal variations as possible precursors. J. Geophys. Res. **93,** pp. 3339–3356

RAI C. S. and HANSON K. E. 1986: Shear-wave birefringence: A laboratory study. Expanded Abstracts, 56th Ann. Int. SEG Meeting, Houston 1986, pp. 471–473

ROBERTS G. and CRAMPIN S. 1986: Shear-wave polarizations in a hot-dry-rock geothermal reservoir: anisotropic effects of fractures. Int. J. Rock Mech. Min. Sci. **23,** 4, pp. 291–302

SHANKLAND T. J. and ANDER M. E. 1983: Electrical conductivity, temperatures and fluids in the lower crust. J. Geophys. Res. **88,** B11, pp. 9475–9484

WILLIS H. A., RETHFORD C. L., BIELANSKI E. 1986: Azimuthal anisotropy: occurrence and effect on shear-wave data quality. Expanded Abstracts, 56th Ann. Int. SEG Meeting, Houston, 1986. pp. 479–481

YOUNG R. P. 1988: Proc. 4th Conf. Acoustic Events/Microseismic Activity in Geologic Materials, Transtech. Publications (in press)

YOUNG R. P. and HILL J. J. 1986: Seismic attenuation spectra in rock mass characterization; a case study in open-pit mining. Geophysics **51,** 2, pp. 302–323

A HÚZÁSI–TÁGULÁSI ANIZOTRÓPIA FÖLDTANI ÉS IPARI KÖVETKEZMÉNYEI

Stuart CRAMPIN

Az utóbbi két-három évben, a világ minden részén — mintegy 30 helyen — a nyíró hullámok polarizációjának viselkedésére végzett kísérletek bebizonyították, hogy a földkéregben előforduló legtöbb kőzetet folyadékokkal kitöltött repedések és mikrorepedések járják át. A folyadék rendszerint folyékony állapotban levő víz, és a mikrorepedések a nyomás hatására irányított eloszlásúak, ezáltal a szeizmikus hullámokkal szemben anizotrop jellegűek. Ezt a repedéseloszlást húzási–tágulási anizotrópiának (EDA) nevezik.

A szeizmikus *P*-hullámok nem nagyon érzékenyek a folyadékokkal kitöltött repedésekre, az *S*-hullámokat viszont erősen befolyásolják az EDA törések. Nyíró hullám hasadást okoznak (kettős törés néven ismert jelenség) és jellegzetes jelalakot hoznak létre. Ezek a jelalakok diagnosztikus értékűek a folyadékkal töltött EDA repedésekre, és felhasználhatók a repedések elrendeződésének becslésére. Nyíró hullám hasadás látható majdnem minden felvételen: kis földrengések felett a világ sok részén; Észak Amerikában 13 nyíró hullám reflexiós szelvényből 12-nél; és számos különböző helyen VSP felvételeken. Nyilvánvaló, hogy a kéreg kőzetét EDA repedések járják át.

A lehetőség, hogy a feszültség által orientált törések és mikrorepedések belső szerkezetét nyíró hullámok analízisével tanulmányozhatjuk, rendkívül jelentős a bányászatban, a mélyfúrások vagy külfejtések során, továbbá a földkéreg deformációs folyamatainak vizsgálatában, mint pl. a földrengés előrejelzésnél. A törési és feszültség geometriai in situ nyomonkövetése a kőzettömegtől távol észlelt nyíró hullámok elemzésével számos alkalmazási lehetőséget rejt magában, a hidraulikus törések irányítottságának előrejelzésétől kezdve, a szénhidrogén tárolók optimális kitermelési stratégiájának tervezésén keresztül a földrengések előrejelzéséig.

ГЕОЛОГИЧЕСКИЕ И ИНДУСТРИАЛЬНЫЕ ПОСЛЕДСТВИЯ АНИЗОТРОПИИ РАСТЯЖЕНИЯ–РАСШИРЕНИЯ

Стюарт КРАМПИН

Опытами, выполненными за последние два-три года примерно в 30 различных пунктах всего мира с целью изучения поляризации поперечных волн, было доказано, что подавляющее большинство пород, слагающих земную кору, пронизано трещинами и микротрещинами, заполненными жидкостью. Последняя обычно представлена жидкой водой, а микротрещины имеют ориентированное под воздействием давления распределение и тем самым — анизотропию в отношении проходящих сейсмических волн. Это распределение трещин называется анизотропией растяжения—расширения.

Продольные сейсмические волны не очень чувствительны к трещинам, заполненным жидкостью, в то время как поперечные волны испытывают сильное влияние со стороны этих трещин. Ими вызывается расщепление поперечных волн (это явление известно под названием двойного лучепреломления) и возникновение сигналов характерной формы. Форма этих сигналов имеет диагностическое значение при изучении рассматриваемых трещин, заполненных жидкостью, и она может быть использована для оценки распределения трещин. Расщепление поперечных волн наблюдается почти на всех записях: над слабыми землетрясениями — во многих районах мира; в Северной Америке — в 12-и из 13-и профилей отраженных поперечных волн; на записях ВСП — в самых разнообразных районах. Совершенно ясно, что большинство пород в земной коре пронизано трещинами рассматриваемого типа.

Возможность изучения внутренней структуры разломов и микротрещин, ориентированных напряжениями, путем анализа волн скалывания может иметь чрезвычайное значение в проходке горных выработок, скважин и карьеров, а также в исследовании процессов деформации земной коры, как например в прогнозе землетрясений. Прослеживание геометрии разломов и напряжений в массиве на основании анализа поперечных волн, зарегистрированных на большом удалении, может иметь различные области применения, начиная от прогноза ориентировки гидравлических разломов, через планирование оптимальной стратегии эксплуатации залежей нефти и газа и вплоть до прогноза землетрясений.

GEOPHYSICAL TRANSACTIONS 1988
Vol. 34. No. 1. pp. 101—119

POLARIZATION ANALYSIS IN THREE-COMPONENT SEISMICS

Christian CLIET and Michel DUBESSET*

The common use of three-component recordings is seismic surveys gives access to knowledge of particle displacement, e.g. at different sonde locations in the case of well seismic profiles. This particle trajectory can be represented by an equivalent ellipsoid over short time windows. This kind of modelling allows one to define parameters which give a good description of how the trajectory looks like (shape parameters) and, also, of what its attitude is in space in relation to a reference trihedron (angular parameters). Other parameters, which are independent of the equivalent ellipsoid, are also defined.

The study of these polarization parameters in the case of VSPs with offset (OVSP) is very instructive. It is shown here by means of examples that the principal plane of polarization of the first down-going *P*-wave is very often not contained in a vertical plane, but is strongly tilted laterally.

Keywords: polarization, amplitude, *S*-waves, vertical seismic profiles, hodograph, three-component seismics

Introduction

For some years now, records of multicomponent profiles have given us knowledge of the particle displacement, which we call particle trajectory. From the properties of this trajectory, polarization filterings have been designed which are useful for multicomponent data processing [BENHAMA et al. 1985, MONTALBETI and KANASEWICH 1970].

Another direction of research, which is developed here, is the precise study of polarization parameters. In order to define these parameters, an ellipsoid (called the "equivalent ellipsoid" or sometimes the "eigenellipsoid") is fitted to the particle trajectory. Two kinds of parameters are then defined [CLIET and DUBESSET 1986, 1987, MATSUMURA 1981, SAMSON 1973]:

— Shape parameters which characterize the shape of the particle trajectory in space.
— Angular parameters which characterize the attitude of this trajectory in space, in relation to a reference trihedron.

Other parameters, which are independent of the equivalent ellipsoid, will also be defined.

In well seismic surveying, it is interesting to plot these parameters for a given type of wave (e.g. the first down-going *P*-wave) as a function of depth. We then get pseudo-logs of polarization parameters. In this paper, some pseudo-logs are presented, in particular lateral tilt or proper rotation pseudo-

* Institut Français du Pétrole, Rueil-Malmaison, France
Manuscript received: 4 December, 1987

logs. So, the fact that the waves do not always travel in a vertical plane is clearly shown by the study of the angles that indicate the rotation of the wave main plane apart from the vertical position.

1. Generalities

1.1 Particle trajectory

The three-component recording of the ground displacement using a special tool (a triphone in conventional seismic surveys or a sonde in well seismic surveys) makes it possible to know the actual motion of the centre of gravity of this receiver. This motion is called "particle trajectory".

This trajectory is a spatial curve in 3-D space, given by its parametrical equations:

$$\begin{aligned} x &= x(t), \\ y &= y(t), \\ z &= z(t). \end{aligned} \tag{1}$$

This curve is in fact a hodograph corresponding to the true trajectory, since the sensors are velocimeters; it is, however, easy to get the true trajectory by integrating. *Figure 1* shows an example of a trajectory corresponding to a VSP with offset (OVSP) recorded in the Paris Basin.

1.2 OVSP's reorientation

The attitude of the velocity vector for a given type of wave can easily be characterized by two angles equivalent to a longitude λ and a latitude φ, as can be seen in *Fig. 2*. In a well, assuming the well is vertical and that its axis is the OZ axis, several trihedrons are defined *(Fig. 3)*:

— The H_1H_2Z trihedron, tied to the sonde, is mobile around Z, i.e. the position of H_1 and H_2 depends upon the recording depth;
— The XYZ trihedron, tied to the ground is the same for all recording depths;
— The NYR trihedron, tied to a seismic arrival, is mobile, i.e. it depends upon which wave we choose for the reorientation.

In the case of OVSPs, the first down-going P-wave is used for the reorientation under the hypothesis that this wave travels in the source-well vertical plane during a time window of about one period. The two angles λ and φ corresponding to this wave are then computed, where:

— λ, the longitude, is the angle between the vertical plane containing the wave and the vertical plane containing the H_1 component. The above-mentioned hypothesis admits that the plane containing the energy arrival indicates the source direction;

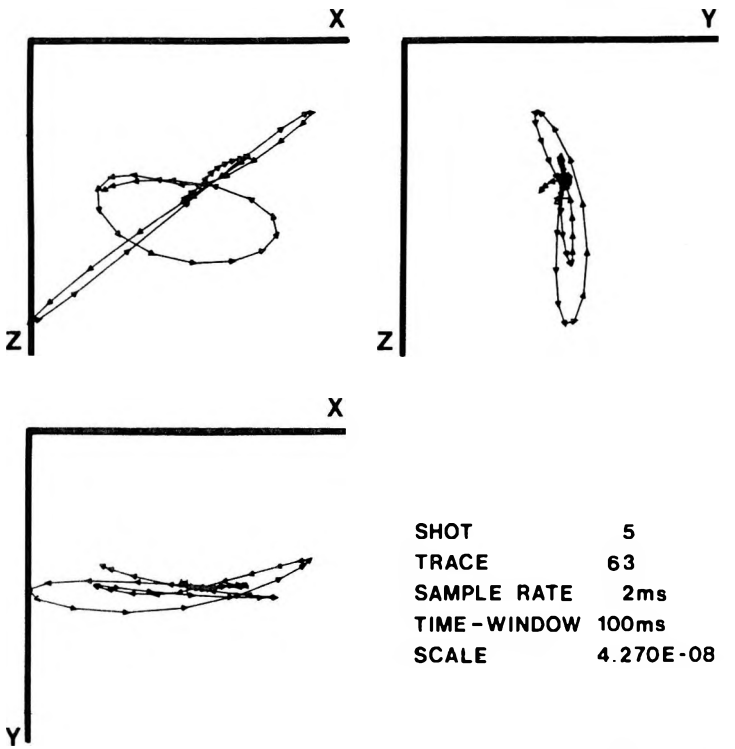

Fig. 1. Particle trajectory recorded at an offset VSP measurement in the Paris Basin

1. ábra. Részecske trajektória a Párizsi-medencében végzett VSP mérésből

Рис. 1. Траектория частиц по измерениям ВСП в Парижском бассейне.

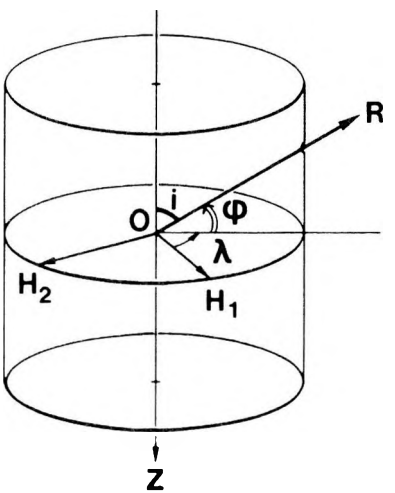

Fig. 2. Characterization of resultant attitude of velocity vector

2. ábra. A sebesség vektor eredőjének szemléltetése

Рис. 2. Результирующий вектор скоростей.

— φ, the latitude, is the angle in the vertical plane containing the wave between the velocity vector and the horizontal plane. In the case of a *P*-wave, φ and the incidence angle i are complementary.

Knowing λ, the X and Y components can be computed. The XZ plane is then, by hypothesis, the source–well plane. Knowing λ and φ, the N, Y and R components can be computed, where R is the radial component and N the component normal to the radial R in the vertical plane (N is called the normal). The vertical plane, formed by R and N, is the plane containing the first down-going *P*-wave, which is also, by hypothesis, the vertical plane containing the well and the source.

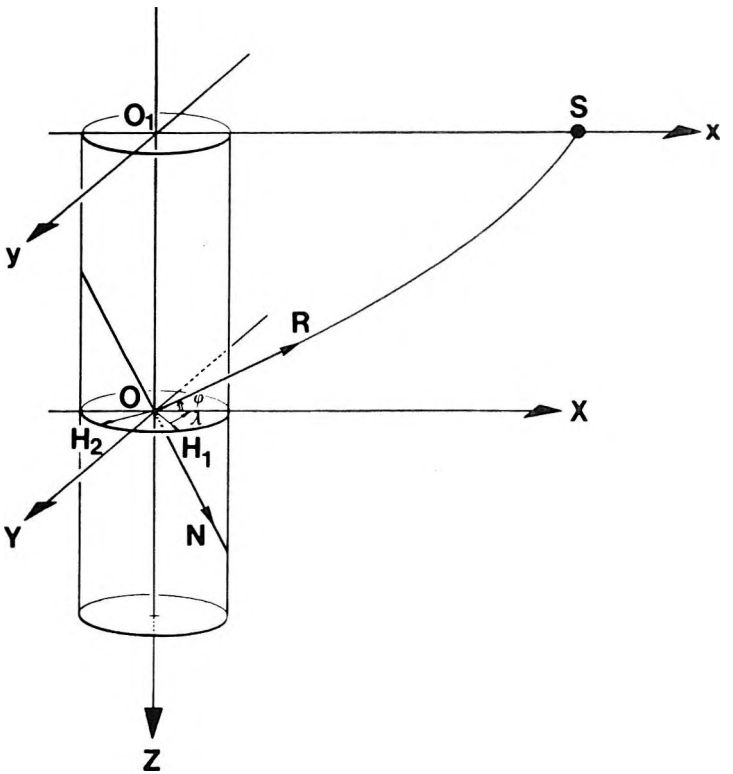

Fig. 3. Relative arrangement of trihedrons in a well

3. ábra. A triéderek relatív helyzete fúrólyukban

Рис. 3. Относительное положение триэдров во скважине.

1.3 Comments

Figures 4, 5 and *6* illustrate the effect of trihedron changes on the particle trajectory corresponding to the first down-going *P*-wave. It is important to notice that in the present case all the polarization information (i.e. incidence angle, ellipticity, etc.) is contained in the *XZ* plane.

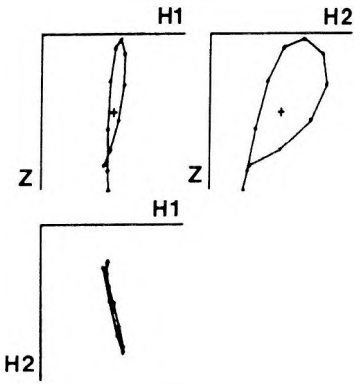

Fig. 4. Particle trajectory in the H_1H_2Z trihedron, without lateral tilt

4. ábra. Részecske trajektória a H_1H_2Z triéderben, oldalirányú dőlés nélkül

Рис. 4. Траектория частиц в триэдре H_1H_2Z без наклона в сторону.

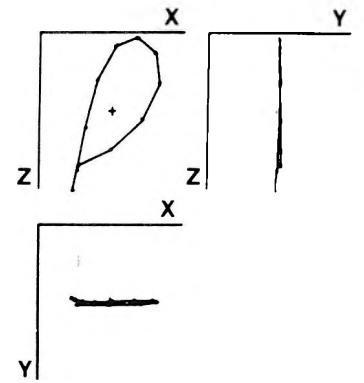

Fig. 5. Particle trajectory in the *XYZ* trihedron, without lateral tilt

5. ábra. Részecske trajektória az *XYZ* triéderben, oldalirányú dőlés nélkül

Рис. 5. Траектория частиц в триэдре *XYZ* без наклона в сторону.

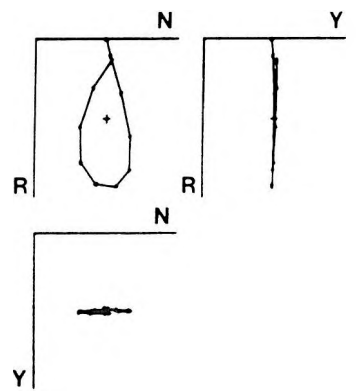

Fig. 6. Particle trajectory in the *NYR* trihedron, without lateral tilt

6. ábra. Részecske trajektória az *NYR* triéderben, oldalirányú dőlés nélkül

Рис. 6. Траектория частиц в триэдре *NYR* без наклона в сторону.

Another example, again taken from an OVSP recorded in the Paris Basin, is presented in *Figs. 7, 8* and *9*. In this case, the elliptical-type motion is no longer in the *XZ* plane after reorientation. Examination of a stereoscopic pair of such a trajectory clearly shows that its principal polarization plane is no longer vertical, but that it is laterally tilted. Angle λ no longer has the same meaning as previously and it is obvious that three angles are now necessary to completely characterize the attitude of the trajectory in space [CLIET and DUBESSET 1986, 1987].

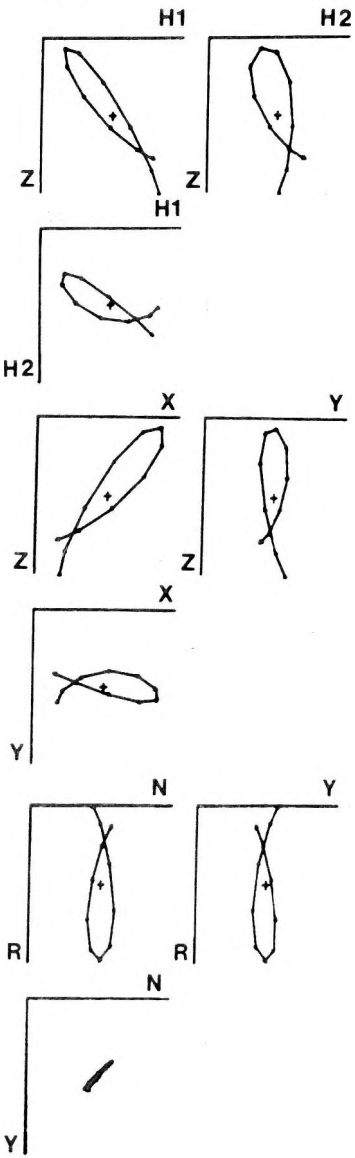

Fig. 7. Particle trajectory in the H_1H_2Z trihedron, with lateral tilt

7. ábra. Részecske trajektória a H_1H_2Z triéderben, oldalirányú dőléssel

Рис. 7. Траектория частиц в триэдре H_1H_2Z с наклоном в сторону.

Fig. 8. Particle trajectory in the *XYZ* trihedron, with lateral tilt

8. ábra. Részecske trajektória az *XYZ* triéderben, oldalirányú dőléssel

Рис. 8. Траектория частиц в триэдре *XYZ* с наклоном в сторону.

Fig. 9. Particle trajectory in the *NYR* trihedron, with lateral tilt

9. ábra. Részecske trajektória az *NYR* triéderben, oldalirányú dőléssel

Рис. 9. Траектория частиц в триэдре *NYR* с наклоном в сторону.

2. Particle trajectory modelling

2.1 Ellipsoid equivalent to the particle trajectory

Covariance matrix

The covariance matrix M_c has been used by many authors in order to model the particle trajectory. Let us consider a time window between times T_1 and T_2 and let us define:

$$\begin{aligned} T &= T_2 - T_1, \\ N_1 &= \frac{T_1}{\tau}, \\ N_2 &= \frac{T_2}{\tau}, \end{aligned} \tag{2}$$

and the sample number $N = N_2 - N_1 + 1$, where τ is the sampling rate.

If the trajectory is considered as a cluster of points of coordinates X_i, Y_i and Z_i, the corresponding covariance matrix between T_1 and T_2 is easily written as follows:

$$\mathbf{M}_c = \frac{1}{N} \begin{pmatrix} \Sigma(x-m_x)^2 & \Sigma(x-m_x)(y-m_y) & \Sigma(x-m_x)(z-m_z) \\ \Sigma(y-m_y)(x-m_x) & \Sigma(y-m_y)^2 & \Sigma(y-m_y)(z-m_z) \\ \Sigma(z-m_z)(x-m_x) & \Sigma(z-m_z)(y-m_y) & \Sigma(z-m_z)^2 \end{pmatrix} \tag{3}$$

noting $\sum_{i=1}^{N}$ by Σ

and with

$$\begin{cases} m_x = \dfrac{1}{N} \displaystyle\sum_{i=1}^{N} x_i \\ m_y = \dfrac{1}{N} \displaystyle\sum_{i=1}^{N} y_i \\ m_z = \dfrac{1}{N} \displaystyle\sum_{i=1}^{N} z_i \end{cases} \tag{4}$$

Equivalent ellipsoid

One can show that this matrix is, in fact, the matrix associated with the quadratic form obtained when computing the inertia of the cluster of points in relation to the three coordinate planes; it is also easy to show that the representative quadric is an ellipsoid, called the "covariance ellipsoid", the length of whose semi-axes are α, β and γ. *Figures 10* and *11* show an example of a trajectory and of its associated ellipsoid. But we want to model the trajectory (e.g. by a least squares method) over a time window of about one period, by

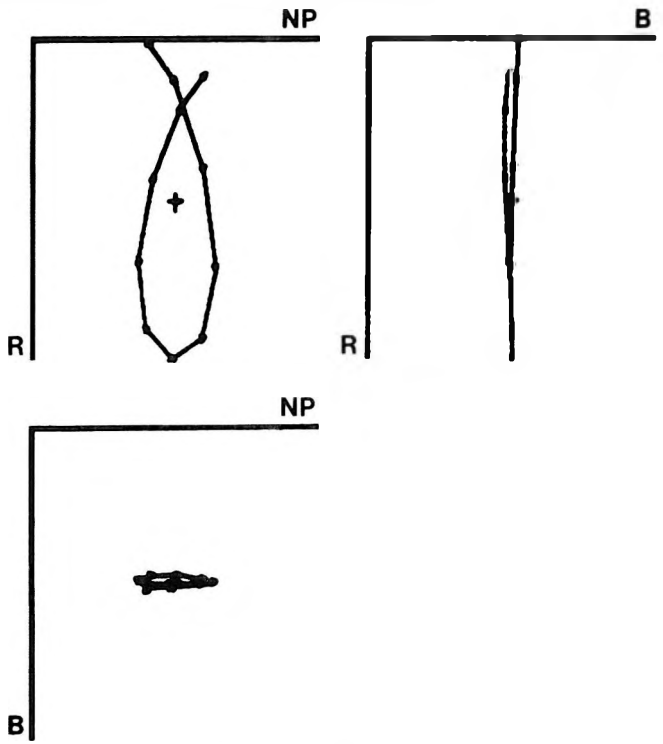

Fig. 10. Trajectory

10. ábra. Egy trajektória

Рис. 10. Траектория.

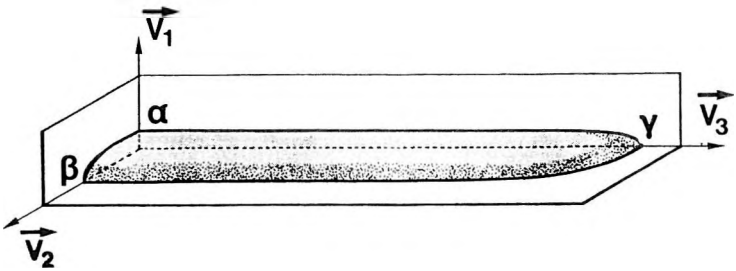

Fig. 11. Covariance ellipsoid associated with the trajectory of Fig. 10

11. ábra. A 10. ábra trajektóriájához tartozó kovariancia ellipszoid

Рис. 11. Ковариантный эллипсоид траектории рис. 10.

the best fitting ellipsoid; if the lengths of the semi-axes of this ellipsoid are a, b and c, we get the following relations:

$$\begin{aligned} a &= m\sqrt{\lambda_1}, \\ b &= m\sqrt{\lambda_2}, \\ c &= m\sqrt{\lambda_3}, \end{aligned} \tag{5}$$

and

where λ_1, λ_2 and λ_3 are the eigenvalues of the covariance matrix ($\lambda_1 \geqq \lambda_2 \geqq \lambda_3 \geqq 0$).

The m coefficient depends upon the kind of model ellipsoid: it equals $\sqrt{3}$ for a hollow ellipsoid, which is — additionally — very similar to the trajectories. In fact, coefficient m is not important since it disappears when computing the ratios of axes for calculating ellipticities, for example.

This *equivalent ellipsoid* is not the covariance ellipsoid and its axes are the inverses of the axes of the second one:

$$a = \frac{m}{\alpha}, \quad b = \frac{m}{\beta}, \quad c = \frac{m}{\gamma} \tag{6}$$

where α, β and γ are the lengths of the semi-axes of the covariance ellipsoid. Comparing Fig. 11 with *Fig. 12*, we can see the difference between the two ellipsoids.

Now, we have been provided with and ellipsoid equivalent to the trajectory. Its three principal axes in space are the three eigenvectors $\vec{V}_1$, $\vec{V}_2$, $\vec{V}_3$ of the

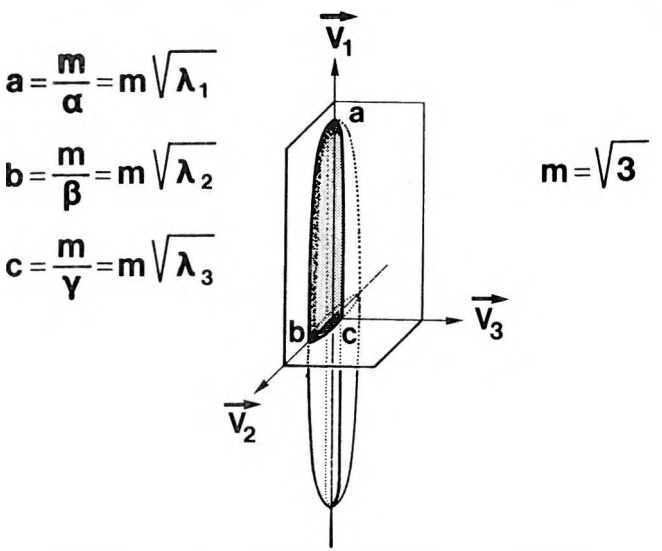

Fig. 12. Equivalent ellipsoid associated with the covariance ellipsoid of Fig. 11

12. ábra. A 11. ábra kovarianca ellipszoidjának megfelelő ekvivalens ellipszoid

Рис. 12. Эквивалентный эллипсоид, соответствующий ковариантному эллипсоиду рис. 11.

covariance matrix and the lengths of its three semi-axes are given by equation (5). This ellipsoid (Fig. 12) is called the equivalent ellipsoid [Cliet and Dubesset 1987]. From this ellipsoid, two kinds of parameters will be defined: the shape parameters and the angular parameters.

2.2 Shape parameters

These parameters give a good description of what the trajectory looks like in space. They are defined from the eigenvalues of $\mathbf{M}_c$.

Ellipticities

First, three ellipticities are defined as follows:

the main ellipticity $$e_{21} = \frac{b}{a} = \frac{\sqrt{\lambda_2}}{\sqrt{\lambda_1}},$$

the cross-ellipticity $$e_{31} = \frac{c}{a} = \frac{\sqrt{\lambda_3}}{\sqrt{\lambda_1}}, \tag{7}$$

and the transverse ellipticity $$e_{32} = \frac{c}{b} = \frac{\sqrt{\lambda_3}}{\sqrt{\lambda_2}}.$$

Polarization coefficient

A global polarization coefficient τ is given by Samson [1973]:

$$\tau^2 = \frac{3\mathrm{tr}(\mathbf{M}_c^2) - (\mathrm{tr}\,\mathbf{M}_c)^2}{2(\mathrm{tr}\,\mathbf{M}_c)^2} \tag{8}$$

where tr marks the trace of matrix $\mathbf{M}$: $\mathrm{tr}\mathbf{M}_c = \sum_{i=1}^{n} m_{ii}$.

This coefficient can also be written as a function of the ellipticities:

$$\tau^2 = \frac{(1-e_{21}^2)^2 + (1-e_{31}^2)^2 + (e_{21}^2 - e_{31}^2)^2}{2(1+e_{21}^2+e_{31}^2)^2} \tag{9}$$

This coefficient equals 1 for a straight line and zero for a sphere.

Oblateness coefficient

It is interesting to characterize the flatness of a given trajectory. For this purpose, an oblateness coefficient f is defined as follows:

$$f = \frac{a+b-2c}{a+b+c} = \frac{\sqrt{\lambda_1}+\sqrt{\lambda_2}-2\sqrt{\lambda_3}}{\sqrt{\lambda_1}+\sqrt{\lambda_2}+\sqrt{\lambda_3}} = \frac{1+e_{21}-2e_{31}}{1+e_{21}+e_{31}} \tag{10}$$

This coefficient equals 1 for any planar trajectory and zero for a sphere.

Linearity coefficient

The linearity coefficient l is given by:

$$l = \frac{1}{2}\,\frac{2a-b-c}{a+b+c} = \frac{1}{2}\,\frac{2\sqrt{\lambda_1}-\sqrt{\lambda_2}-\sqrt{\lambda_3}}{\sqrt{\lambda_1}+\sqrt{\lambda_2}+\sqrt{\lambda_3}} = \frac{2-e_{21}-e_{31}}{2(1+e_{21}+e_{31})} \tag{11}$$

This coefficient equals 1 for a straight line and zero for a sphere. All these coefficients lie between 0 and 1 [CLIET and DUBESSET 1987].

2.3 Angular parameters

In order to characterize the particle trajectory attitude completely, it is necessary to introduce the three eulerian angles. These angles make it possible, knowing the recording trihedron H_1H_2Z, to obtain the "eigentrihedron" $V_1V_2V_3$ *(Fig. 13)*:

- Precession ψ is the angle between H_1 and Y in the horizontal plane; it corresponds to a rotation around the OZ axis: $H_1 \rightarrow h$.
- Nutation θ is the angle between R and Z; it corresponds to a rotation around the Oh axis. For a P-wave, θ is equal to the incidence angle i; $Z \rightarrow R$ (alias $\vec{V}_1$) and $X' \rightarrow N'$.
- Proper rotation φ is the angle of rotation of the principal plane of polarization (defined by $\vec{V}_1$ and $\vec{V}_2$) around R, alias $\vec{V}_1$; $N' \rightarrow N_p$ alias $\vec{V}_2$ and $h \rightarrow B$ alias $\vec{V}_3$. N_p is called the "proper normal".

Owing to practical considerations of occasional inaccuracy of the φ value, a fourth angle β, called the "lateral tilt", is introduced. It is defined as the angle between the normal $\vec{V}_3$ to the principal polarization plane ($\vec{V}_3$ is called the "binormal" by analogy with the Serret–Frenet gliding trihedron) and the horizontal plane. One can notice that, if the common hypothesis is true, the trajectory plane is vertical (in the case of a P-wave), the binormal B is therefore in the horizontal plane and, thus, the lateral tilt β is zero.

ψ, θ, φ and β are the angular parameters. They can be expressed as functions of $\vec{H}_1$, $\vec{H}_2$, $\vec{Z}$, $\vec{V}_1$, $\vec{V}_2$ and $\vec{V}_3$ (all these vectors being normalized to 1) as follows:

$$\psi = \tan^{-1}\left[\frac{\vec{V}_1\vec{H}_1}{-\vec{V}_1\vec{H}_2}\right] \tag{12}$$

$$\theta = \cos^{-1}(\vec{V}_1\vec{Z}) \tag{13}$$

$$\varphi = \tan^{-1}\left(\frac{\vec{V}_3\vec{Z}}{\vec{V}_2\vec{Z}}\right) \tag{14}$$

$$\beta = \sin^{-1}(\vec{V}_3\vec{Z}) = \sin^{-1}(\sin\varphi \sin\theta) \tag{15}$$

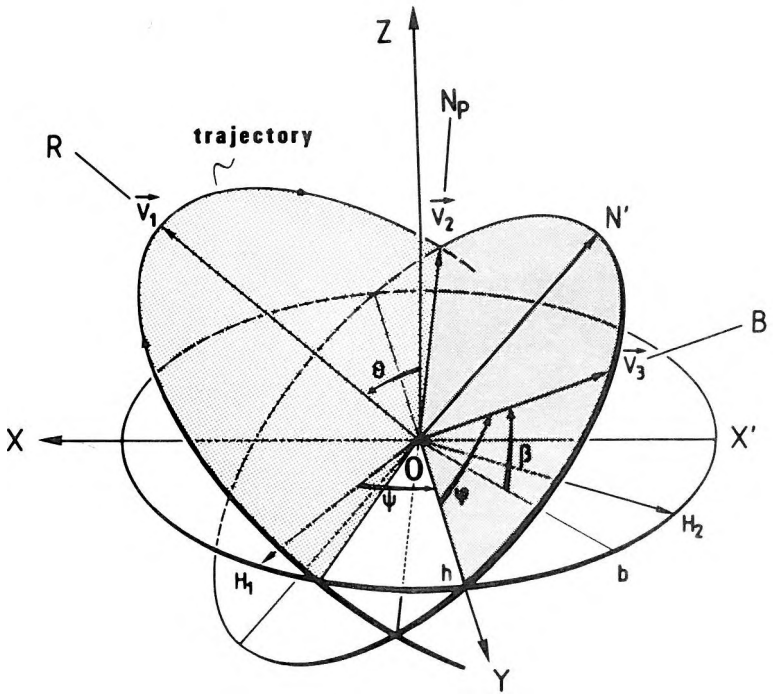

Fig. 13. Trajectory attitude and Eulerian angles

13. ábra. A trajektória helyzete és az Euler-féle szögek

Рис. 13. Положение траектории и эйлеровские углы.

2.4 Complementary parameters

3-C picking time

It is also helpful to define a picking time, $T_{S\max}$, corresponding to the sample of maximum amplitude, the nearest to the sample that has maximum global polarization coefficient. This time is called 3-C picking time.

Amplitudes

The amplitude associated with the 3-C picking time $T_{S\max}$ is computed and we call it the maximum amplitude $S_{\max}$. It is also possible to use the value a (semi-major axis length of the equivalent ellipsoid) as a resultant, called the "eigenresultant" S_p.

Lastly, the quadratic resultant S_{rms} is defined as:

$$S_{\text{rms}} = \frac{1}{N} \sum_{i=N_1}^{N_2} \left(X_i^2 + Y_i^2 + Z_i^2 \right) \tag{16}$$

Over a short time window containing a seismic arrival, it is possible to show [CLIET and DUBESSET 1987] that:

$$S_p \cong S_{\text{rms}} \cong \frac{1}{m} S_{\max} \tag{17}$$

Ellipsoid-independent parameters

It is also possible to define some ellipsoid-independent parameters, for example:

— the tortuosity (entropy of the trajectory),
— the radius of curvature,
— the radius of torsion, etc.

We have not used these parameters in this paper, but they can be very useful. In particular, the tortuosity can enable one to distinguish between signal and noise.

3. Applications to OVSPs

3.1 Seismic pseudo-logs

The kind of representation of all these polarization parameters depends upon what kind of seismics is available:

— in well surveying, parameters are plotted versus depth for a given type of wave, so that pseudo-logs are obtained;
— in conventional surveying, the plot is performed versus offset and pseudo-horizons are obtained.

The correlations between the pseudo-logs, and their comparison with a sonic log, for example, offer interesting possibilities which will not be studied here.

3.2 Sonde location in the horizontal plane

The difference of ψ and longitude λ is $\pi/2$. In fact, ψ gives the direction normal to the direction of energy arrival in the horizontal plane *(OX)*. If the

medium is tabular and isotropic, the arrival direction is the actual direction of the source. In this case, OX is the horizontal direction of the source. In the general case, OX is always the direction of arrival of energy, but not necessarily the source direction: thus, it is essential to precisely know the attitude of the sonde in the well.

The following example comes from a site where no dip is known. Two OVSP's were recorded with the same azimuth and with offsets of 500 m and 1000 m. At each recording depth, both offsets are shot without moving the sonde. The comparison between the two pseudo-logs of the precession angle for these two shots shows remarkable agreement *(Fig. 14)*. The zones with a weak gap would deserve a thorough study to decide whether this is caused by interferences or by anisotropy.

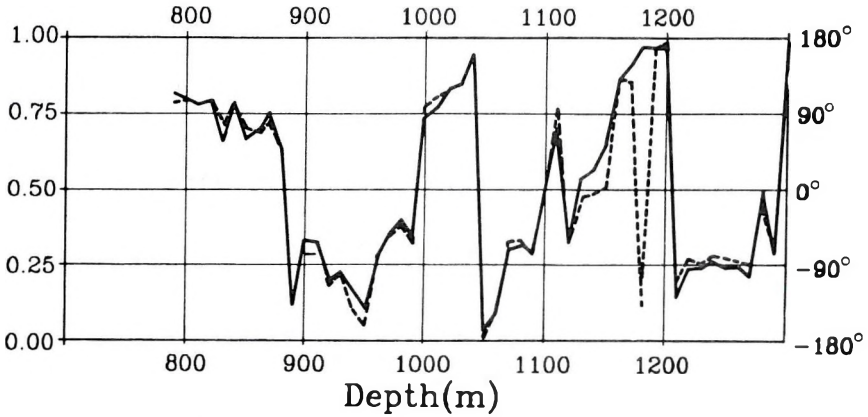

Fig. 14. Precession (ψ) pseudo-logs, offsets: 500 m (broken line) and 1000 m (continuous line)

14. ábra. A precessziós szög (ψ) pszeudo-szelvénye, fokban. A rengésforrás távolsága a fúrólyuktól 500 méter (szaggatott vonal), illetve 1000 méter (folytonos vonal)

Рис. 14. Псевдо-профил прецессионного угла (ψ) в градусах; расстояние источника волн от скважины — 500 м (прерывистая линия) или 1000 м (сплошная линия).

3.3 Amplitudes study

The comparison of the three above-defined amplitudes is interesting. We have seen that (Eq. 17):

$$S_p \cong S_{rms} \cong \frac{1}{m} S_{max},$$

with m being theoretically equal to $\sqrt{3}$ when a hollow ellipsoid is chosen for the trajectory modelling. On an actual example, one can see (for a first P-arrival) that these relations are well verified. For each depth of an OVSP, S_{max} is plotted as a function of S_p *(Fig. 15)*. In this figure, we can see that the function is a

quasi-line with a slope of 1.66 reasonably close to $\sqrt{3}$. The fact that we get a straight line confirms in a way the coherence of the arrival; the slope value justifies the validity of using a hollow ellipsoid as the trajectory model.

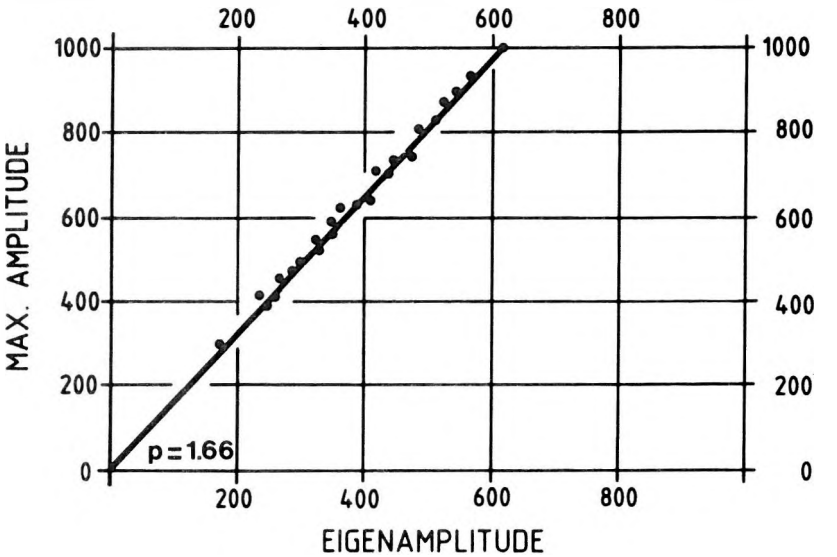

Fig. 15. Amplitude ratio

15. ábra. Amplitudó arányok

Рис. 15. Соотношения амплитуд.

3.4 The phenomenon of lateral tilt

The phenomenon of lateral tilt can be illustrated by means of two angles:
— the angle of proper rotation,
— the angle of lateral tilt.

The sines of these two angles are related by the sine of the nutation (see Eq. 15) and, depending on the given case, both angles can be useful.

Examples of lateral tilt

Example 1 *(Fig. 16)* is taken from an OVSP from the Paris Basin. It was shot with a vertical vibrator with an offset of 1173 m. The recording depths varied from 2060 to 1100 m in steps of 15 m.

Example 2 *(Fig. 17)* was recorded in Houston, USA. The source was the Marthor M3® and the recording depths were from 170 to 5 m in steps of 5 m. The offset was 200 m. One may think that the lateral tilt could be produced by

® SH weight-drop source. IFP trademark.

the sonde. That is why the OVSP shown in Fig. 17 was not recorded with a mobile receiver but with 11 stations of three geophones (X, Y and Z-oriented) sealed in the well at different depths. All the X geophones were carefully aligned towards the source in the horizontal plane. The 11 stations were recorded with one single shot. Figure 17 shows that, for one and the same shot, some stations present a lateral tilt effect and others do not; this means that the lateral tilt is connected with the local layers and not with a source effect, nor with a sonde effect.

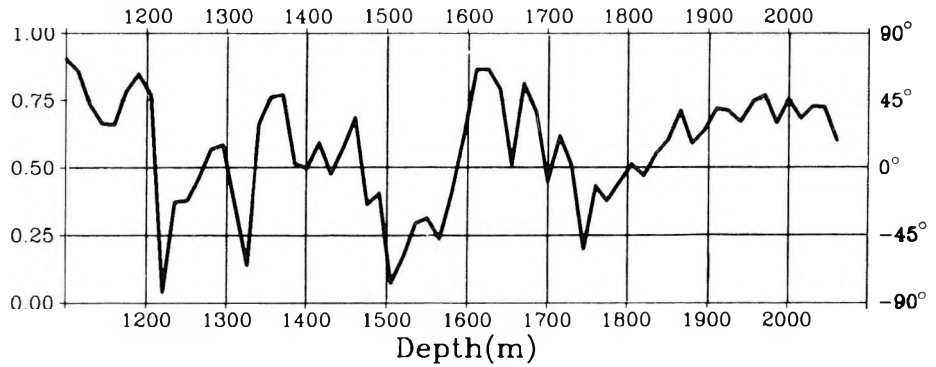

Fig. 16. Lateral tilt (β) pseudo-log from an OVSP measurement in the Paris Basin

16. ábra. Oldalirányú dőlés (β) pszeudo-szelvénye egy, a Párizsi-medencében végzett távoli VSP mérésből

Рис. 16. Псевдо-профиль наклона (β) в сторону по дальнему измерению ВСП в Парижском бассейне.

Example of proper rotation

This example *(Fig. 18)* was also recorded in the Paris Basin on a site of Gaz de France. The source was a P-shooter and the recording depths were from 785 to 736 m in steps of 1 metre. The offset was 460 m. This example is particularly interesting because it corresponds to a gas reservoir divided in two parts:

— the upper part (742–753 m) is composed of sands; the proper rotation has a mean value of −160°;
— the lower part (754–780 m) is principally composed of sandstones; the proper rotation has a remarkably constant mean value of −36°.

From these three examples we see that the phenomena are not anecdotal but, on the contrary, almost omnipresent and with surprising amplitude. It is difficult to make pertinent comments about these variations since their interpretation seems rather delicate; it is perhaps possible to attribute them either to interferences or — more probably — to anisotropy or to sudden lateral changes of attenuation.

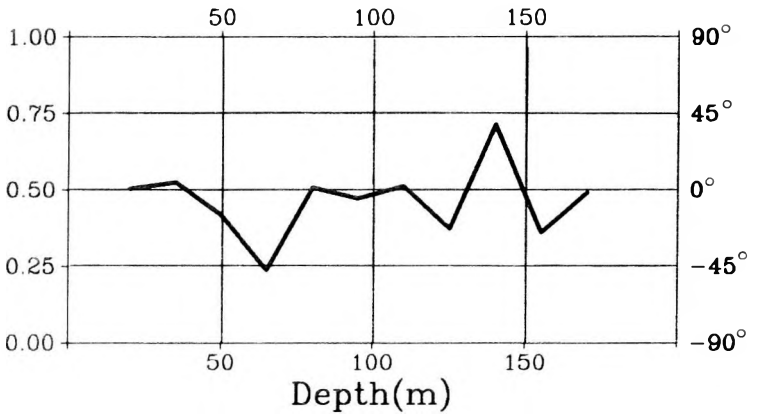

Fig. 17. Lateral tilt (β) pseudo-log from an OVSP measurement in Houston (USA)

17. ábra. Oldalirányú dőlés (β) pszeudo-szelvénye egy Houstonban (USA) végzett távoli VSP mérésből

Рис. 17. Псевдо-профиль наклона (β) в сторону по дальнему измерению ВСП в Хьюстоне (США).

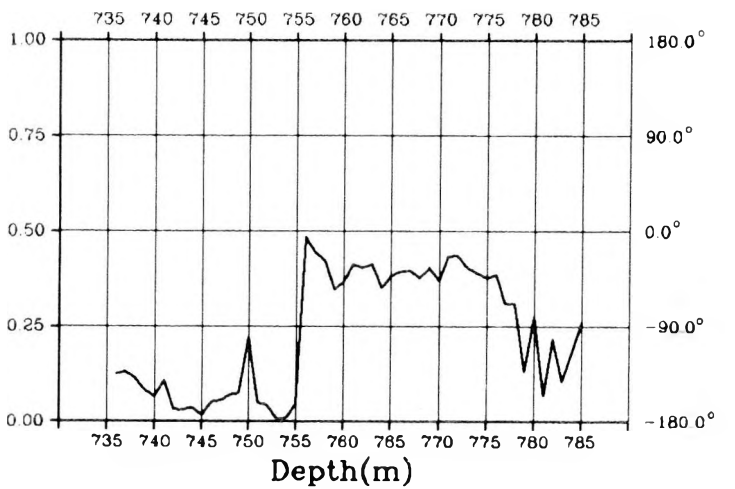

Fig. 18. Proper rotation (φ) pseudo-log

18. ábra. A megfelelő elfordulás (φ) pszeudo-szelvénye

Рис. 18. Псевдо-профиль соответствующего поворота (φ).

Conclusion

The precise characterization of the spatial attitude of the trajectory (notably the principal plane of polarization) seems essential and lead to extremely interesting results. In particular, the proof that this plane of polarization is not vertical but strongly laterally tilted, leads us to revise the way of analysing wave propagation and also the description and use of polarization phenomena.

There are two main points:

— first, it seems essential to precisely know the orientation of the sonde in the well;

— secondly, it would be desirable to record OVSP's with smaller depth intervals, for example with a sampling interval of 1 or 2 metres.

REFERENCES

Benhama A., Cliet C. and Dubesset M. 1985: Study and applications of spatial directional filterings in three-component recordings. Presented at the 47th Ann. Meeting of EAEG, Budapest

Cliet C. and Dubesset M. 1986: Premier aperçu sur les nouveaux paramètres de polarisation en sismique à trois composantes. IFP report n° 34 882

Cliet C. and Dubesset M. 1987: La paramétrisation des trajectoires de particules; 1ère partie; théorie. IFP report n° 35 080

Matsumura S. 1981: Three-dimensional expression of seismic particle motions by the trajectory ellipsoid and its application to the seismic data observed in the Kants district, Japan. J. Phys. Earth, **29**, 3, pp. 221–239

Montalbeti J. F. and Kanasewich E. R. 1970: Enhancement of teleseismic body phases with a polarization filter. Geophys. J. R. Astr. Soc. **21**, 2, pp. 119–129

Samson J. C. 1973: Description of the polarization states of vector processes: Application of ULF magnetic fields. Geophys. J. R. Astr. Soc. **34**, 4, pp. 403–419

POLARIZÁCIÓS ELEMZÉS A HÁROM KOMPONENSES SZEIZMIKÁBAN

Christian CLIET és Michel DUBESSET

A három komponenses jelrögzítés általános használata a szeizmikus kutatásban lehetővé teszi a részecske elmozdulások ismeretét is, például a különböző szondahelyzetekben fúrólyukbeli mérések során. A részecske trajektória rövid időablakokban ekvivalens ellipszoiddal ábrázolható. Az ilyen típusú modellezés lehetővé teszi a trajektóriákat jól leíró paraméterek meghatározását (alakparaméterek) és azok térbeli viszonyát a referencia tridederekhez képest (szögparaméterek). Egyéb, az ekvivalencia ellipszoidtól független paraméterek is meghatározhatók. Ezen polarizációs paraméterek tanulmányozása a távoli VSP-k esetén igen tanulságos. Példákon mutatjuk be, hogy az első lefelé haladó *P*-hullám fő polarizációs síkja gyakran nem esik a függőleges síkba, hanem oldalirányban dől.

ПОЛЯРИЗАЦИОННЫЙ АНАЛИЗ В ТРЕХКОМПОНЕНТНОЙ СЕЙСМОРАЗВЕДКЕ

Кристиан КЛИЕ и Мишел ДЮБЕССЕ

Всеобщее применение трехкомпонентной записи сигналов в сейсморазведке обеспечивает возможность знать и смещение частиц, например, при производстве скважинных измерений с различным положением зонда. Траектории частиц могут изображаться эквивалентными эллипсоидами в коротких окнах времени. Моделирование данного типа обеспечивает возможность определения параметров траекторий (параметров морфологии) и их пространственных соотношений с опорными триэдрами (параметры углов). Могут быть определены также и прочие параметры, не зависимые от эквивалентного эллипсоида. Изучение этих поляризационных параметров является весьма поучительным при дальних ВСП. Приводятся примеры, иллюстрирующие несовпадение главной плоскости поляризации первой проходящей вниз продольной волны с вертикальной плоскостью и ее наклон в сторону.

GEOPHYSICAL TRANSACTIONS 1988
Vol. 34. No. 1. pp. 121—131

EXAMPLES OF *S*-WAVE SPLITTING ANALYSES FROM VSP DATA

(Expanded Abstract)

Charles NAVILLE and Gildas OMNÈS*

Keywords: Vertical seismic profiles, *S*-waves, anisotropy, polarization, birefringence, three-component seismics, hodograph

Vertical Seismic Profiles offer a unique possibility to observe and analyse the Shear Wave Splitting phenomenon:

— Three-component signals can be recorded at various levels, consequently dinates *(Figs. 1–2)*. In many cases, when no steep dips are present near the
— The S/N is higher than for surface obsevation and the bandwidth is broader.
— Shear Wave Splitting effects associated with different raypaths can be compared and interpreted in terms of lateral changes moving away from the well.

Before analysis can be started it is necessary to go through a preprocessing phase comprising:

— A reorientation of the three-component data relative to geographical coordinates *(Figs. 1–2)*. In many cases, when no steep dips are present near the well, the displacement vector associated with the *P*-wave first arrival from an offset source may be used as an orientation reference. In other cases it is recommended that one should use the bearings given by a gyroscope linked rigidly to the tool. Gyroscopes using the earth's rotation as an absolute reference are particularly attractive because they can be stopped during seismic data acquisition; moreover, they are not affected by drift.
— A separation of *P*- and *S*-waves when studying converted *P*–*S*-waves.

Analysis is based on the following three methods:

1) Qualitative observations on VSP seismograms
— The appearance of transmitted energy on a given component below a certain depth may be interpreted as the polarization effect associated with a given layer *(Fig. 3)*.
— When the appearance of transmitted energy occurs on a given *S*-wave train at different depths the cause may be a lateral heterogeneity, for example a fractured zone at a distance from the well *(Fig. 4)*.
2) The study of hodographs: one must be aware of the respective effects of time lags and differential attenuation. Increasing time lags make the Shear Wave Splitting phenomenon more visible (see *Fig. 5*). Differential attenuation may simply rotate the hodographs's main axis *(Fig. 6)*.

* CGG, Massy, 6 rue Galvani — B.P. 56, France

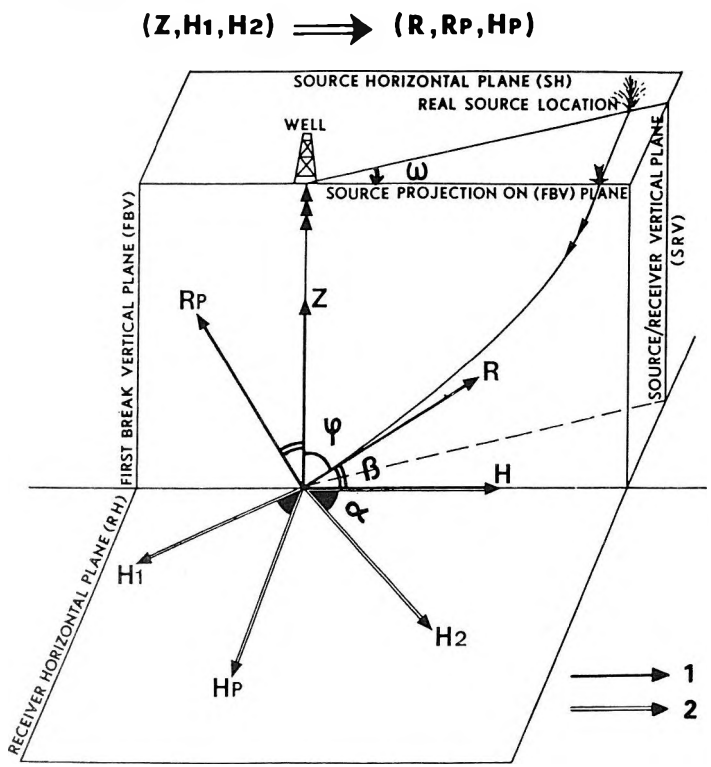

Fig. 1. 3-component reorientation before processing
1 — vector in vertical plane; 2 — vector in horizontal plane; α — horizontal rotation angle; β — vertical rotation angle; φ — angle of *P*-wave first arrival with vertical; ω — angle of *P*-wave first arrival with *SRV* plane (angle projected on horizontal plane)

1. ábra. Koordináta-rendszer váltás feldolgozás előtt
1 — függőleges síkbeli vektorok; 2 — vízszintes síkbeli vektorok; α — vízszintes forgatási szög; β — függőleges forgatási szög; φ — a *P*-hullám első beérkezésének a függőlegessel bezárt szöge; ω — a *P*-hullám első beérkezésének az *SRV* síkkal bezárt szöge (a vízszintes síkra vetített szög)

Рис. 1. Изменение системы координат до обработки:
1 — векторы в вертикальной плоскости; 2 — векторы в горизонтальной плоскости; α — угол горизонтального поворота; β — угол вертикального поворота; φ — угол, образованный первым вступлением продольных волн с вертикалью; ω — угол, образованный первым вступлением продольных волн с плоскостью *SRV* (проекция угла на горизонтальную плоскость).

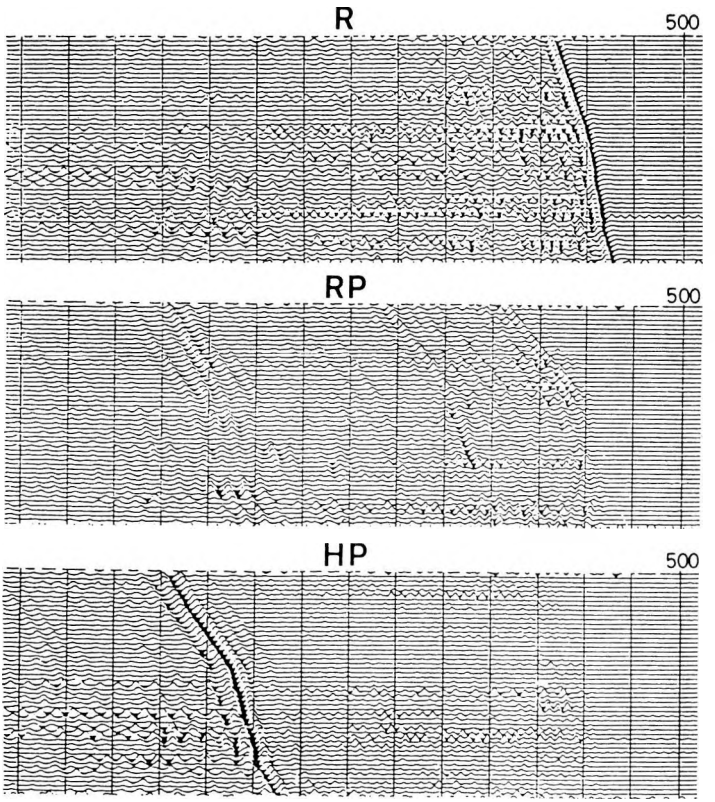

Fig. 2. Raw data reorientated (constant rotation versus time)

2. ábra. A terepi adatok az új koordináta rendszerben (időben változatlan elforgatás)

Рис. 2. Данные полевых измерений в новой системе координат (поворот, неизменяющийся во времени).

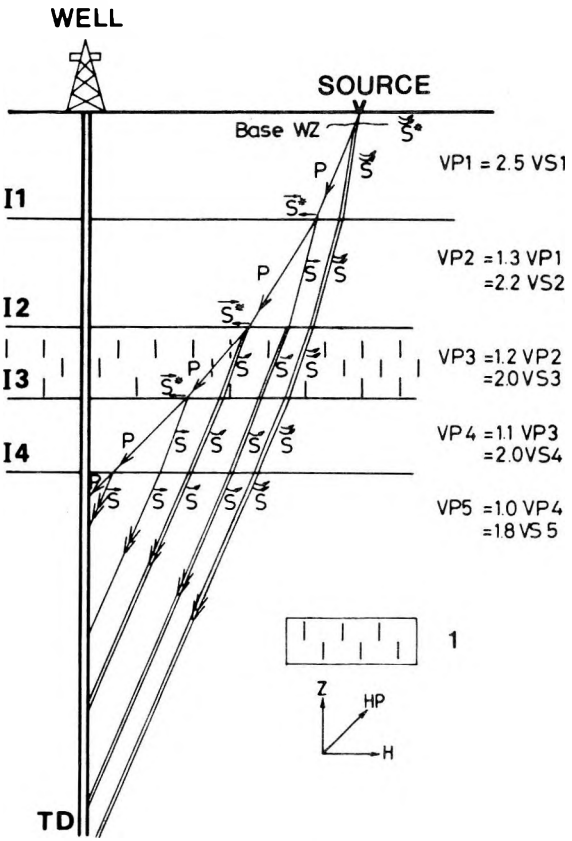

Fig. 3. *S*-wave splitting in a layered medium
1 — anisotropic layer; $\vec{S}$ — linear polarization; $\vec{S}$ — elliptic polarization (*S*-wave splitting); S^* — virtual source; $\vec{S}$ — ordinary elliptic polarization

3. ábra. *S*-hullám hasadás rétegzett közegben
1 — anizotróp réteg; $\vec{S}$ — lineáris polarizáció; $\vec{S}$ — elliptikus polarizáció (*S*-hullám hasadás); S^* — virtuális forrás; $\vec{S}$ — közönséges elliptikus polarizáció

Рис. 3. Разщепление поперечных волн в слоистой среде:
1 — анизотропный слой; $\vec{S}$ — линейная поляризация; $\vec{S}$ — эллиптическая поляризация (двупреломление поперечных волн); S^* — виртуальный источник; $\vec{S}$ — обычная эллиптическая поляризация.

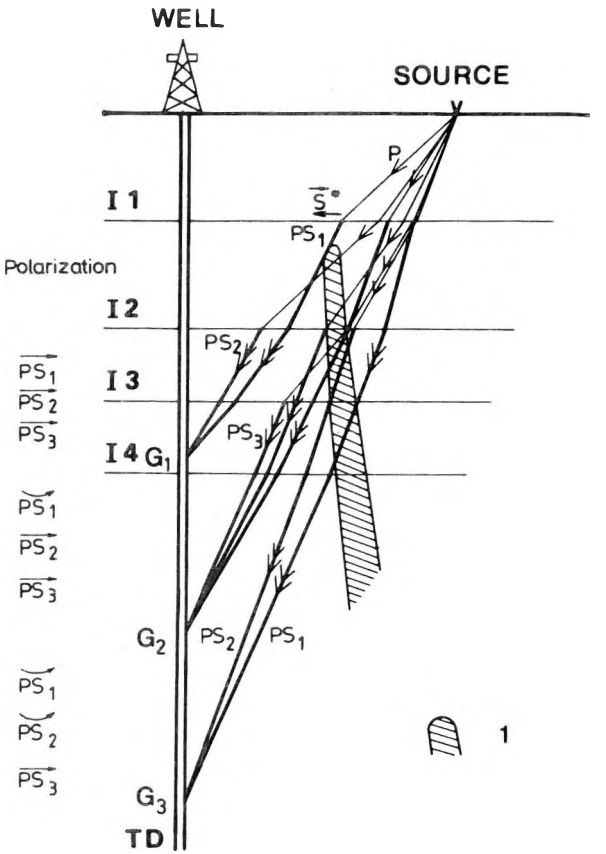

Fig. 4. Detection of an anisotropic body at a distance from the well. Anisotropy is azimuth dependent and appears at different levels
1 — anisotropic body (fractured zone)

4. ábra. Anizotrop test észlelése a fúrólyuktól távol. Az anizotrópia irányfüggő és különböző szinteken jelenik meg
1 — anizotrop test (töredezett zóna)

Рис. 4. Выявление анизотропного тела вдали от скважины. Анизотропия зависит от ориентировки и проявляется на различных уровнях:
1 — анизотропное тело (зона трещиноватости).

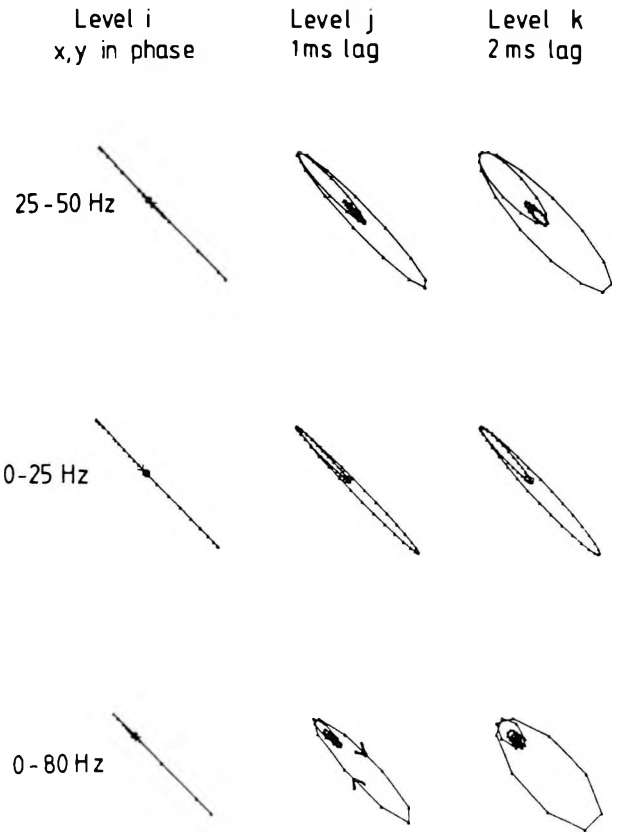

Fig. 5. Hodographs affected by velocity anisotropy only; 2 ms sampling rate

5. ábra. Csak a sebesség anizotrópia által befolyásolt trajektóriák. Mintavétel 2 ms

Рис. 5. Траектории, испытывающие влияние одной лишь анизотропии скоростей. Отсчеты — через 2 мс.

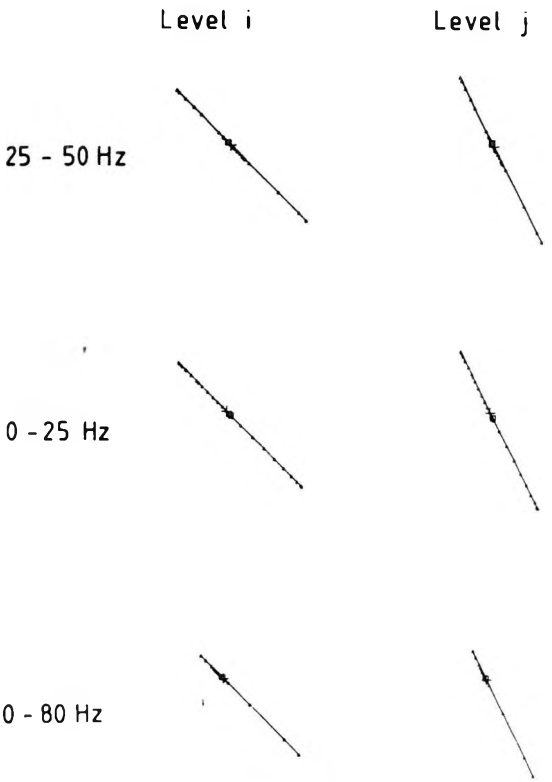

Fig. 6. Hodographs affected by attenuation anisotropy only; x and y are in phase

6. ábra. Csak a csillapítási anizotrópia által befolyásolt trajektóriák; x és y komponens fázisban

Рис. 6. Траектории, испытывающие влияние одной лишь анизотропии затухания; компоненты x и y находятся в фазе.

3) A quantitative Shear Wave Splitting detection method based on the analysis of crosscorrelations of traces recorded at different levels.

The complexity of polarization effects calls for a more refined method than the observation of multicomponent seismograms and hodographs. It may even be impossible to define the orientation of anisotropy axes on the basis of qualitative observations alone. *(Fig. 7)*

When the recording axes have an orientation different from the orientation of natural axes the two waves generated by splitting interfere with each other.

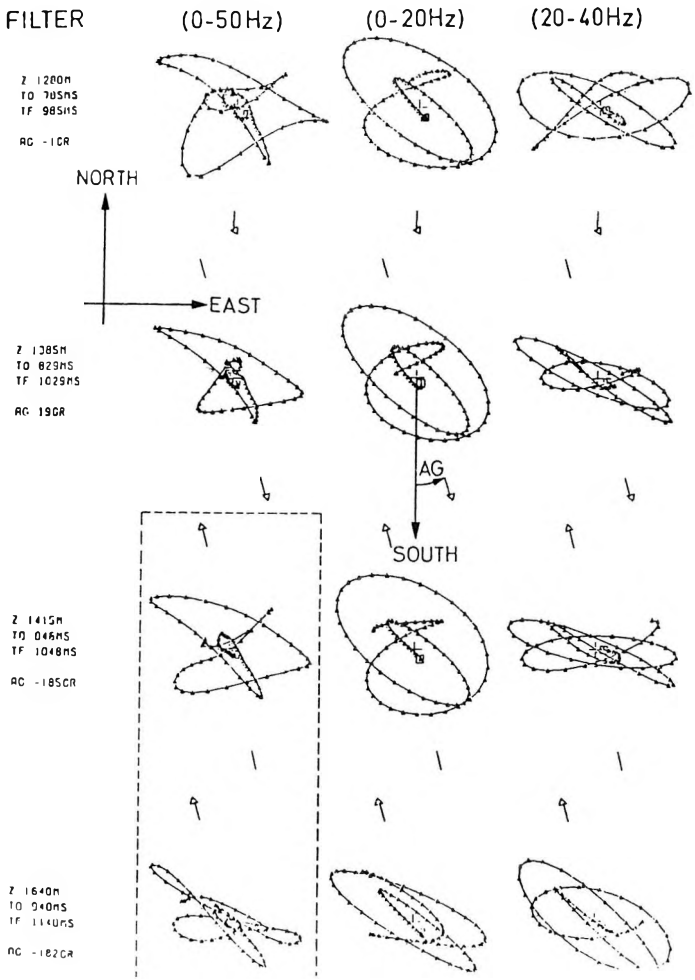

Fig. 7. Hodographs of a trace collection of the same tool orientation

7. ábra. Felvétel sorozat trajektóriái, azonos szonda irányítottság esetén

Рис. 7. Траектории по серии записей при постоянной ориентировке зонда.

When the recording axes X and Y at two different levels, i and j, coincide with the natural axes, the two waves are separated on their respective axes. Consequently, when a series of crosscorrelations $C_{XX} = X_i * \bar{X}_j$ and $C_{YY} = Y_i * \bar{Y}_j$ corresponding to a rotation scan is produced, pseudo autocorrelations, i.e. symmetrical wave shapes, are obtained when the rotation scan reaches the natural axes *(Fig. 8)*. The crosscorrelation of crosscorrelations $C_{XX} * \bar{C}_{YY}$ is a band limited pulse, the intercept of its phase spectrum corresponds to the time lag separating the two waves. The results, including differential attenuation are presented in a comprehensive listing *(Table I)*.

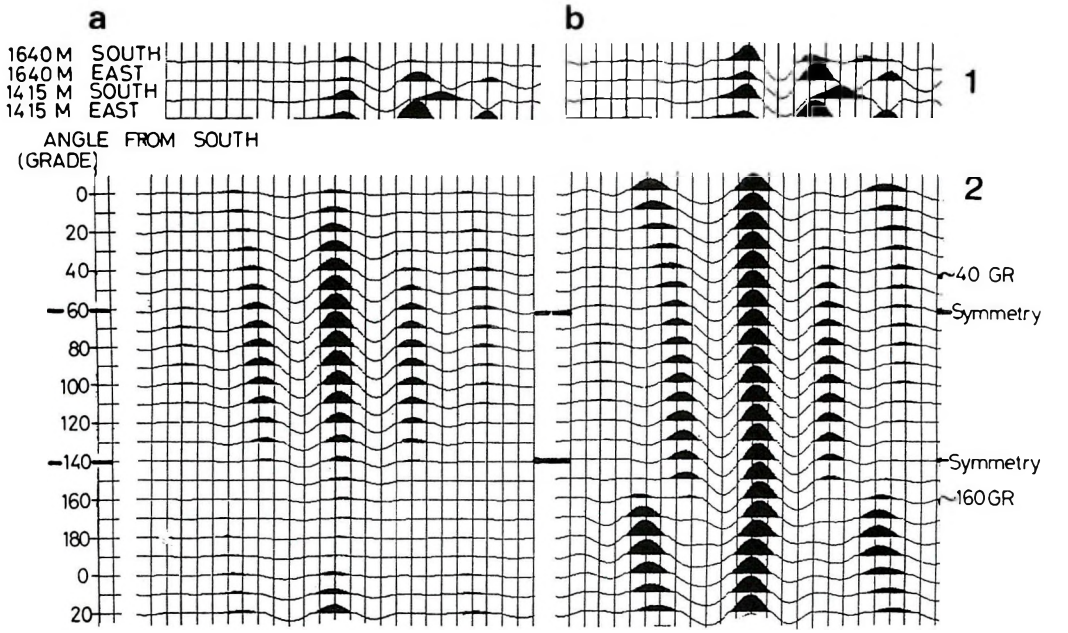

Fig. 8. Correlation scan on VSP seismograms
1 — data; 2 — correlation scan; a — constant gain traces; b — normalized traces
Symmetry is observed at 60 and 140 GR (360° = 400 GR), thus directions of polarization axes are 40 and 160 GR

8. ábra. VSP szeizmogramok korrelációs vizsgálata
1 — adatok; 2 — korrelációs vizsgálat; a — konstans erősítésű csatornák; b — normált csatornák
Szimmetria észlelhető 60 és 140 GR-nél (360° = 400 GR), így a polarizáció tengelyirányai 40 és 160 GR

Рис. 8. Корреляционное исследование сейсмограмм ВСП:
1 — данные; 2 — корреляционное исследование; a — каналы с постоянным усилением; b — нормированные каналы
Симметрия наблюдается при 60 и 140 гр (360° = 400 гр), так что оси поляризации ориентированы по 40 и 160 гр.

	DEPTH1 METER	DEPTH2 METER	ANGLE1 NORTH DEG.	ANGLE2 NORTH DEG.	V2–V1 / V PER CENT	INTVL TIME MILLISEC	QD: 10–20 Hz A2/A1 ARE IN DECIBELS	QD: 20–30 Hz	QD: 30–40 Hz	INDICE AVERAGE 100
1	900.0	660.0	162.0	90.0	−.1	215.0	−.7	−4.9	4.6	62.0
2	920.0	640.0	180.0	72.0	−.2	242.0	−.5	−3.2	−2.0	62.0
3	1160.0	760.0	135.0	27.0	−1.2	274.0	3.0	6.3	2.8	68.0
4	1240.0	800.0	108.0	.0	−1.2	286.0	−.8	3.2	−2.5	51.0
5	1200.0	920.0	153.0	63.0	.7	163.0	−1.0	−3.7	.9	122.0
6	1320.0	1080.0	108.0	.0	−.6	129.0	1.8	−.1	1.3	48.0
7	1300.0	1200.0	162.0	54.0	2.6	59.0	−.2	−.9	2.5	143.0
8	1460.0	1160.0	108.0	.0	−1.0	169.0	−1.1	1.1	−3.4	90.0
9	1440.0	1300.0	135.0	63.0	−.6	81.0	.6	−2.0	−1.5	100.0
10	1520.0	1240.0	99.0	−9.0	−.3	148.0	−1.2	1.7	1.0	101.0
11	1500.0	1320.0	171.0	81.0	.6	89.0	.5	−.7	2.5	117.0
12	1600.0	1460.0	153.0	81.0	−.4	54.0	−2.0	.6	.6	138.0
13	1640.0	1440.0	270.0	9.0	−1.2	78.0	−1.2	1.7	.5	153.0
14	1680.0	1520.0	171.0	81.0	.0	67.0	−.3	−.5	.4	104.0
15	1720.0	1640.0	108.0	.0	−.2	41.0	.0	−1.4	−2.8	83.0
16	1760.0	1620.0	270.0	18.0	.1	72.0	−1.5	−.5	.7	128.0
17	1825.0	1600.0	153.0	72.0	−.6	121.0	2.3	4.7	−5.4	94.0
18	1800.0	1680.0	162.0	90.0	−3.6	69.0	.9	−1.1	−1.1	185.0
19	1845.0	1760.0	108.0	9.0	−2.1	48.0	3.3	1.3	−1.1	152.0

Table I. Comprehensive list of crosscorrelation results

I. táblázat. A keresztkorreláció eredményei

Таблица I. Результаты перекрестной корреляции.

S-HULLÁM HASADÁS ELEMZÉSE VSP ADATOKBÓL

Charles NAVILLE and Gildas OMNÈS

A VSP adatok jó lehetőséget biztosítanak az S-hullám hasadás tanulmányozására, mert különböző mélységekben (különböző kőzetekben) lehet 3-komponenses jelet rögzíteni, a jel/zaj viszony nagyobb, mint a felszíni szeizmikában és a különböző sugárutakhoz kapcsolódó jelenségek értelmezhetők a fizikai paraméterek horizontális változásaként. A vizsgálatot — amely a következő három módszeren alapul: kvalitatív megfigyelések a VSP szeizmogramon, a részecske trajektóriák tanulmányozása és keresztkorrelációs analízis — meg kell hogy előzze a 3-komponenses adatok koordináta transzformációja és a *P*- és *S*-hullámok szétválasztása.

АНАЛИЗ РАСЩЕПЛЕНИЯ ПОПЕРЕЧНЫХ ВОЛН, ПО ДАННЫМ ВСП

Шарль НАВИЛЬ и Жильдас ОМНЕС

По данным ВСП легко изучается расщепление поперечных волн, поскольку представляется возможность регистрации трехкомпонентного сигнала на различных глубинах (в различных породах), далее, соотношение сигнал/шум выше, нежели в обычной сейсморазведке, и, наконец, явления, связанные с различными траекториями лучей, могут интерпретироваться в качестве горизонтальных изменений физических параметров. Исследования, основывающиеся на трех методах: качественных наблюдениях по сейсмозаписям ВСП, изучении траекторий частиц и перекрестно-корреляционном анализе, — должны опережаться преобразованием координат трехкомпонентных данных, а также разделением продольных и поперечных волн.

BOOK REVIEW

Multilingual Thesaurus of Geosciences
by G. N. Rassam, J. Gravesteijn and R. Potenza
Pergamon Press, New York, Oxford, etc.
1988 LII + 516 pages
ISBN 0-08-036431-4
Sponsored by the International Council for Scientific and Technical Information (ICSTI) and International Union of Geological Sciences (IUGS)

Fourteen years of work of several committees, many national and international organizations and an uncountable number of researchers and others have gone into this book. It might be thought that as, in this case, multilingual means six languages (English, French, German, Russian, Spanish and Italian) that this Multilingual Thesaurus (MT) involved only six national committees: this is not so. A side effect of the ICSTI–IUGS MT project is the reinforcement of nine European countries (Czechoslovakia, Finland, France, FRG, Hungary, Italy, Poland, Romania and Spain) and the United States (represented by the American Geological Institute, AGI) in participating in an information network contributing to the updating of the two international databases, GeoRef and PASCEL–GEODE, and using a common indexing language fully compatible with the MT. Thus, it seems that the MT is or will become the tool enabling us to create a unified international network of geological information.

The MT is based on the *Glossary of Geology* by Batesand Jackson (published by the American Geological Institute) whose first edition, comprising about 33000 terms, was published in 1972. It is worth mentioning that 36000 terms were contained in the second edition (published in 1980), and the predecessor of the Glossary — under the title *Glossary of Geology and related Sciences* (published in 1957) — contained only 14000 terms. One may suppose that the difference in the number of terms between the 1972 and the 1980 edition (375 terms/year) comes more from the evolution of science than from the differences in principles of compiling the glossary, which have to answer for the 19000 extra terms between 1957 and 1972.

The change of title reminds me of the real scientist of whom it is said: the more he learns the more modest he becomes. It is this train of thought that I should like to follow. In this respect, one needs to question the extent to which the MT meets the requirements of being a thesaurus of geosciences? As a geophysist, my judgement is made from the point of view of geophysics. The MT contains 4871 terms. Each term is assigned to one of the 36 fields of the geosciences. Of these 36 fields 2 have geophysics in their name, viz. Applied geophysics and Solid Earth geophysics, the first containing 88 terms, the second 171. Two more fields: Instruments — equipment (38) and Mathematical geology (104) contain such words that if a thesaurus for geophysics were to be compiled, all these words should be incorporated. From other fields, such as

Physical and chemical properties, Processes, Sedimentology, etc. a given percentage of words can be regarded as related to geophysics. Thus, altogether 837 terms were found to be strongly linked with geophysics; this means 17% of the whole stock.

It is terribly difficult to make any assessment on the percentage of geophysical terms from the whole of geosciences but I think the ratio would be higher if equal weights were assigned to each discipline. Clearly some branches of geophysics, e.g. Atmosphere and space physics, are completely left out. But even applied geophysics with its 88 terms cannot be regarded as having the same importance as, say, paleontology with 243 + 460 terms.

But enough of these statistics, my view is that the Multilingual Theseaurus is an extremely concise thesaurus of geology with a very good coverage of related sciences. But, apart from the challenge of creating a national version of this book, there is the much bigger challenge of continuing the international effort and compiling a Multilingual Thesaurus of Geophysics. In making my comments, my intention has not been to diminish the value of the MT but, on the contrary, to suggest that it is so valuable that lack of a similar book in geophysics is felt very much more than before.

Éva Kilényi

Prospektagent GMK
GÉPSZEV VDG GT